

A LABORATORY AND NUMERICAL INVESTIGATION  
OF SOLUTE TRANSPORT IN  
DISCONTINUOUS FRACTURE SYSTEMS

CENTRE FOR NEWFOUNDLAND STUDIES

**TOTAL OF 10 PAGES ONLY  
MAY BE XEROXED**

(Without Author's Permission)

JAMES WILLIAM ROBINSON



00479





National Library  
of Canada

Bibliothèque nationale  
du Canada

Canadian Theses Service

Services des thèses canadiennes

Ottawa, Canada  
K1A 0N4

## CANADIAN THESES

## THÈSES CANADIENNES

### NOTICE

The quality of this microfiche is heavily dependent upon the quality of the original thesis submitted for microfilming. Every effort has been made to ensure the highest quality of reproduction possible.

If pages are missing, contact the university which granted the degree.

Some pages may have indistinct print especially if the original pages were typed with a poor typewriter ribbon or if the university sent us an inferior photocopy.

Previously copyrighted materials (journal articles, published tests, etc.) are not filmed.

Reproduction in full or in part of this film is governed by the Canadian Copyright Act, R.S.C. 1970, c. C-30.

**THIS DISSERTATION  
HAS BEEN MICROFILMED  
EXACTLY AS RECEIVED**

### AVIS

La qualité de cette microfiche dépend grandement de la qualité de la thèse soumise au microfilmage. Nous avons tout fait pour assurer une qualité supérieure de reproduction.

S'il manque des pages, veuillez communiquer avec l'université qui a conféré le grade.

La qualité d'impression de certaines pages peut laisser à désirer, surtout si les pages originales ont été dactylographiées à l'aide d'un ruban usé ou si l'université nous a fait parvenir une photocopie de qualité inférieure.

Les documents qui font déjà l'objet d'un droit d'auteur (articles de revue, examens publiés, etc.) ne sont pas microfilmés.

La reproduction, même partielle, de ce microfilm est soumise à la Loi canadienne sur le droit d'auteur, SRC 1970, c. C-30.

**LA THÈSE A ÉTÉ  
MICROFILMÉE TELLE QUE  
NOUS L'AVONS REÇUE**

A  
LABORATORY AND  
NUMERICAL INVESTIGATION  
OF SOLUTE TRANSPORT  
IN  
DISCONTINUOUS FRACTURE SYSTEMS

by

(C) J. W. Robinson, BSc.

A thesis  
submitted to the  
School of Graduate Studies  
in partial fulfillment of the  
requirements for the degree of  
Master of Science

Department of Earth Sciences  
Memorial University of Newfoundland

January 1987

St. John's

Newfoundland



Permission has been granted to the National Library of Canada to microfilm this thesis and to lend or sell copies of the film.


The author (copyright owner) has reserved other publication rights, and neither the thesis nor extensive extracts from it may be printed or otherwise reproduced without his/her written permission.

L'autorisation a été accordée à la Bibliothèque nationale du Canada de microfilmer cette thèse et de prêter ou de vendre des exemplaires du film.

L'auteur (titulaire du droit d'auteur) se réserve les autres droits de publication; ni la thèse ni de longs extraits de celle-ci ne doivent être imprimés ou autrement reproduits sans son autorisation écrite.

ISBN 0-315-37010-6

Dedicated  
to  
Laura, Joel and Michael  
who didn't complain  
(too much)  
and to  
my beloved Patty  
who was willing to give up much  
to see this work through to the end.



# ABSTRACT

The mixing of fluids at fracture intersections was examined, in the laboratory, using fourteen plexiglass models that simulated open fractures with no contact between the fracture walls. Twelve models contained two fully intersecting fractures. One model contained two intersecting but offset fractures (parallel flow model) and one fracture system model contained a total of eleven fractures in two sets of intersecting fractures, all with the same aperture. One set was composed of five parallel fractures and the other set was composed of six parallel fractures. The twelve fully intersecting fracture models were designed to investigate the effects, on mixing, of seven angles of intersection and three fracture apertures. Iodide solution of known concentration was injected into one fracture and distilled water into another (inlet ports). At each of the outlet ports the concentration of iodide and the discharge volume were measured. The ratio of the volumes of distilled water and iodide solution in each of the discharge fractures was compared to calculate the percent mixing at the fracture intersection.

Testing, conducted at three hydraulic gradients, indicated that essentially no mixing occurred in the fully intersecting fracture models and only nominal mixing occurred in the parallel flow model. In general mixing was found to be



dependent only upon the relative size of the inlet and outlet fractures. Testing, using the fracture system model, indicated a similar lack of mixing at six intersections through which the fluid moved.

A two dimensional finite element model was written to simulate the transport of a conservative solute in a discontinuous, random, fracture system. Mixing at fracture intersections in the numerical model was based on the results of the physical model study. Hence no mixing was allowed to take place at the fracture intersections except that which was due to the differences in the apertures of the inlet and discharge fractures. Using this mixing algorithm the numerical model indicates that more longitudinal and less lateral dispersion takes place than when complete mixing at fracture intersections is assumed. In addition, more longitudinal transport takes place in discontinuous than in continuous fracture systems. These findings indicate that contaminants migrating through fractured media, where the fracture walls are not in contact, will not be dispersed and diluted to the extent that past numerical models have predicted and hence the contaminant will be discharged to the biosphere in much greater concentration than expected.

#### ACKNOWLEDGEMENTS

I wish to thank the many people who made this work possible. Dr. Wasi Ullah, Director of the Water Resources Division for putting many hours into obtaining approval from the Newfoundland Department of Environment for educational leave. Mr. Allister Kinsmen and Mr. Dave Jeans, deputy and assistant deputy minister of the Department of Environment for giving their approval of further training and making the necessary submissions to the Newfoundland Public Service Commission. Miss Lyne Houle for her able help in conducting the laboratory tests. Mr. Lee Atkinson for many helpful discussions concerning the numerical transport model. Mr. Don Cameron for his ever ready help in the laboratory. Mr. Alain Rouleau and Mr. Bob MacLeod for their help with the workings of the fracture flow model. Mr. Jim Keating for his help in drafting some of the more complicated figures. Most importantly my supervisor Dr. John Gale for the excellent one-on-one courses and conversations concerning fractured rock hydrology and his patience, guidance and financial support with regard to the present study. Last but by no means least I thank my wife for her help in typing the major portion of the text and who's patience and support was nothing short of monumental during the long years of study.

## TABLE OF CONTENTS

ABSTRACT . . . . .	i
ACKNOWLEDGEMENTS . . . . .	iii
LIST OF TABLES . . . . .	vi
LIST OF FIGURES . . . . .	vii
CHAPTER ONE	
INTRODUCTION . . . . .	1
1.1 STATEMENT OF PROBLEM . . . . .	1
1.2 OBJECTIVES AND SCOPE . . . . .	3
1.3 LITERATURE REVIEW . . . . .	5
CHAPTER TWO	
PHYSICAL MIXING MODELS . . . . .	12
2.1 MODEL DESIGN AND CONSTRUCTION . . . . .	12
2.2 TESTING PROCEDURE . . . . .	18
2.3 DETERMINATION OF PERCENT MIXING . . . . .	20
2.4 MIXING TEST RESULTS . . . . .	26
2.5 DISCUSSION . . . . .	28
CHAPTER THREE	
COMPUTER MODELING . . . . .	30
3.1 INTRODUCTION . . . . .	30
3.2 FRACTURE NETWORK AND FLOW GENERATION . . . . .	32
3.3 UPSTREAM WEIGHTED FINITE ELEMENT FORMULATION . . . . .	34
3.4 EXPORT - A FINITE ELEMENT TRANSPORT MODEL . . . . .	43
3.4.1 The Main Program . . . . .	43
3.4.2 Subroutine BREAKUP . . . . .	54
3.4.3 Subroutine CONCENTRATION . . . . .	61
3.4.4 Subroutines MATRICIES and PARTITION . . . . .	61
3.4.5 Subroutines SOLVEC and RECONSTITUTE . . . . .	68
3.5 RESULTS OF NUMERICAL MODEL . . . . .	74
CHAPTER FOUR	
NUMERICAL SIMULATION OF SOLUTE TRANSPORT IN FRACTURED SYSTEMS . . . . .	83
4.1 MODEL FOURTEEN . . . . .	83
4.2 RANDOM FRACTURE SYSTEMS . . . . .	86
4.2.1 Equivalent Fracture Sets . . . . .	87
4.2.2 Unequal Aperture Model . . . . .	90
4.2.3 Equal Apertures and Unequal Spacing and Density . . . . .	90
4.3 STRIPA FRACTURE MODEL . . . . .	93



CHAPTER FIVE	
CONCLUSIONS AND RECOMMENDATIONS FOR FURTHER WORK . . . . .	99
APPENDIX A	
TESTING RESULTS OF PLEXIGLASS FRACTURE MODELS . . . . .	105
APPENDIX B	
LONG HAND DETERMINATION OF TRANSPORT IN A FRACTURE SYSTEM	135
APPENDIX C	
FORTTRAN LISTING OF NUMERICAL MODEL EXPORT AND ALL SUBROUTINES . . . . .	143
APPENDIX D	
DATA FILE USED TO GENERATE FIGURE 4.3 AND THRED.DAT FOR FIGURE 4.4 . . . . .	173

# LIST OF TABLES

Table 1:	Design Details of Fracture Mixing Models . . . .	16
Table 2:	Average Adjusted Mixing Values . . . . .	28
Table 3:	Control file "choice.dat" . . . . .	49
Table 4:	Fracture information file "element.dat*" . . . . .	52
Table 5:	Concentration Values ( $C/C_0$ ) Determined in Model # 14. . . . .	86
Table 6:	Data File CHOICE.DAT . . . . .	87

# LIST OF FIGURES

Figure 1.1	Schematic showing idealized concentration distribution with equal flow in all directions and a) assuming 100 percent mixing and b) assuming no mixing at fracture intersections. . . . .	3
Figure 2.1	Typical Plexiglass Fracture Model . . . . .	13
Figure 2.2	Fracture configuration of parallel flow model . . . . .	14
Figure 2.3	Fracture configuration in the fracture system model with selected port numbering . . . . .	15
Figure 2.4	Enlargement of typical saw cut, viewed looking down into the fracture. . . . .	19
Figure 2.5	Schematic of (a) 100 percent mixing and (b) less than 100 percent mixing at the intersection node. . . . .	22
Figure 2.6	Schematic flow diagram for forced mixing . . . . .	25
Figure 3.1	(a) Linear element basis functions and (b) Upstream weighting functions for $\alpha = 1$ . (After Huyakorn and Pinder, 1983) . . . . .	41
Figure 3.2	Flow chart of main program in the code EXPORT . . . . .	44
Figure 3.2	(continued) Flow chart of main program in the code EXPORT . . . . .	45
Figure 3.2	(continued) Flow chart of main program in the code EXPORT . . . . .	46
Figure 3.2	(continued) Flow chart of main program in the code EXPORT . . . . .	47
Figure 3.2	(continued) Flow chart of main program in the code EXPORT . . . . .	48
Figure 3.3	Flow chart of Subroutine BREAKUP . . . . .	56
Figure 3.3	(continued) Flow chart of Subroutine BREAKUP . . . . .	57
Figure 3.3	(continued) Flow chart of Subroutine BREAKUP . . . . .	58
Figure 3.3	(continued) Flow chart of Subroutine BREAKUP . . . . .	59
Figure 3.4	Four way fracture intersection showing (a) the angles that determine the direction of solute movement from inlet fractures to discharge fractures and (b) the renumbering of the intersection nodes. . . . .	60
Figure 3.5	Flow chart of subroutine CONCENTRATION . . . . .	62
Figure 3.5	(continued) Flow chart of subroutine CONCENTRATION . . . . .	63
Figure 3.6	Flow chart for subroutine MATRICES . . . . .	64
Figure 3.6	(continued) Flow chart for subroutine MATRICES . . . . .	65
Figure 3.7	Flow chart for subroutine PARTITION . . . . .	66
Figure 3.7	(continued) Flow chart for subroutine PARTITION . . . . .	67
Figure 3.8	Flow chart for subroutine SOLVEC. . . . .	69



Figure 3.8	(continued) Flow chart for subroutine SOLVEC. . . . .	70
Figure 3.9	Flow chart for subroutine BRIDGIT. . . . .	71
Figure 3.10	Flow chart for subroutine MULTIPLY. . . . .	72
Figure 3.11	Flow chart for subroutine RECONSTITUTE. . . . .	73
Figure 3.12	Fracture configuration used to test the numerical model. . . . .	74
Figure 3.13	Concentration profiles using $dt = 0.4$ , $t = 6.4$ ; (a) $Pe = 10$ ; (b) $Pe = 100$ (after Huyakorn and Nilkuha, 1979) . . . . .	75
Figure 3.14	Concentration profiles using $dt = 0.4$ , $t = 6.0$ and $Pe = 10$ (Using the analytical solution and the numerical transport model EXPORT). . . . .	76
Figure 3.15	Concentration profiles using $dt = 0.3$ , $t = 6.0$ and $Pe = 10$ (Using the analytical solution and the numerical transport model EXPORT). . . . .	77
Figure 3.16	Concentration profiles using $dt = 0.2$ , $t = 6.0$ and $Pe = 10$ (Using the analytical solution and the numerical transport model EXPORT). . . . .	78
Figure 3.17	Concentration profiles using $dt = 0.3$ , $t = 6.0$ , $Pe = 10$ , $\alpha = 0.0$ , $\alpha = 0.13$ and $\alpha = 0.2$ (Using the analytical solution and the numerical transport model EXPORT). . . . .	79
Figure 3.18	Concentration profiles using $dt = 0.3$ , $t = 6.0$ , $Pe = 100$ , $\alpha = 0.0$ , $\alpha = 0.13$ and $\alpha = 0.2$ (Using the analytical solution and the numerical transport model EXPORT). . . . .	80
Figure 3.19	Fracture configuration used to examine the mixing algorithm used in EXPORT. . . . .	81
Figure 3.20	Concentration profiles using $dt = 0.4$ , $t = 6.0$ , $Pe = 10$ , $\alpha = 0.0$ and implementing the subroutine BREAKUP (Using the analytical solution and the numerical transport model EXPORT). . . . .	82
Figure 4.1	3-D plot of solute concentrations in model # 14 assuming perfect mixing at the fracture intersections. . . . .	84
Figure 4.2	3-D plot of solute concentrations in model # 14 assuming no mixing at the fracture intersections. . . . .	85
Figure 4.3	Configuration of equal density/equal aperture fracture model. . . . .	88
Figure 4.4	3-D plot of nodal concentrations for equal density/equal aperture fracture model. . . . .	89
Figure 4.5	3-D plot of nodal concentrations for equal density-equal spacing fracture model in which the fracture set at 15 degrees from the horizontal has twice the aperture as the	

other set. . . . .	91
Figure 4.6 Configuration of equal aperture fracture model with unequal density and length (set one, 15 degrees from horizontal, has twice the length and twice the density of set two). . . . .	92
Figure 4.7 3-D plot of nodal concentrations for fracture model with equal aperture and unequal density and length. . . . .	94
Figure 4.8 Fracture network configuration generated by NETWORK from data obtained in Stripa Sweden. . . . .	95
Figure 4.9 Concentration of solute at fracture intersections using EXPORT without BREAKUP . . . . .	96
Figure 4.10 Concentration of solute at fracture intersections using EXPORT with BREAKUP . . . . .	97
Figure A-1 Diagram of experimental setup. . . . .	106
Figure B-1 Fracture configuration and element numbering . . . . .	136

## CHAPTER ONE

### INTRODUCTION

#### 1.1 STATEMENT OF PROBLEM

Rock masses are characterized by fracture systems consisting of a number of fracture sets. Individual fractures in each set are discontinuous within their own planes. Hence the hydraulic conductivity of rock masses, having a low permeability matrix, is a function of the interconnection of the individual fractures. In order to simulate the transport of a solute through a discontinuous intersecting fracture network, or system, one must know the degree of solute mixing at the fracture intersections.

Most numerical studies of mass transport in discrete fracture systems have assumed complete mixing at fracture intersections ie; Castillo (1972), Krizek et al. (1972), and Schwartz et al. (1983). This assumption was based on the results of laboratory studies by Castillo (1972) and Krizek et al. (1972), using a plexiglass model of two fractures. In Castillo's model the fractures intersected at right angles and in the model by Krizek, et al. (1972) the two fractures intersected at 60 degrees. Both studies concluded that one could assume complete mixing at fracture intersections. This work however was not conclusive because only one inflow element was considered.



A more general situation involving two inflow elements was considered by Wilson and Witherspoon (1976). Studying the effect of orthogonal pipe intersections on total flow they reported that a qualitative dye experiment showed that little or no mixing took place at the intersection of the two pipes. Endo et al. (1984) presented a numerical fracture transport model based on the work of Wilson in which it was assumed that no mixing occurred at the fracture intersections. This work however was not based on any physical testing, in fact, there appears to have been no additional laboratory testing of mixing at fracture intersections despite the markedly dissimilar conclusions that were reached by the above laboratory studies.

The importance of determining the correct mixing algorithm is illustrated in Figure 1.1. This figure shows an idealized network of orthogonal fractures with equal apertures, lengths and spacings into which a contaminant, at a concentration of 100 mg/L, is introduced at one node. A concentration of 0 mg/L is assumed for all other inlets. Figure 1.1a illustrates the substantial lateral dispersion of contaminant in the direction of flow when complete mixing at fracture intersections is assumed. Figure 1.1b, in contrast, indicates that no lateral dispersion of contaminant is possible if no mechanical mixing takes place at the intersections. In both networks zero diffusion is assumed.

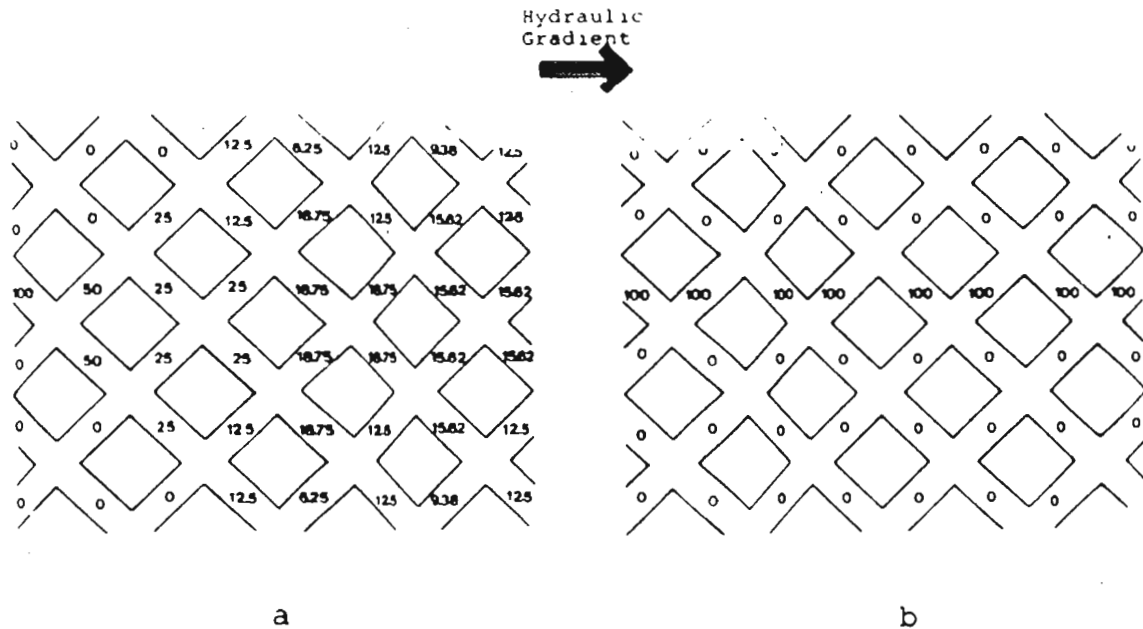


Figure 1.1 Schematic showing idealized concentration distribution with equal flow in all directions and a) assuming 100 percent mixing and b) assuming no mixing at fracture intersections.

## 1.2 OBJECTIVES AND SCOPE

The objectives of the present study were; 1) to determine the degree of mixing that takes place at fracture intersections, 2) to determine the effects of this mixing on lateral dispersion and 3) to simulate, by means of a numerical finite element model, incorporating the appropriate fracture intersection mixing algorithm, the two-dimensional transport of a conservative solute in fractured media. In order to accomplish these objectives, a laboratory study of the dynamics of mixing at fracture intersections was conducted. Twelve plexiglass, fracture intersection models were used to investigate the effects of the angle of intersection,

and the apertures of intersecting fractures on mixing. A thirteenth model was used to determine the amount of mixing that takes place between two streams of fluid, one contaminated and the other not, flowing side by side in one fracture. Finally a fourteenth model was used to investigate solute mixing in a fracture system containing multiple fracture intersections. A potassium iodide solution and distilled water were used in the models to determine the amount of mixing that takes place under various flow rates and fracture configurations. These tests are described in Chapter 2.

A finite element model, based on the mixing test results, was developed to simulate the transport of a contaminant in fractured media. For this purpose, realistic network configurations and flow conditions were used. The network generator and flow model of Rouleau (1984) were used to define the physical structure of the fracture system and to determine the dynamics of flow within it. The transport model was written to accept the output of these programs and to determine the time dependent movement of a conservative solute through the system. The model incorporated advective-dispersive transport within the fracture plane and the assumption of an impervious matrix. The numerical model is described in Chapter 3.

In Chapter 4, a comparison is made of the transport

patterns that are determined from the numerical model, in continuous and discontinuous fracture systems. The comparison also shows the effects of making the assumption of perfect mixing at fracture intersections.

The study does not consider mixing under turbulent flow conditions. In nature, flow in fractured media is usually laminar. Low hydraulic gradients and the small size of natural fractures contribute to this fact. Some exceptions to this rule are solution channels in soluble rocks, such as limestones, and radial flow around bore holes. These situations, however, are usually well defined and very localized. For this reason the laboratory testing and the numerical model results are limited to laminar flow conditions. The results are also limited to open fractures. Fractures that were in contact or fractures that were partially filled were not investigated in this study.

### 1.3 LITERATURE REVIEW

A number of workers have contributed to the understanding of transport in discrete fracture systems and specifically the degree of mixing that takes place at fracture intersections. G de Josselin de Jong, et al (unpublished), developed a probabilistic approach of subdividing lamina at each fracture intersection according to the relative flow

rates of the fractures flowing into the intersection and those draining it. He assumed essentially no mixing at these intersections. In contrast to this view, Castillo (1972), using a plexiglass model of two orthogonally intersecting fractures, concluded from laboratory testing that complete mixing could be assumed at fracture intersections. Subsequent numerical modelling of a system of orthogonal fractures of equal spacing and aperture by the same author used this mixing relationship. Other workers (Krizek, 1972) put forward the same conclusion based on similar testing conditions using an additional plexiglass model. This model simulated two fractures intersecting at 60 degrees.

While it is true that the work of Castillo (1972) and Krizek (1972) did show the importance of longitudinal dispersion of solutes within the fracture plane, their conclusion concerning complete mixing at intersections in a fracture system is questionable. The physical configuration of their fracture model, in which the tests were conducted, preclude such a finding. When the measurements of concentration were being made by these workers, the only flow into the system was that of the contaminant. The end of one fracture received this flow while drainage was allowed, at atmospheric pressure, from the other three outlets. Since no flow of uncontaminated water was allowed into the system, it is only logical that the concentration in each outlet fracture would

eventually be equal. Equality of concentration under these conditions is independent of the degree of mixing because no uncontaminated fluid is allowed to flow into the intersection. A more realistic intersection model was tested by Wilson, et al (1976). This work, although qualitative, involved the use of a circular pipe model made from two intersecting, orthogonal holes drilled into a plexiglass block. When a dyed fluid was allowed to flow through one pipe and a colourless fluid, at the same head, flowed through an adjacent pipe, little or no mixing was reported.

Besides the dynamics of mixing at fracture intersections, the effects of various transport mechanisms in the plane of discrete fractures has been discussed by numerous workers. Diffusion into the matrix was modelled by Foster (1975). He used a one-dimensional analytical solution to explain an anomalous low level of tritium in a Chalk aquifer in Britain. Physically, his analysis was limited to a single uniform continuous fracture. Further modelling based on single fractures was carried out by Grisak, et al (1980), who used a finite element model to simulate nonreactive and reactive solute transport by advection, mechanical dispersion and diffusion into the matrix. Following the work of Barker (1980), who developed Laplace transform solutions for solute transport in fissured media, several workers contributed analytical models to the growing body of transport simula-

tions. Tang, et al (1981) provided an analytical solution to single fracture transport which accounted for each of the transport processes mentioned above, plus adsorption onto the face of the matrix, adsorption within the matrix and radioactive decay. A similar but less comprehensive solution was given by Grisak, et al (1981). Although they are not very realistic, being limited to single fractures, their analytical solutions do provide an accurate way of investigating the relative importance of the various transport processes, given that the underlying boundary conditions such as hydraulic gradients and empirical relationships, describing mixing and diffusion within the fracture plane are correct.

Transport in parallel fissures was modelled numerically by Barker, et al (1981) and analytically by Sudicky, et al (1982). The first of these studies concerned only diffusion into the matrix while the second accounts for all of the transport processes mentioned so far. Further work on parallel fractures was done by Rasmuson, et al (1982) in which a three-dimensional numerical model of advective, diffusive transport was verified against the analytical solution of Neretnieks (1982). While providing further insight into the relative importance of the various transport mechanisms, such modelling still suffers from the physical restrictions imposed by the assumption of a system of parallel, unconnected, continuous fractures.



One of the limitations of numerical modelling of transport in fractures is the oscillation of the concentration profile. This happens when advection is the dominate transport mechanism. Huyakorn, et al (1979) developed an efficient technique of reducing this oscillation while maintaining a relatively coarse temporal discretization. This was done using upstream weighing functions. Using this technique, Noorishad, et al (1982) developed a two-dimensional model in which fractures were represented by one-dimensional line elements with two nodal points. Huyakorn, et al (1983) developed a discrete fracture model using a similar finite element technique for advective transport in fracture systems. To avoid the limitations of a parallel fracture system, his model incorporated a spherical idealization of matrix blocks for the simulation of diffusion into the matrix. In his model, single-species transport only is considered. In a later model, (Huyakorn, et al (1983) nuclide decay and chain transport are included. Since both models approximate the blocky nature of fractured media using spheres, of necessity, they simulate only regular continuous fractured systems.

Flow modelling in discontinuous random fracture networks has been done by Long, et al (1982) and Rouleau (1984). Each of these models generates a two-dimensional fracture network

represented by sets of line elements. The orientations, apertures and lengths of the fractures, thus represented, are generated according to a user-specified distribution. To calculate the flow distribution in each of the connected segments a finite element solution is used. Transport models in such networks have been presented by only a few workers. Schwartz, et al (1983) modeled mass transport in a network of discrete fractures by use of a particle-tracking technique. The model was based on a finite difference technique and therefore the fractures intersect orthogonally. In addition the assumption is made that complete mixing occurs at the fracture intersections. This assumption was based on the work by Krizek, et al (1972). Endo et. al. (1984) presented a transport model which assumed no mechanical mixing at the fracture intersections. Fluid transport was simulated by means of stream tubes. As a fluid moved through a fracture system the original stream subdivided at each intersection and therefore the number of stream tubes increase and their thickness decreased requiring substantial computer memory for even modest sized fracture systems.

More recently Hwang et. al (1984) developed a model which used an eigenvalue solution. This model avoided much of the stability problems that are encountered in the Galerkin finite element formulation. Another model that avoids the same problems was developed by Hwang (1985). This

model used a new solution approach which was called, by the authors, "the finite analytic method". In this method a system of linear equations are developed by application of the appropriate analytic solution to the transport of a solute between two nodes. The results are comparable with those obtained using the upstream weighted finite element method. While extensive numerical studies have been conducted on transport in fractured media the laboratory studies designed to examine the empirical relationships involved in the transport process have been limited in both number and scope.

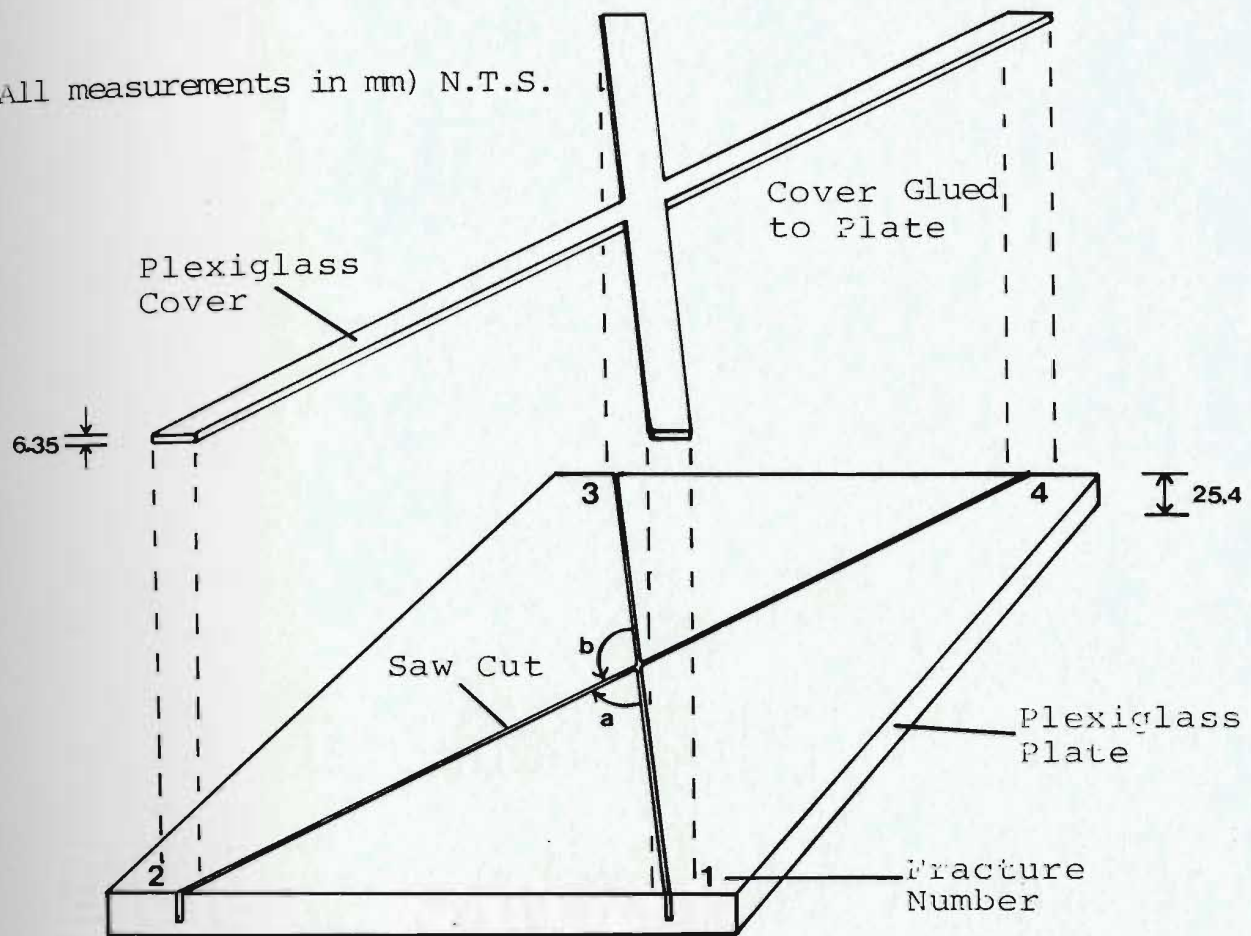
## CHAPTER TWO

### PHYSICAL MIXING MODELS

#### 2.1 MODEL DESIGN AND CONSTRUCTION

Using a design similar to that of Krizek et al (1972), illustrated in Figure 2.1, fourteen plexiglass fracture models were constructed. Twelve of the models were constructed with fully intersecting fractures as shown in Figure 2.1. One model was constructed with an offset fracture intersection as depicted in Figure 2.2. A final model was constructed with two sets of five and six fractures, respectively, which intersected fully as shown in Figure 2.3. The model fractures were cut into a 25 mm thick, clear, plexiglass base using Dormer, model HSS saws with a diameter of 70 mm and 72 teeth. The nominal width of the saws used were 0.254 mm (0.010 in), 0.381 mm (0.015 in), and 0.508 mm (0.020 in). These saws produced cuts with measured apertures of .28, .36 and .50 mm, respectively. The cutting was done on a Aciera F5 milling machine. Throughout all the milling and cutting processes a 50:1 ratio of water to cutting fluid (Esso Kutwell 45 #50754 lubricating oil) was used to reduce friction on the saw blade and to dissipate any heat that was generated in order to produce a uniform aperture along the fracture length.

(All measurements in mm) N.T.S.



# FRACTURE END ASSEMBLY

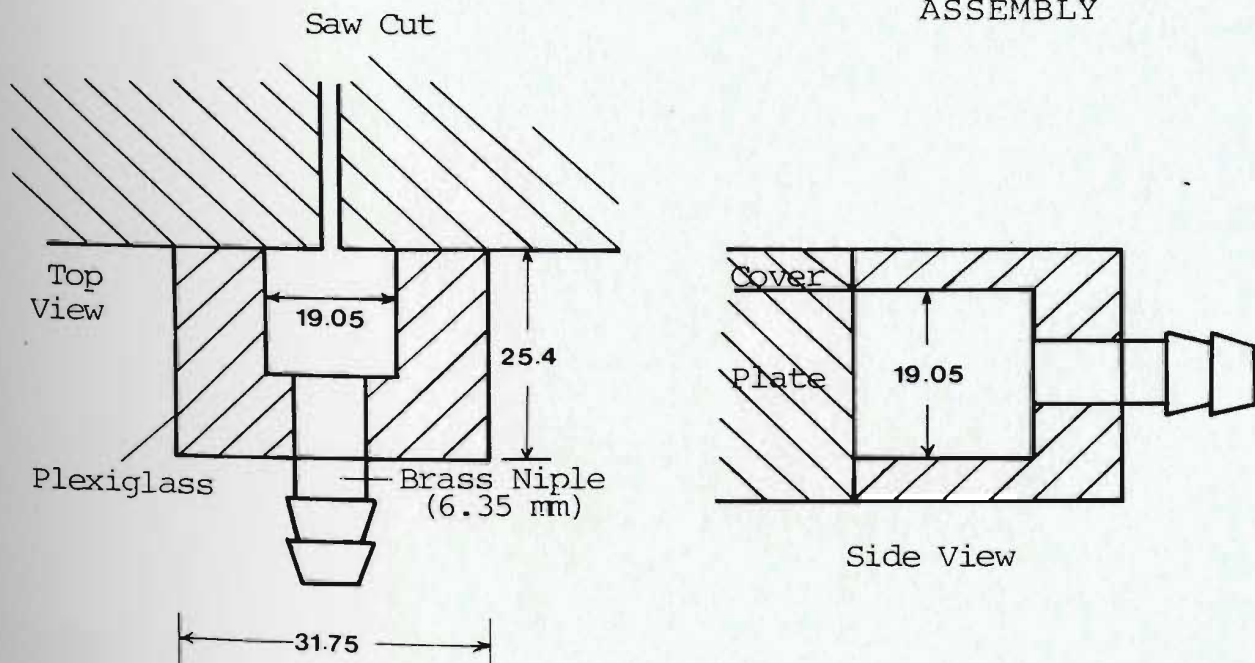


Figure 2.1 Typical Plexiglass Fracture Model

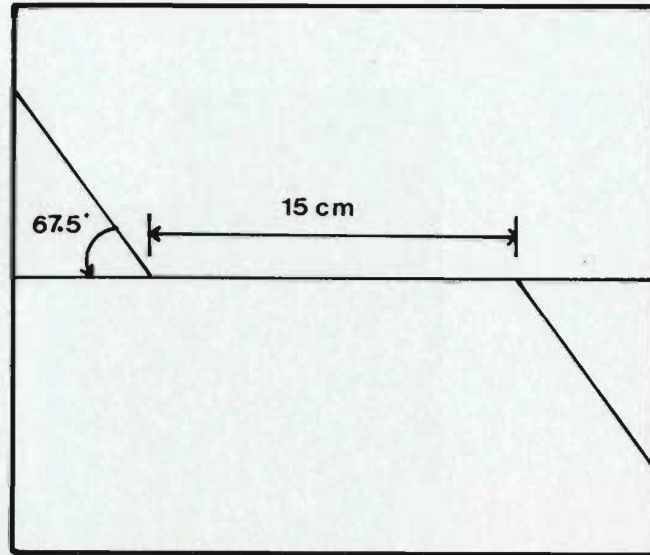


Figure 2.2 Fracture configuration of parallel flow model

The twelve models constructed with fully intersecting fractures were used to examine the three variables that were thought to be important to mixing; (1) the angle of intersection between the two fractures, (2) the velocity of flow in the contributing fractures, and (3) the difference in fracture aperture. The twelve models were divided into four groups of three models each. Each model in a given group had the same angle of fracture intersection. In addition the aperture of one fracture in each group was 0.5 mm, while the second fracture in each model had an aperture of 0.28 mm, 0.36 mm or 0.5 mm respectively for the three models in the group. The various fracture intersection angles used in each



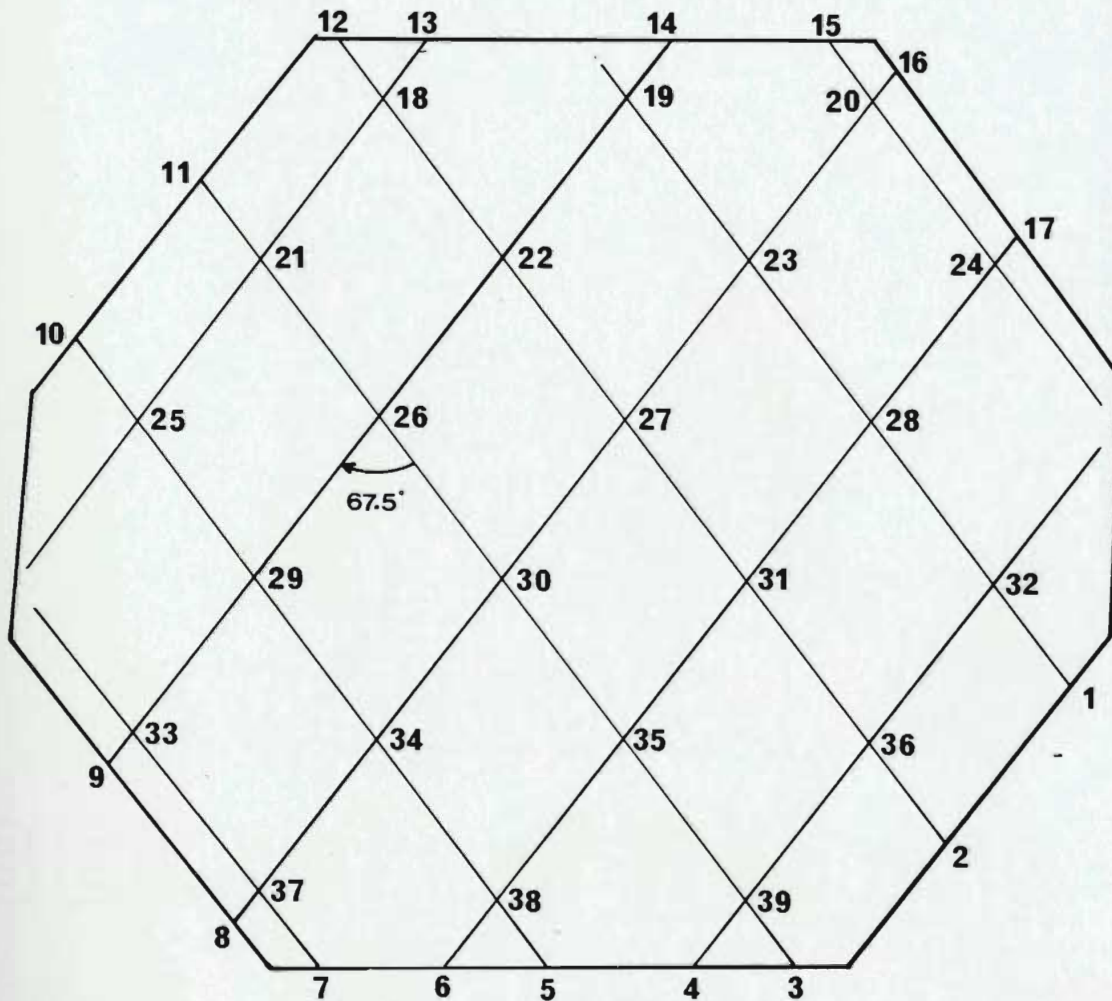


Figure 2.3 Fracture configuration in the fracture system model with selected port numbering

group and the fracture apertures used in each model are listed in Table 1. As shown in this table, by varying the inlet and outlet ports, it was possible to investigate seven different intersection angles ranging from 22.5 to 157.5 degrees.

The flow regulating system consisted of two Marriotte bottles, approximately 100 mm in diameter, which provided a continuous flow of solution at a constant pressure head. The



Table 1: Design Details of Fracture Mixing Models

Series	Model #	Angle a* degrees	Angle b* degrees	Aperture of #1 - #3 mm	Aperture of #2 - #4 mm
1	1	22.5	157.5	0.25	0.50
	2	22.5	157.5	0.33	0.50
	3	22.5	157.5	0.50	0.50
2	4	45.0	135.0	0.25	0.50
	5	45.0	135.0	0.33	0.50
	6	45.0	135.0	0.50	0.50
3	7	67.5	112.5	0.25	0.50
	8	67.5	112.5	0.33	0.50
	9	67.5	112.5	0.50	0.50
4	10	90.0	90.0	0.25	0.50
	11	90.0	90.0	0.33	0.50
	12	90.0	90.0	0.50	0.50
other	13	67.5	112.5	0.50	0.50
other	14	67.5	112.5	0.50	0.50

\* see Figure 2.2

capacity of each bottle was about 6 L, which ensured an ample supply of solution for several tests to be run.

The effect of flow velocity on mixing was examined by using three different hydraulic gradients. To have the same fluid velocity all fracture segments were designed with a constant length of 150 mm and a depth that was equal to 44 to 51 times the aperture. This was thought to be sufficient to eliminate differential friction losses and end effects in the fractures.

The thirteenth model (parallel flow model) was designed

to examine the mixing of two streams of fluid in a single fracture plane. The basic construction of this model was similar to the fully intersecting models, except for the configuration of fracture segments and their number. As depicted in Figure 2.2, the model was designed with 2 intersection nodes and 4 end nodes. The fracture segments were designed with apertures of .5 mm and intersection angles of 17.5 degrees. The design details of this thirteenth model are listed in Table 1.

The fourteenth model (the fracture system model) was designed to investigate the mixing that takes place in a fracture system of several intersecting fractures. The fracture configuration used in this model, as depicted in Figure 2.3, consisted of two sets of intersecting fractures. One set contained five parallel and equally spaced fractures with the same aperture. The other set contained six fractures with the same spacing and aperture as the first set but intersecting it at 67.5 degrees. This configurations resulted in a total of 21 internal intersections and 20 boundary intersections. The design details of this model are listed in Table 1.

The fracture system model was run at only one hydraulic gradient. Three tests were run using node #5 as the contaminant injection node (see Figure 2.3). Distilled water was

injected into nodes #1 through #9 (except #5) at exactly the same pressure as that of the solute injection node to insure a similar flow rate in all fractures. It is noted that the node next to #14 was plugged with cement during the construction phase and therefore the flow rates were somewhat different in the fractures directly connected to this node.

The photographic enlargement in Figure 2.4 shows that the cutting process produced a surface with a very low relative roughness and a sharp, well defined fracture intersection. When all of the fractures had been cut into each base plate, the saw cuts were thoroughly cleaned to remove any pieces of plexiglass sawdust, and all traces of the oil base cutting fluid. The cover plate was then applied.

## 2.2 TESTING PROCEDURE

The first twelve physical models were tested by injecting a solution of potassium iodide, with a concentration of about 100 mg/L into one fracture segment and distilled water at the same hydraulic pressure into one of the other fracture segments. When the model was completely flushed with fresh solution, a sample of the discharge from the remaining fracture segments was collected. From inflow and outflow measurements the volume of distilled water used and the

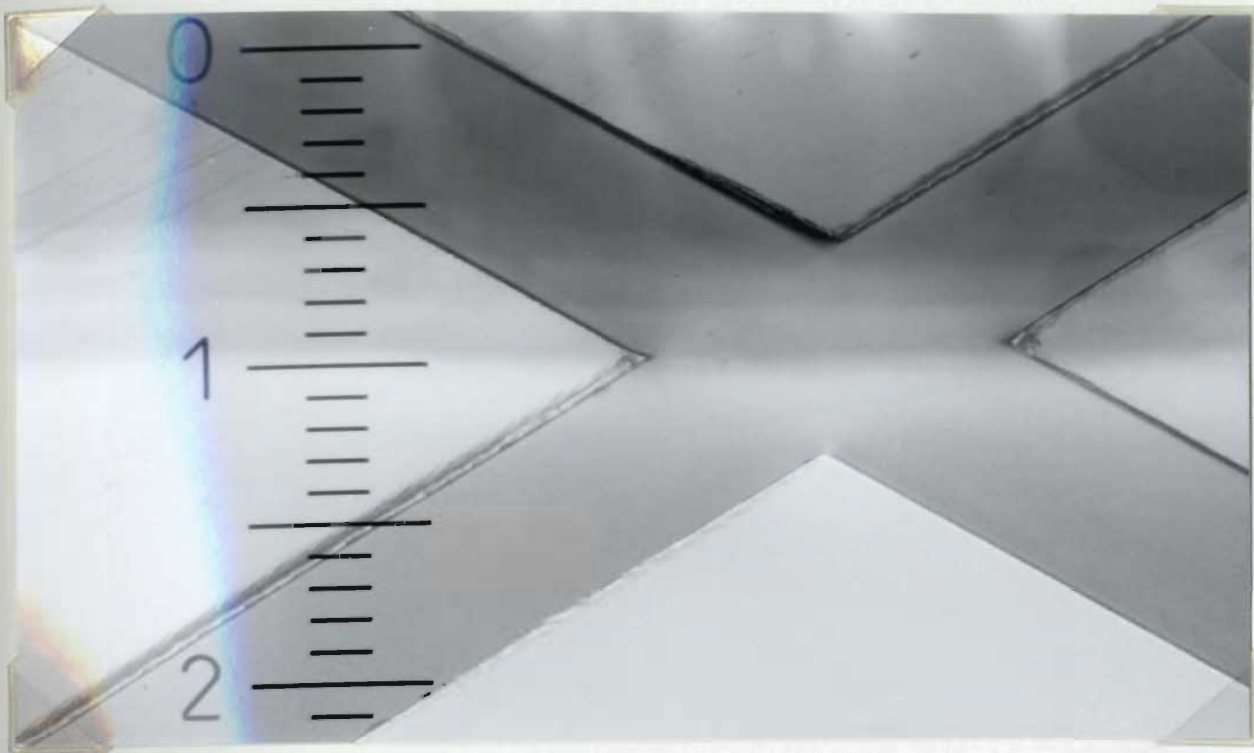


Figure 2.4 Enlargement of typical saw cut, viewed looking down into the fracture (Scale shown in mm).

velocity of flow in each fracture segment were calculated. A single junction reference electrode and an Orion iodide electrode connected to a Radiometer pH meter were used. Readings were recorded in mV and converted to mg/L using the calibration curve.

The concentration of iodide in each of the outlet fractures was determined by injecting distilled water and the iodide solution into ports 1 and 2, 1 and 3, and 1 and 4 (see Figure 2.1). All three possible conditions of intersection angle and aperture were tested. The mixing that occurs when two streams meet at 180 degrees was included in these tests.

This case, however, was thought to be trivial and is not reported in detail here. Each flow configuration of inlet and outlet ports (a setup) was tested three times at hydraulic gradients of 3.33, 1.67 and 0.33 and the results were averaged. Three hundred tests were run to determine the degree of mixing in all fourteen models.

The testing procedure used for the parallel flow model was similar to that described above except that only one inlet configuration was used. The same three hydraulic gradients were imposed. With reference to Figure 2.2, the iodide solution was injected at node 1, at a known flux, and the distilled water was introduced, at the same rate of flow, into node 2. Samples were obtained at nodes 3 and 4 and the same determinations were made as described for the previous 12 models. A sketch of the experimental setup is shown in Appendix A.

### 2.3 DETERMINATION OF PERCENT MIXING

A convenient definition for determining the percentage of mixing that takes place at fracture intersections is given by Krizek, et al (1972) as follows: "Complete mixing is characterized by the fact that all of the fluid mixture which leaves the intersection node has the same concentration." This definition of 100 percent mixing is illustrated in Figure 2.5a. Here a given volume of iodide solution,  $V_s$ , of

concentration  $C$  flows through fracture segment 1 and enters the intersection. At the same time a volume of distilled water,  $V_w$ , flows through fracture segment 2 and also enters the intersection. The two fluids are assumed to mix at the intersection node and the mixture is discharged through fracture segments 3 and 4. If it is assumed that 100 percent mixing occurs, then the ratio of the component volumes of distilled water to iodide solution, in both discharge segments 3 and 4, must be equal to  $V_s/V_w$ . This ratio, therefore, is characteristic of 100 percent mixing.

Figure 2.5(b) illustrates the case where less than 100 percent mixing occurs. In segment 3, in order to calculate the actual percentage of mixing that has occurred, the ratio,  $V_{s3}/V_{w3}$ , must be compared to the ratio  $V_s/V_w$ , resulting in

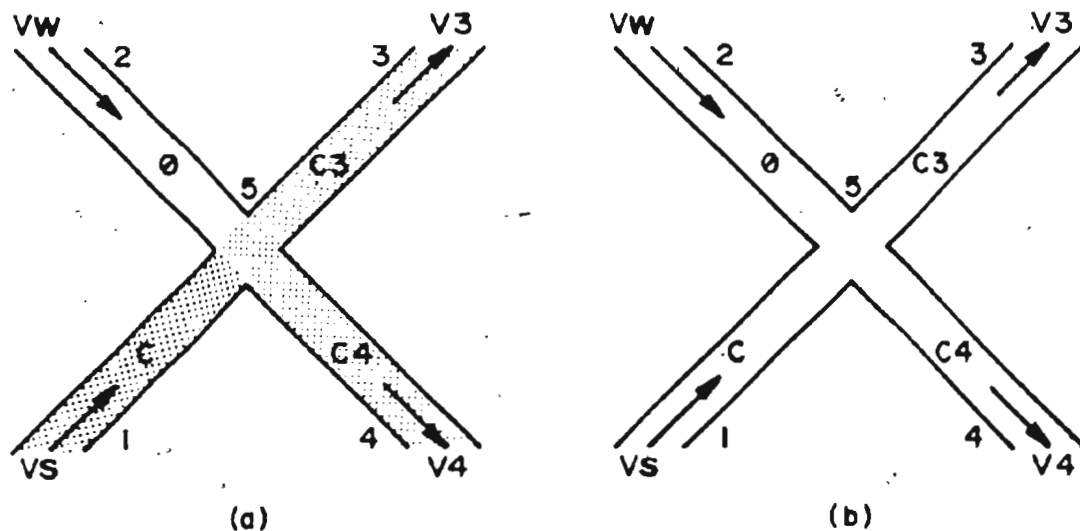


Figure 2.5 Schematic of (a) 100 percent mixing and (b) less than 100 percent mixing at the intersection node.

the following equation:

$$M3 = \frac{Vs3/Vw3}{Vs/Vw} 100 \quad (2.1)$$

where M3 is the percentage of mixing in fracture segment 3.

In order to determine the percentage of mixing in segment 4 it is necessary to invert the ratios of the volumes as follows:

$$M4 = \frac{Vw4/Vs4}{Vw/Vs} 100 \quad (2.2)$$

where M4 is the percentage of mixing in fracture segment 4. To understand why this inversion is necessary, consider the following set of hypothetical data:

Vw = 1.3 L  
Vs = 0.7 L  
Vw3 = 0.7 L  
Vs3 = 0.0 L  
Vw4 = 0.6 L  
Vs4 = 0.7 L

Applying Equation (2.1) would give the following:

$$M3 = \frac{0.0/0.7}{0.7/1.3} 100 = \frac{0.0}{0.54} 100 = 0.0$$

This gives us the correct value of 0 percent but if the same ratios were used in Equation (2.2) we would get the following value:



$$M4 = \frac{0.7/0.6}{0.7/1.3} 100 = \frac{1.17}{0.54} 100 = 216.7$$

This value of 216% is clearly in error, however if we invert the ratios as in Equation (2.2) we have:

$$M4 = \frac{0.6/0.7}{1.3/0.7} 100 = \frac{0.86}{1.86} 100 = 46.2$$

This value of 46.2% is the correct value of mixing in segment 4.

In order to apply Equations (2.1) and (2.2) the component volumes of distilled water and iodine solution in each fracture segment must be determined. The fundamental relationships are given below:

$$C_i = \frac{V_{si} C}{V_{si} + V_{wi}} \quad (2.3)$$

$$V_i = V_{si} + V_{wi} \quad (2.4)$$

where C is the initial concentration, in mg/L, of injected iodide solution,  $C_i$  is the concentration in the  $i$ th fracture segment,  $V_i$  is the total volume of solution passing through the  $i$ th fracture segment and  $V_{si}$  and  $V_{wi}$  are as defined above for the  $i$ th fracture. Rearranging and substituting (2.4) into (2.3) we have:

$$C_i = \frac{(V_i - V_{wi}) C}{V_i}$$

Solving for  $V_{wi}$  we have:

$$V_{wi} = \frac{V_i (C - C_i)}{C} \quad (2.5)$$

And then the value for  $V_{si}$  is simply:

$$V_{si} = V_i - V_{wi} \quad (2.6)$$

Once the component volumes of the influent streams in each effluent stream are determined by use of Equations (2.5) and (2.6), Equations (2.1) and (2.2) can be applied specifically to the discharge segments in the appropriate form as follows:

$$M_3 = 100 \frac{V_{s3}/V_{w3}}{V_s/V_w} \quad (2.7)$$

$$M_4 = 100 \frac{V_{w4}/V_{s4}}{V_w/V_s} \quad (2.8)$$

From mass balance considerations it is apparent that there will be a certain percentage of mixing when the hydraulic properties of the fracture segments are unequal. When the intersecting fractures have unequal apertures and the iodide solution enters one of these fractures and distilled water the other, the flow configuration at the

intersection will force some of the larger volume to mix with the smaller volume (See Figure 2.6).

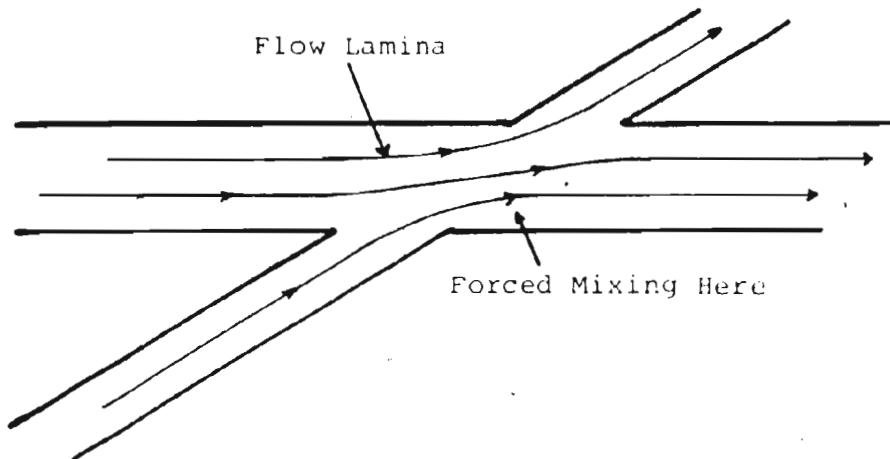


Figure 2.6 Schematic flow diagram for forced mixing

The mixing that results from this simple mechanism, will be referred to as "forced mixing". While more prominent in the unequal aperture models, the fact that each model differs slightly due to construction techniques means that in each model some percentage of the mixing that takes place is forced mixing. The percentage of mixing that is not forced is determined from the following equation:

$$M_i' = TM_i - FM_i \quad (2.9)$$

where  $M_i'$  is the adjusted mixing value for discharge  $i$ ,  $TM_i$  is the total mixing value determined and  $FM_i$  is the forced mixing value.  $FM_i$  is determined from the following equation:

$$FM_i = 100 \frac{V_{si}/V_{wi}}{V_s/V_w} \quad (2.10)$$

where  $V_{wi}$  is the volume of distilled water forced into discharge fracture segment  $i$ . The ratio terms on the right hand side of Equation (2.10) must, of course, be inverted for the same reasons as outlined for Equations (2.1) and (2.2). The test results and error values for models one through thirteen are listed in Appendix A. The results for model fourteen are listed in Table 5.

## 2.4 MIXING TEST RESULTS

It is noted that when Equation (2.9) is used some of the adjusted mixing values are negative. This is thought to reflect small measurement errors in both the fracture apertures and the determination of iodide concentration in the discharge streams. When negative mixing values were obtained it was assumed that no mixing took place and the adjusted mixing values were given a value of 0.0%. This appears to be a reasonable assumption since the negative values obtained were small.

The accuracy of the mixing results was determined by examining the mass balance of the flow system. The percentage difference between the amount of iodide flowing into the

model and that flowing out was attributed to measurement errors. It was assumed that no reaction took place and there was no change in storage in the model. These values were calculated by use of the following equation:

$$E = 100 \frac{\text{abs}[(V_s C) - (V_3 C_3) - (V_4 C_4)]}{V_s C} \quad (2.11)$$

where E is the percent error, abs is the absolute value of the expression and V<sub>3</sub>, C<sub>3</sub>, V<sub>4</sub>, C<sub>4</sub> are as defined in Figure 2.5. The significance of E is illustrated by varying the value of V<sub>3</sub>, C<sub>3</sub>, V<sub>4</sub>, and C<sub>4</sub>. When one of these variables is changed enough to cause a change in percent mixing of 0.5 percent, E changes about 5.0 percent. Most of the error values listed in Appendix A were less than 10 percent.

The mixing values, and the adjusted mixing values are listed in Appendix A. All the negative adjusted mixing results are given a value of 0.0 percent as noted above. For comparison purposes, the **actual** component volumes of iodide solution and distilled water, and those that would result from 100 percent mixing, are also listed in Appendix A. A diagram of the experimental setup and the calculations that were used to determine these results are also presented in Appendix A. For the purposes of discussion, the averages of the three adjusted mixing values that were obtained, for each

of the testing configurations, are listed in Table 2.

## 2.5 DISCUSSION

It is apparent from the Figures 2:8 - 2.10 that very little mixing takes place. Considerably more mixing occurs when the two inlet fractures intersect at 180 degrees, however, the possibility of this happening in nature is remote.

Table 2: Average Adjusted Mixing Values

	Apertures of .5mm			Apertures of .36mm & .5mm			Apertures of .28mm & .5mm		
Grad	3.3	1.6	0.3	3.3	1.6	0.3	3.3	1.6	0.3
Angle	Percent mixing			Percent Mixing			Percent Mixing		
22.5	4.5	2.3	0.0	NA	NA	NA	1.8	0.7	1.3
45.0	1.0	9.2	4.9	1.9	1.9	0.4	0.6	0.3	0.4
67.5	6.9	5.2	1.4	2.8	2.1	1.1	7.4	2.5	0.7
90.0	5.7	4.6	2.3	3.7	4.1	0.2	15.4	7.0	3.9
112.5	5.2	6.1	1.9	1.7	1.0	0.7	14.0	10.4	3.8
135.0	1.0	0.9	1.7	1.8	2.0	0.9	2.1	1.1	0.7
157.5	0.7	1.2	0.5	NA	NA	NA	0.8	0.6	0.1

NA - Data not available

Table 2 indicates three minor trends in the results: 1) In general, less mixing was observed in all models when the lower gradients were imposed, 2) Less mixing was observed in

the models with unequal fracture apertures and, 3) It was observed that the highest mixing values occurred where the fractures intersected at the middle angle of 67.5 - 112.5 degrees and the lowest values occurred at the smallest and largest intersection angles tested (i.e., 22.5 - 67.5 degrees and 112.5 - 157.5 degrees). How real these trends are is not certain since the total amount of mixing is so small. For example, the overall average adjusted mixing percentage is less than 3%. This is considered to be within the range of error expected in the testing procedure.

The results of testing models thirteen and fourteen appear to support the above findings. In the first of these models, when two streams, one of solute and one of distilled water, were forced to flow together in the same fracture over a length of 15 cm (as in model thirteen), only an average of 13.2 percent mixing was observed. This is considered to be within the range of error that can be expected in the model. In model fourteen, as is shown in Table 5, little mixing occurred, although the solute was forced to encounter six intersections while traversing the model. It may be concluded, on the basis of these tests, that no mixing occurs at fracture intersections except that which is forced to take place due to the flow differential that may exist in the two intersecting fractures.

## CHAPTER THREE

### COMPUTER MODELING

#### 3.1 INTRODUCTION

The transport of solute species in fractured media has been investigated by a number of workers (see Section 1.3) using both numerical and analytical procedures. Because of the limitations of initial and boundary conditions, analytical solutions are restricted in their application to the simpler fracture geometries and flow boundary conditions (Noorishad and Mehran, 1982). Numerical solutions, on the other hand, are subject to computational round off errors because of the iterative calculations that they require (Rasmuson and Neretnieks, 1981). Oscillations of the concentration profile are more severe where the transport is dominated by advection (Huyakorn and Pinder, 1983). Advective transport is dominant in fractured media and therefore the problem is acute in fractured systems especially when using the standard Galerkin finite element method (Huyakorn, 1977). To avoid this problem Hwang and Cho (1984) have developed an eigenvalue method which is exact in time and allows the solute concentration at any node to be calculated at any given instant with a direct computation. More recently Hwang et. al. (1985) have developed a finite



analytic numerical solution which uses local analytic solutions to generate the matrix coefficients. Another approach is that of (Huyakorn and Nilkuha, 1979) who have used upstream weighing functions to reduce the oscillation of the concentration profile in the finite element formulation. Noorishad and Mehran (1982) have shown how these functions can be applied in an efficient finite element model of transport in fractured media. The main advantage to their use is that accurate solutions of the nodal concentration can be obtained without having to use an overly fine mesh and small time steps while retaining the flexibility that is inherent with the finite element method.

In this study the weighing functions developed by Huyakorn and Nilkuha, (1979) are used in a finite element model to investigate the pattern of contaminant transport in two-dimensional fracture systems of various geometry. In this model, the individual fractures are treated discretely as a mesh of one-dimensional line elements. It was assumed that the fracture walls are parallel plates in which no adsorption or chemical reaction takes place. The contaminant is assumed to be conservative and to have a density equal to that of water. The movement of the contaminant is assumed to be by advection and longitudinal dispersion only.

In order to simulate the geometry of real fracture sets,

the two dimensional fracture network was generated using the program "NETWRK" (Rouleau, 1984). This program also models the fracture network in a discrete fashion as a mesh of one-dimensional line elements. The velocity of flow in each of the fractures of this network was calculated using the program "NETFLO" (Rouleau, 1984).

The fortran program, EXPORT, is a finite element model, which was written for this study to simulate the transport of a solute through a fracture system. It was designed to reflect the findings of the mixing tests that were reported in section 3. In this model it is assumed that no mixing occurs at the fracture intersections unless the flow rates in the elements are different. When this is the case forced mixing, as defined above, is assumed to take place.

In the following sections the two programs NETWRK and NETFLO are described; the upstream weighing functions are discussed; the transport model, EXPORT; is developed and explained and the results of this model are compared to those of the analytical solution given by Ogata and Banks (1961).

### **3.2 FRACTURE NETWORK AND FLOW GENERATION**

The fracture network generation code, NETWRK, developed by Rouleau (1985) uses a Monte Carlo approach to generate a

pattern of lines of specified length and orientation. Figures 4.5 and 4.10 are examples of a rectangular and a circular boundary pattern respectively. Each of the lines in the figure represents the trace of a fracture, of unit depth, that is exposed on the planar surface of a rock. The apertures of the fractures are specified or selected, by NETWRK, from a given distribution and assigned to each line. The code NETWRK executes the following sequence of operations:

1. reading of input data,
2. generation of a line pattern,
3. computation of spacing values (optional),
4. location of all the effective intersections in the network, ie. that are part of a continuous flow path,
5. generation of a plotting file (optional),
6. definition of the elements, ie. every line segment between two consecutive effective intersections and
7. recording the node numbers that identify each element.

The input data for the program is of two types. One describes the geometry of the fracture pattern and the other is related to the geometry of the boundary.

The code NETFLO is a finite element model that simulates the steady state flow that takes place in a discrete two dimensional, random fracture network generated by the code NETWRK. In the simulation, the matrix is assumed to be impermeable. The model calculates the hydraulic head at each node by solving the simultaneous equations which can be written for each node (ie. the sum of the flow rates at any

node must equal zero). Once the equations for each element are written, the corresponding matrix equations are solved for hydraulic head using the Choleski algorithm. The hydraulic head is used to calculate, the flow rate in every segment using the cubic law for fluid flow between two smooth parallel plates which is written as:

$$q = \frac{w^3 \delta}{12\mu} I \quad (3.1)$$

where  $q$  is the Darcy velocity per unit cross sectional area,  $w$  is the plate separation or aperture,  $\delta$  is the weight density of the fluid,  $\mu$  is the dynamic viscosity and  $I$  is the hydraulic gradient.

The code NETWRK was altered slightly, for this study, in order to output the data file needed to simulate solute transport in the network.

### 3.3 UPSTREAM WEIGHTED FINITE ELEMENT FORMULATION

When the Galerkin finite element method is used to solve the advective-dispersive transport equation, it exhibits considerable oscillatory behaviour and/or excessive numerical dispersion near the concentration front (Huyakorn, 1977). The intensity of such errors increases with the dominance of the advective term and is exhibited in overshoot and under-

shoot. These are the erroneously high and low values of concentration encountered upstream of the front. When severe enough these errors can prevent convergence of the solution scheme.

The cause of this behaviour, according to Pinder and Gray (1977), is the inability of the numerical approximation to propagate, accurately, short wavelength harmonics of the Fourier series. It has been determined that where linear basis functions are used, the oscillation can be virtually eliminated if the value of the Peclet number does not exceed 2.0. The local element Peclet number ( $Pe$ ) is defined as  $Pe = V \cdot L / D$ , where  $V$  is the velocity of flow,  $L$  is the element length and  $D$  is the dispersion coefficient. Normally  $Pe$  is reduced by selecting sufficiently small element lengths. This adjustment however, in large fracture systems, would be prohibitive in both computer time and the amount of computer memory that is needed. In order to avoid this difficulty an upstream weighted finite element technique is used in this study.

The finite element model for the above transport problem is developed using the method of weighted residuals. We state first the one dimensional differential equation for advective-dispersive transport of a conservative solute which is written as follows:

$$\frac{\partial C}{\partial t} = D \frac{\partial^2 C}{\partial x^2} - \frac{\partial}{\partial x} (vC) \quad (3.2)$$

where  $C$  is the concentration,  $t$  is the time,  $D$  is the dispersion coefficient,  $x$  is the distance along the fracture, and  $v$  is the average velocity of flow. In this study the concentration is defined as  $C/C_0$ , where  $C$  is the actual concentration of solute and  $C_0$  is the initial concentration of solute. The trial solution for  $C$  is written as:

$$\zeta = \sum_{i=1}^n C_i(t) N_i(x) \quad (3.3)$$

where  $\zeta$  is the approximate value of  $C$ ,  $n$  is the number of nodes ( $n=2$ , for the one dimensional line element) and  $N_i$  denotes the standard basis functions. With the Galerkin method a set of weighting functions,  $W_i$ , is defined which are identical to the basis functions. For the upstream method the weighting functions are different from the basis functions. Now weighting the spatial derivative terms with the asymmetric upstream weighting functions,  $W_i$  and the remaining terms with the standard basis functions,  $N_i$  and substituting the trial solution for  $C$ , we have:

$$W_i \left( D \frac{\partial^2 \zeta}{\partial x^2} - \frac{\partial}{\partial x} (v_1 \zeta) \right) - N_i \frac{\partial \zeta}{\partial t} = 0 \quad (3.4)$$

In order to minimize the residuals in the estimate of  $C$  we require that the integration of this equation over the problem domain be zero. This is shown in the next equation:

$$\int_R w_i \left[ D \frac{\partial^2 \zeta}{\partial x^2} - \frac{\partial}{\partial x} (v_i \zeta) \right] dR - \int_R N_i \frac{\partial \zeta}{\partial t} dR = 0 \quad (3.5)$$

where  $R$  is the problem domain. We now integrate by parts to reduce the second order derivative as follows:

$$\begin{aligned} \int_R \frac{\partial w_i}{\partial x} \left[ D \frac{\partial \zeta}{\partial x} - v_i \zeta \right] dR + \int_R N_i \frac{\partial \zeta}{\partial t} dR \\ - \int_b w_i D \frac{\partial \zeta}{\partial x} n_i db + \int_b w_i \zeta v_i n_i db = 0 \quad (3.6) \end{aligned}$$

where  $b$  is the boundary of the solution domain and  $n_i$  is the outward normal vector on the boundary. Substitution of Equation (3.3) into the first two terms of Equation (3.6) yields:

$$\begin{aligned} \int_R \left[ D \frac{\partial w_i}{\partial x} \frac{\partial N_j}{\partial x} - v_i \frac{\partial w_i}{\partial x} N_j \right] C_j dR \\ + \int_R N_i N_j \frac{\partial C_j}{\partial t} dR \end{aligned}$$

$$- \int_b w_i D \frac{\partial C}{\partial x} n_i db + \int_b w_i C v_i n_i db = 0 \quad (3.7)$$

The equation in matrix form is as follows:

$$[R]\{C\} + [S] \frac{\partial \{C\}}{\partial t} + [F] = 0 \quad (3.8)$$

where  $[R]$ ,  $[S]$  and  $[F]$  are the diffusion-advection, storage, and source matrices respectively and defined by the first, second and third lines of Equation (3.7). The source matrix is equal to 0 at all nodes except where the solute is injected where it equals  $q_i C_i$ ;  $q_i$  is the flux at node  $i$ .

Time integration of Equation (3.8) is done by the mid-difference finite difference scheme. In this method the values of the unknown are assumed to vary linearly with time in the time interval  $dt$ . The resulting recurrence formula, as given by Norishad et. al (1982), is of the form:

$$\left[ \frac{2}{dt} [S] + [R] \right] \{C\}_{t+dt/2} - \frac{2}{dt} [S]\{C\}_t + [F] = 0 \quad (3.9)$$

where  $\{C\}_{t+dt} = 2\{C\}_{t+dt/2} - \{C\}_t$ .



In order to evaluate Equation (3.9) the basis and weighting functions must be defined. The linear basis functions  $N_j$  are illustrated in Figure 3.1(a) and given below.

$$N_1 = 1 - \frac{x}{L} \quad (3.10)$$

$$\frac{dN_1}{dx} = -\frac{1}{L} \quad (3.11)$$

$$N_2 = \frac{x}{L} \quad (3.12)$$

$$\frac{dN_2}{dx} = \frac{1}{L} \quad (3.13)$$

The upstream weighting functions,  $w_i$  are defined by Huyakorn and Nilkuha (1979) as follows:

$$w_1 = \frac{1}{4} [(1 + \Phi)(3\alpha\Phi - 3\alpha - 2) + 4] \quad (3.14)$$

$$w_2 = \frac{1}{4} [(1 + \Phi)(-3\alpha\Phi + 2)] \quad (3.15)$$

where  $\Phi$  is a local iso-parametric co-ordinate and  $\alpha$  is the upstream parameter associated with the element.

The derivatives of these functions are as follows:

$$\frac{dw_1}{dx} = -\frac{1}{L} + 3\alpha \left( \frac{2x}{L^2} - \frac{1}{L} \right) \quad (3.16)$$

$$\frac{dw_2}{dx} = \frac{1}{L} - 3\alpha \left( \frac{2x}{L^2} - \frac{1}{L} \right) \quad (3.17)$$

where  $L$  is the element length.

If  $\alpha$  is greater than or equal to 1 then the formulation will be unconditionally stable (Huyakorn, 1977). The expression for the optimum value for  $\alpha$  is given by Christie et. al. (1976) as:

$$\alpha_{\text{opt}} = \coth \left[ \frac{vL}{2D} \right] - \frac{2D}{vL} \quad (3.18)$$

For a value of  $\alpha = 1$  these weighting functions are depicted in Figure 3.1(b). When the derivatives of the weighting functions and the value of  $v$  are substituted, and the appropriate integration completed we have the individual elemental matrices as given by Noorishad and Mehran (1982):

$$[R^{\text{fe}}] = \frac{D}{L} \begin{bmatrix} 1 & -1 \\ -1 & 1 \end{bmatrix} + \frac{v}{2} \begin{bmatrix} -(1 - \alpha) & (1 - \alpha) \\ -(1 + \alpha) & (1 + \alpha) \end{bmatrix} \quad (3.19)$$

$$[S^{\text{fe}}] = \frac{L}{6} \begin{bmatrix} (2 - \alpha/4) & (1 - \alpha/4) \\ (1 + \alpha/4) & (2 + \alpha/4) \end{bmatrix} \frac{2}{dt} \quad (3.20)$$

$$[F] = vc \quad (\text{for each input node}) \quad (3.21)$$

When we specify a certain concentration at the inflow boundary or at certain nodes along a boundary the nodes



Figure 3.1(a) Linear element basis functions and (b) Upstream weighing functions for  $\alpha = 1$ . (After Huyakorn and Pinder, 1983)

involved are said to be constrained. These nodes do not change during the simulation except in the case of discontinuous sources. All other nodes are said to be free nodes because it is at these points that the concentration is determined. To reduce the size of the matrices and thus conserve computer time the constrained nodes are partitioned out of the solution in the following manner. Allowing the subscript c to denote a constrained condition, f to denote a free condition and letting  $[A] = [S] + [R]$  we write Equation (3.9) again as:

$$\begin{bmatrix} A_{cc} & | & A_{cf} \\ \hline A_{fc} & | & A_{ff} \end{bmatrix} \begin{Bmatrix} C_c \\ C_f t + dt/2 \end{Bmatrix} = \begin{bmatrix} S_{cc} & | & S_{cf} \\ \hline S_{fc} & | & S_{ff} \end{bmatrix} \begin{Bmatrix} C_c \\ C_f t \end{Bmatrix} - \begin{Bmatrix} F_c \\ F_f \end{Bmatrix} \quad (3.22)$$

Equation (3.22) implies the following relationship when  $F_f$  is equal to 0:

$$[A_{fc}] \{C_c\}_{t+dt/2} + [A_{ff}] \{C_f\}_{t+dt/2} = [S_{fc}] \{C_c\}_t + [S_{ff}] \{C_f\}_t \quad (3.23)$$

For continuous injection of solute  $\{C_c\}_{t+dt/2}$  and  $\{C_c\}_t$  are equal to 1.0,  $[A_{fc}]$  and  $[S_{fc}]$  have only one entry per row, and Equation (3.23) further reduces to:

$$[A_{ff}] \{C_f\}_{t+dt/2} = [S_{fc}] + [S_{ff}] \{C_f\}_t - [A_{fc}] \quad (3.24)$$

To further simplify the expression it is noted that all the terms on the right hand side of Equation (3.24) have the same dimensions (since the matrix  $[S_{fc}]$  becomes a vector when multiplied by  $\{C_c\}$ ) and therefore can be combined into a single vector,  $\{B\}$ . Thus we have finally:

$$[A_{ff}] \{C_f\}_{t+dt/2} = \{B\}_t \quad (3.25)$$

where

$$\{C_f\}_{t+dt} = 2\{C_f\}_{t+dt/2} - \{C_f\}_t$$

If the injection of solute is discontinuous then the terms  $\{C_c\}_{t+dt/2}$  and  $\{C_c\}_t$  become equal to 0.0 and  $\{B\}_t$  can be defined as follows:

$$\{B\}_t = [S_{ff}] \{C_f\}_t$$

The program EXPORT, which is described in the next

section, solves Equation (3.25) for a specified injection time. The longhand solution to an example problem is given in Appendix B.

### 3.4 EXPORT - A FINITE ELEMENT TRANSPORT MODEL

#### 3.4.1 The Main Program

The FORTRAN program EXPORT has been written to execute the mathematical operations described in the preceding section as illustrated in the example in Appendix B. The flow chart for EXPORT is shown in Figure 3.2. EXPORT begins by declaring the size and type of the arrays and the type of variables that are used in the main program and the various subroutines.

The next step is the opening of the five input and output files. The first file is "element.dat" which is generated by the program NETFLO (Rouleau, 1985). This file contains all the information concerning the fracture network. The second file, "nodconc.dat" contains all intermediate matrix calculations and concentration values. The present version has commented out most of the references to this file in order to conserve computer memory. The third file is "choice.dat", contains the control parameters for each simulation. The fourth file is "brkthr.dat". It contains an unformatted listing of the concentration at

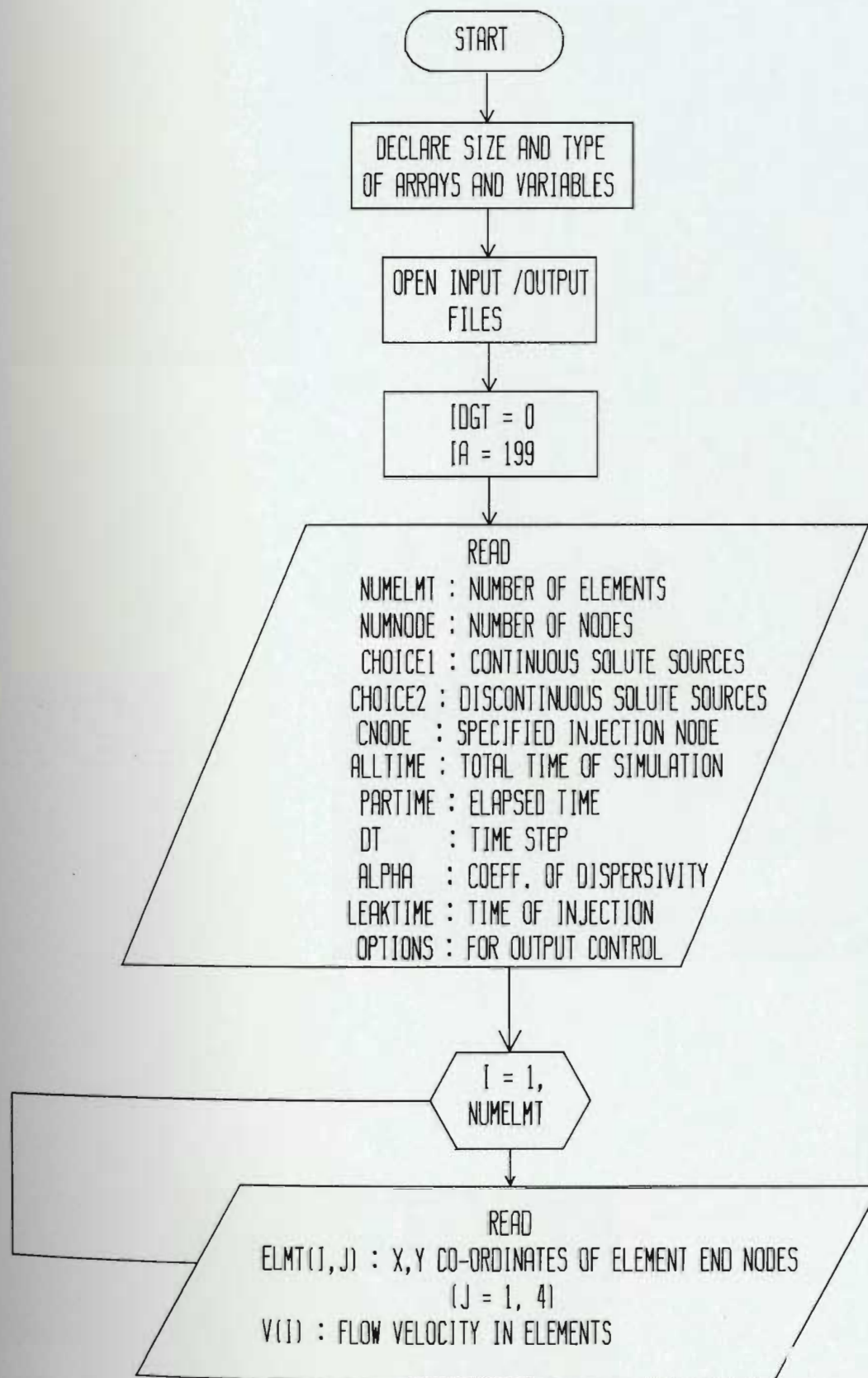


Figure 3.2 Flow chart of main program in the code EXPORT

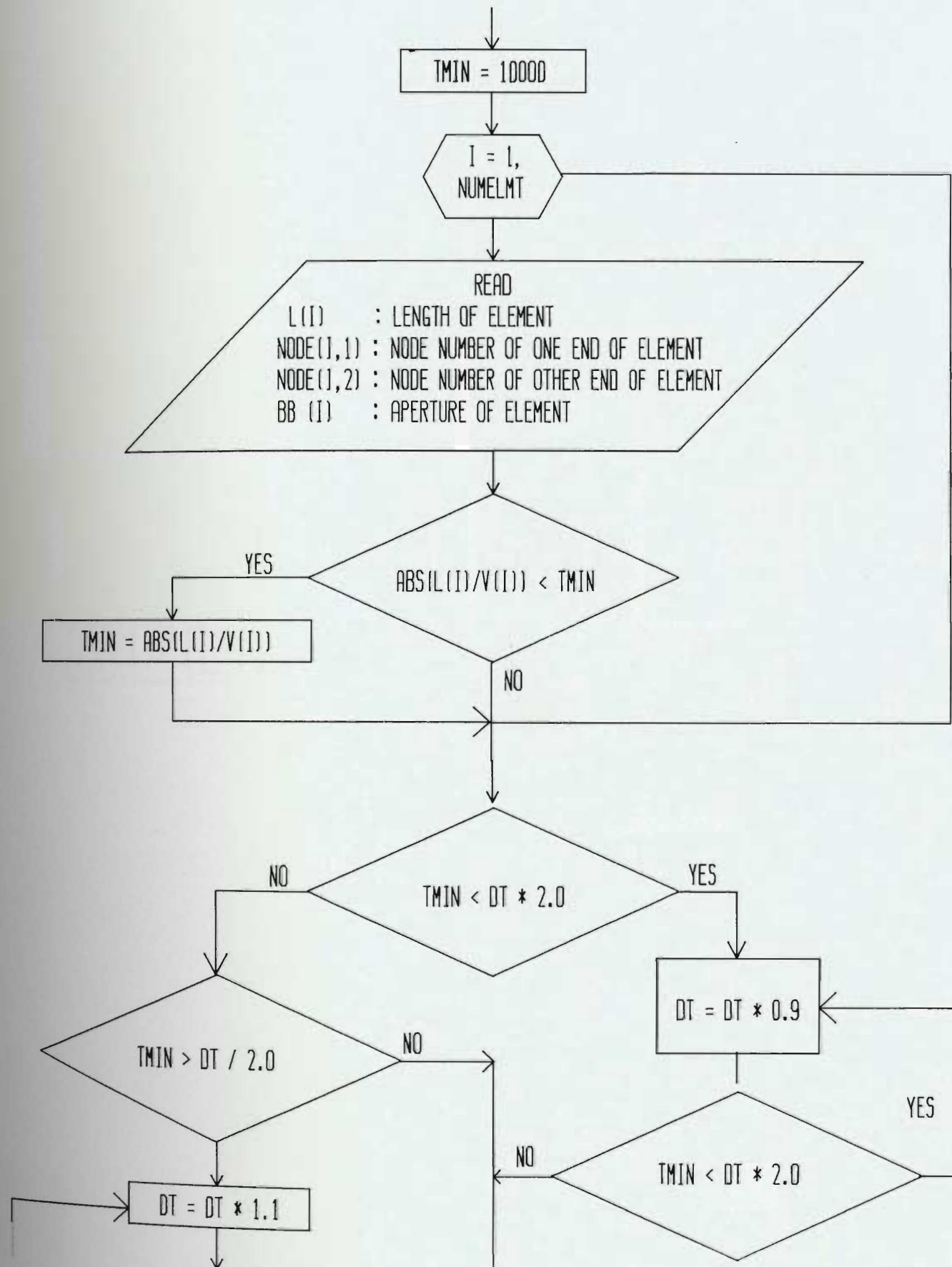


Figure 3.2 (continued) Flow chart of main program in the code EXPORT

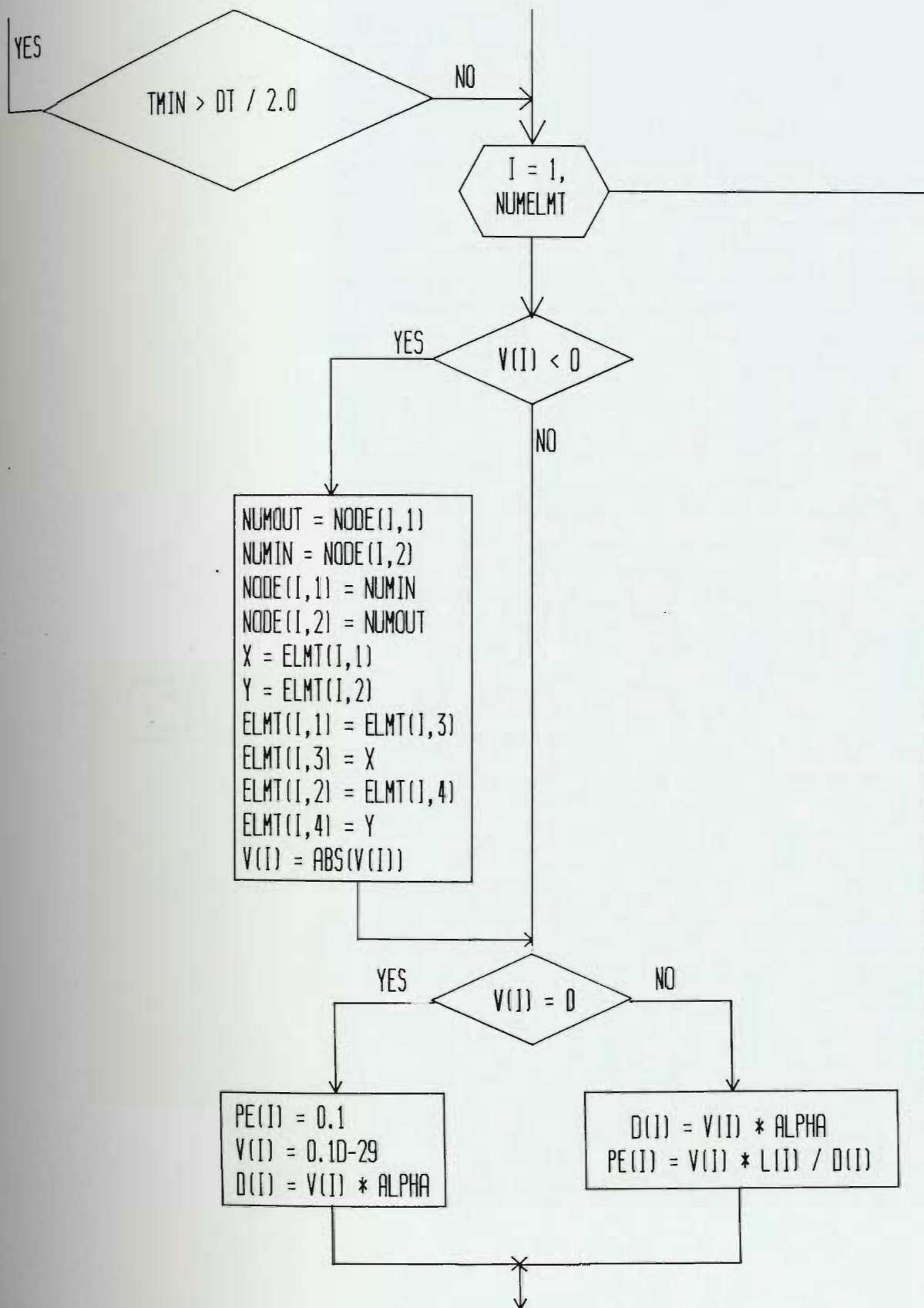


Figure 3.2 (continued) Flow chart of main program in the code EXPORT



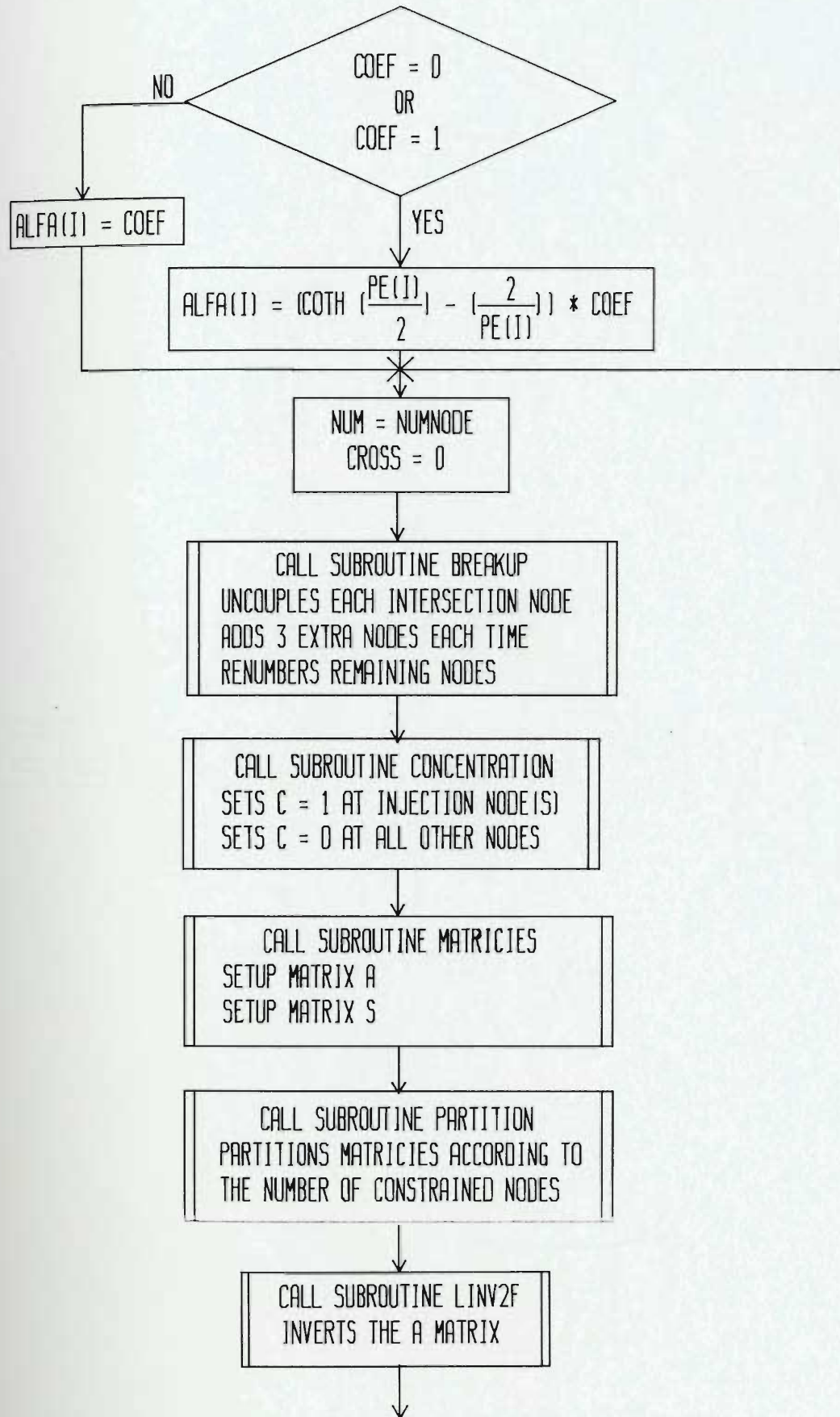


Figure 3.2 (continued) Flow chart of main program in the code EXPORT

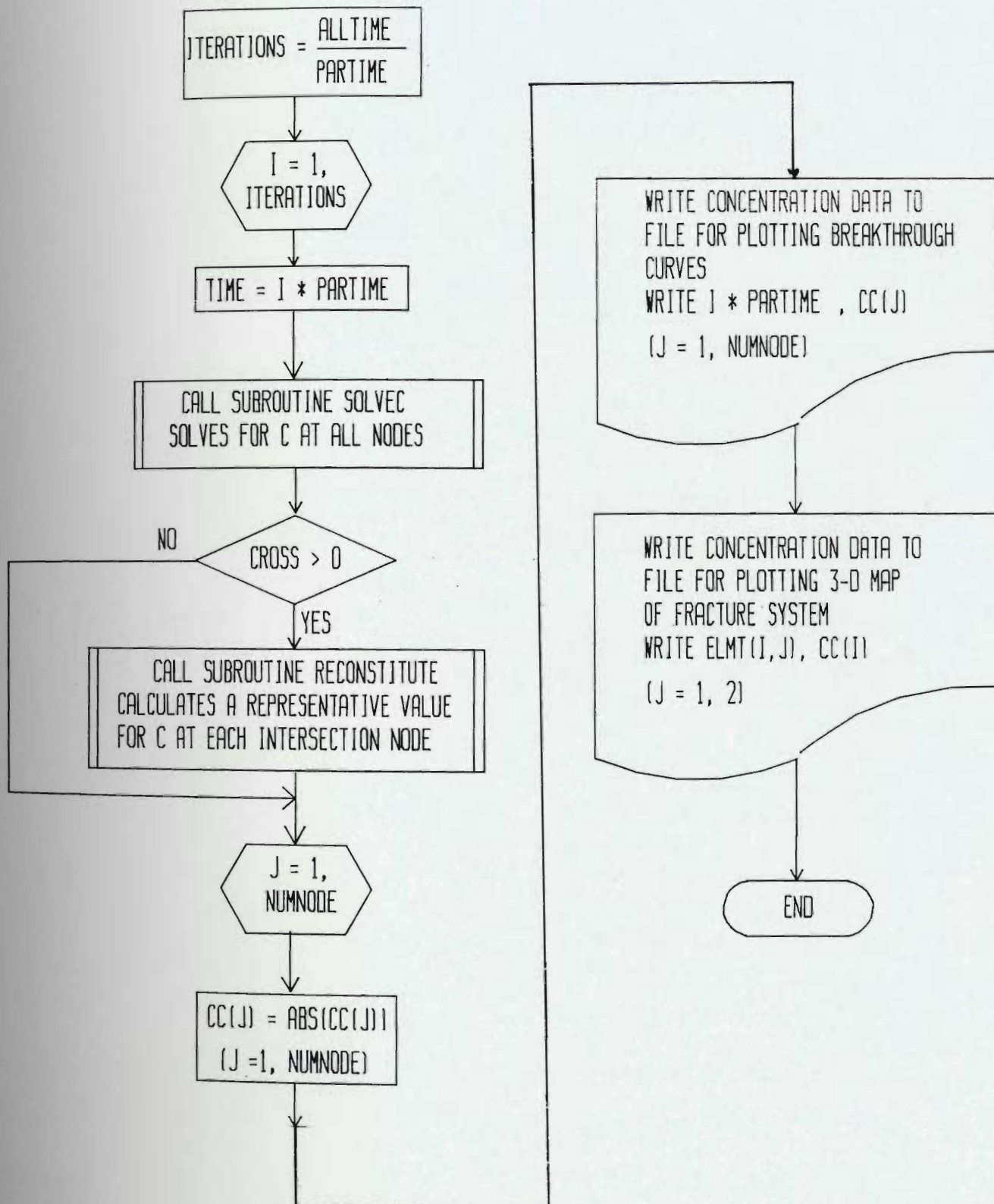


Figure 3.2 (continued) Flow chart of main program in the code EXPORT

each node at the specified time. This fourth file is designed to be read directly into a spreadsheet program on a micro computer for plotting the breakthrough curves at specified nodes. The last file "3-d.dat" contains the co-ordinates of each node and the concentration at that node at the end of the simulation. This file is used by the plotting program to produce a plot file for a 3-D plot of the concentration at each node.

To begin execution, EXPORT reads the control parameters and the fracture information in choice.dat and element.dat. The form and content of choice.dat and element.dat are shown in Tables 3 and 4 respectively. The first two control parameters specify the physical nature of the solute source. They indicate a continuous (c) or discontinuous (d) source

Table 3: Control file "choice.dat"

choicel =	c	(19x,a)
choice2 =	n	(19x,a)
cnode =	4	(11x,i10)
alltime =	10	(11x,i10)
partime =	1	(11x,i10)
dt =	0.400000d+00	(11x,d12.6)
alpha =	0.500000D-01	(11x,d12.6)
coef =	0.000000D+00	(11x,d12.6)
leaktime=	0.000000D+00	(11x,d12.6)
options =	y n y n n n n	(11x,7(a,4x))

and whether the solute is introduced at one node (n), at a boundary (b) or at a specified node on a circular or other

type of boundary (c). If the latter type of boundary is specified then the node is given by the next parameter, cnode. The next three parameters specify the time components of the calculation, namely the total simulation time, the elapsed time at which the concentration values are printed to a file, and finally the initial value of the time step. This value can be adjusted so that solute does not flow further than the length of the shortest element in less than one time step. The next three parameters are the coefficient of dispersion, the upstream weighing coefficient and the injection time to be used if discontinuous sources are simulated. The format for this file is given on the right side of the table.

The last record contains a yes or a no (y/n) and directs EXPORT to implement the following work according to the control variables that take on the y/n value. These character variables are as follows:

- 1) brk - do you want to use the BREAKUP subroutine?
- 2) bkth - Do you want to output concentration data for breakthrough curves?
- 3) pr3\_d- Do you want to output concentration data for the 3D plot?
- 4) prn1 - Do you want to output general element data for verification?
- 5) prn2 - Do you want to output the matrix values?
- 6) prn3 - Do you want to output concentration values inreadable form?
- 7) dtad - Do you want automatic adjustment to the initial dt value?

The first two parameters in element.dat are specified by the program NETFLO and indicate the number of effective elements and the number of effective nodes that are in the system under investigation. Following these are a list of the co-ordinates of the element ends and the flow velocity for each element. Lastly length, the end node numbers and the aperture of each element is listed.

It is a requirement of the upstream finite element scheme that the sign of the velocity be the same as that of the damping factor (Huyakorn, 1977). It is evident, however, from Equation (3.18) that no matter what sign velocity has, the sign of the damping factor will be positive. This is because the sign of the dispersivity coefficient is the same as that of the velocity. When velocity is negative, greater weighing will be given to the downstream end of the element which will tend to cause oscillation. To ensure that this situation does not occur, EXPORT takes each element with negative velocity and exchanges the node numbers and the end node co-ordinates. When this has been done the sign of the velocity is made positive. At the same stage, the Peclet number is calculated.

Once the preliminary assignment statements are made EXPORT calls the subroutine BREAKUP which uncouples the element mesh at all four way intersections so that the

Table 4: Fracture information file "element.dat"

```

numelmt =      10
numnode =      11
0.000D+00  0.100D+00  0.500D+00  0.100D+00  0.50D+00
0.500D+00  0.100D+00  0.100D+01  0.100D+00  0.50D+00
0.100D+01  0.100D+00  0.150D+01  0.100D+00  0.50D+00
0.150D+01  0.100D+00  0.200D+01  0.100D+00  0.50D+00
0.200D+01  0.100D+00  0.250D+01  0.100D+00  0.50D+00
0.250D+01  0.100D+00  0.300D+01  0.100D+00  0.50D+00
0.300D+01  0.100D+00  0.350D+01  0.100D+00  0.50D+00
0.350D+01  0.100D+00  0.400D+01  0.100D+00  0.50D+00
0.400D+01  0.100D+00  0.450D+01  0.100D+00  0.50D+00
0.450D+01  0.100D+00  0.500D+01  0.100D+00  0.50D+00
0.500D+00      1      2  0.100D-03
0.500D+00      2      3  0.100D-03
0.500D+00      3      4  0.100D-03
0.500D+00      4      5  0.100D-03
0.500D+00      5      6  0.100D-03
0.500D+00      6      7  0.100D-03
0.500D+00      7      8  0.100D-03
0.500D+00      8      9  0.100D-03
0.500D+00      9     10  0.100D-03

```

\* This Table does not show the real format of ELEMENT.DAT. The format used is as follows: For the first two records (11x,i10); For the next numelmt records (1x,5(d14.6)); For the last numnode records (1x,d15.7 ,2i10,d15.7)..

correct mixing algorithm can be applied. If these intersections were not uncoupled then the model would solve for one concentration at the intersection node and each discharge fracture would receive the same concentration of solute. This would amount to perfect mixing which has been shown to be incorrect.

The next subroutine to be called is CONCENTRATION. This subroutine assigns a value of 1.0 to each of the source nodes as specified in the control parameters. All other nodes are

assigned a value of 0.0. Using all the information that has been assigned so far the matrix coefficients for the diffusion-advection, storage and source matrices, as defined in Equations (3.19) to (3.21), are assigned in the subroutine MATRICES. After this has been completed, the matrices are partitioned according to the constrained nodes as in Equation (3.23). The subroutine PARTITION is called to execute this step and also to assemble [B].

In order to solve Equation (3.25), [A] is inverted using the subroutine LINV2F from the IMSL library. Once [A] is inverted the times at which the concentration is required, are determined from the control parameters. For each time step the subroutine SOLVEC is called. This routine solves Equation (3.25) by an iterative time stepping procedure.

When the specified time for the output of the concentration values is reached the subroutine RECONSTITUTE is called. This routine calculates a representative concentration at each of the four way intersections and outputs all the concentration values for the original node numbers.

The complete listing for the main program EXPORT is in Appendix C. The subroutines that are called are described briefly in the following sections. The listings for these subroutines are also given in Appendix C.

### 3.4.2 Subroutine BREAKUP

This subroutine is central to the implementation of imperfect mixing as determined in the laboratory tests discussed in Chapter 2. The conclusion in that chapter was, that essentially, no mixing takes place at fracture intersections. The only exception was the mixing that is forced to take place due to different sized fractures as depicted in Figure 2.6. The normal finite element solution for transport solves for concentration at each node. This node is common to each of the discharge fractures that intersect it, thus, the same concentration of solute is used for each discharge fracture. The concentration leaving each node therefore is the same in each fracture. This is the perfect mixing model of Castillo et. al. (1972) and Smith et. al. (1985), which has been shown to be incorrect. In order to avoid this problem and still maintain the advantages of the finite element method, the four way nodes are uncoupled by assigning a new node number to the ends of those elements that meet at these intersections. When the new node numbers are added the number of nodes in the system increases by 3 for each intersection. The new total number of nodes is stored in the variable NUM. Although the mesh of line elements are still in contact geometrically, they are treated as if they were dead-end elements by the program so that the solute can be directed into the correct discharge fracture at the right



concentration. The flow chart for the subroutine BREAKUP is shown in Figure 3.3.

BREAKUP first finds each of the four way intersections in the mesh. At each such node it rennumbers the end node of three of the elements involved and leaves one with the original node number. This renumbering is ordered so that later subroutines can direct the solute to the correct fracture. The order is determined by the angle of intersection of the four elements. The results that are reported in Chapter 2 indicate that flow from a given inlet fracture is transferred to the outlet fracture having the smallest angle. This is illustrated in Figure 3.4. Solute entering the intersection from element 5 would be preferentially transferred to element 9. BREAKUP numbers the nodes (see Figure 3.4(b)) so that later subroutines will make this transfer in the correct manner.

In order to assign the concentration value to the correct node, as they were originally given by NETFLO, an array NODC, is setup to store the original number of all nodes and the number to which the node changes when new nodes are added.

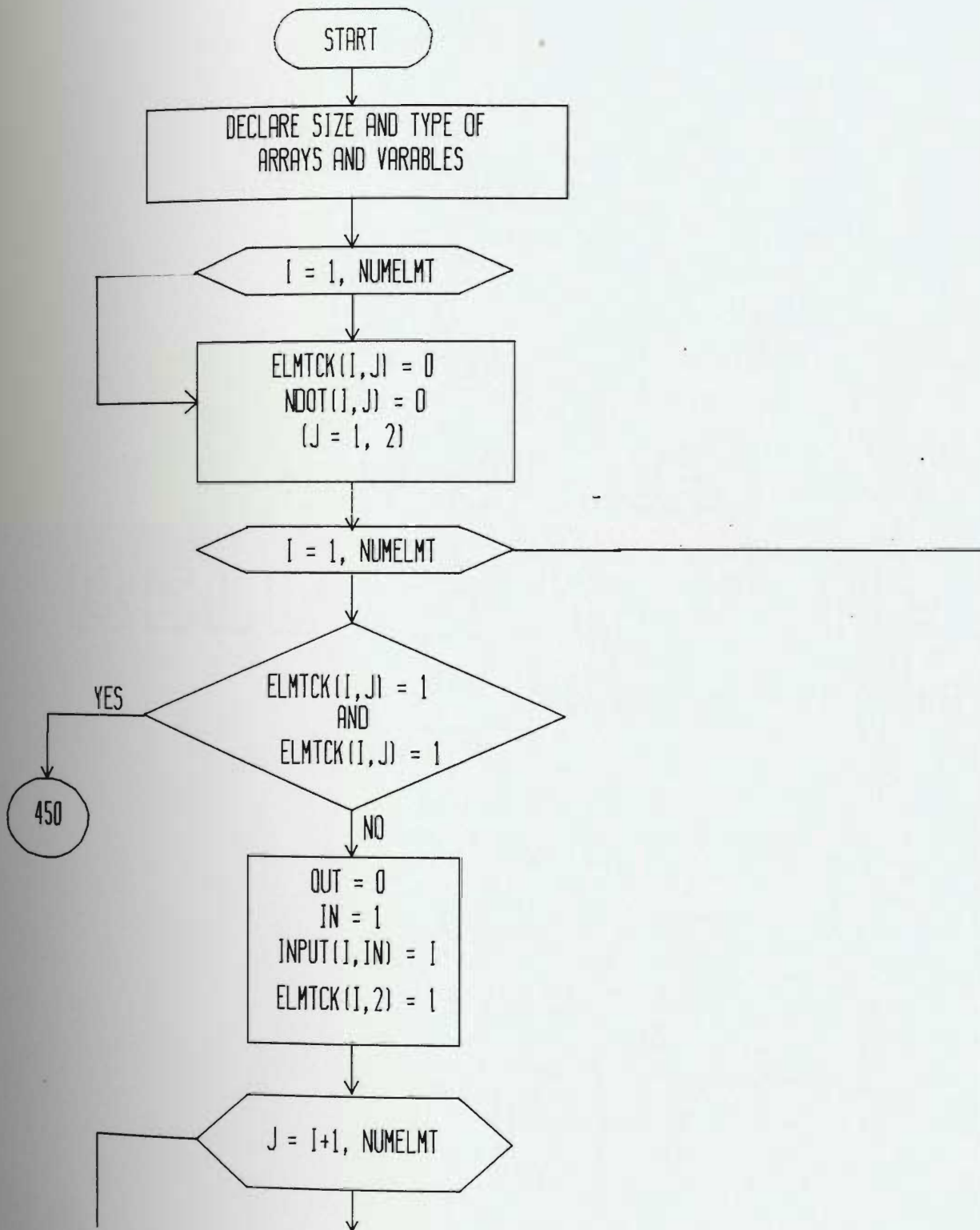


Figure 3.3 Flow chart of Subroutine BREAKUP

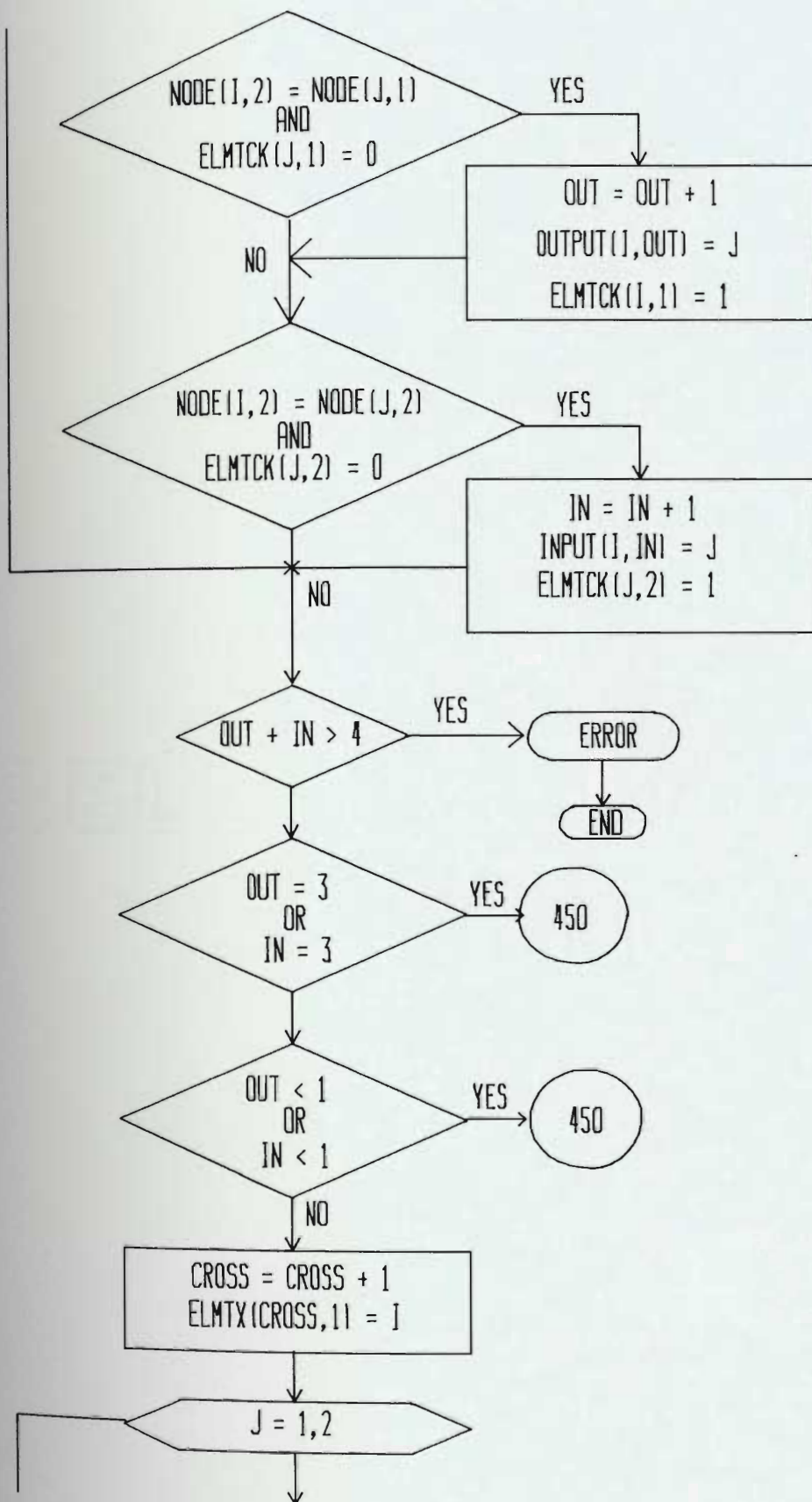


Figure 3.3 (continued) Flow chart of Subroutine BREAKUP

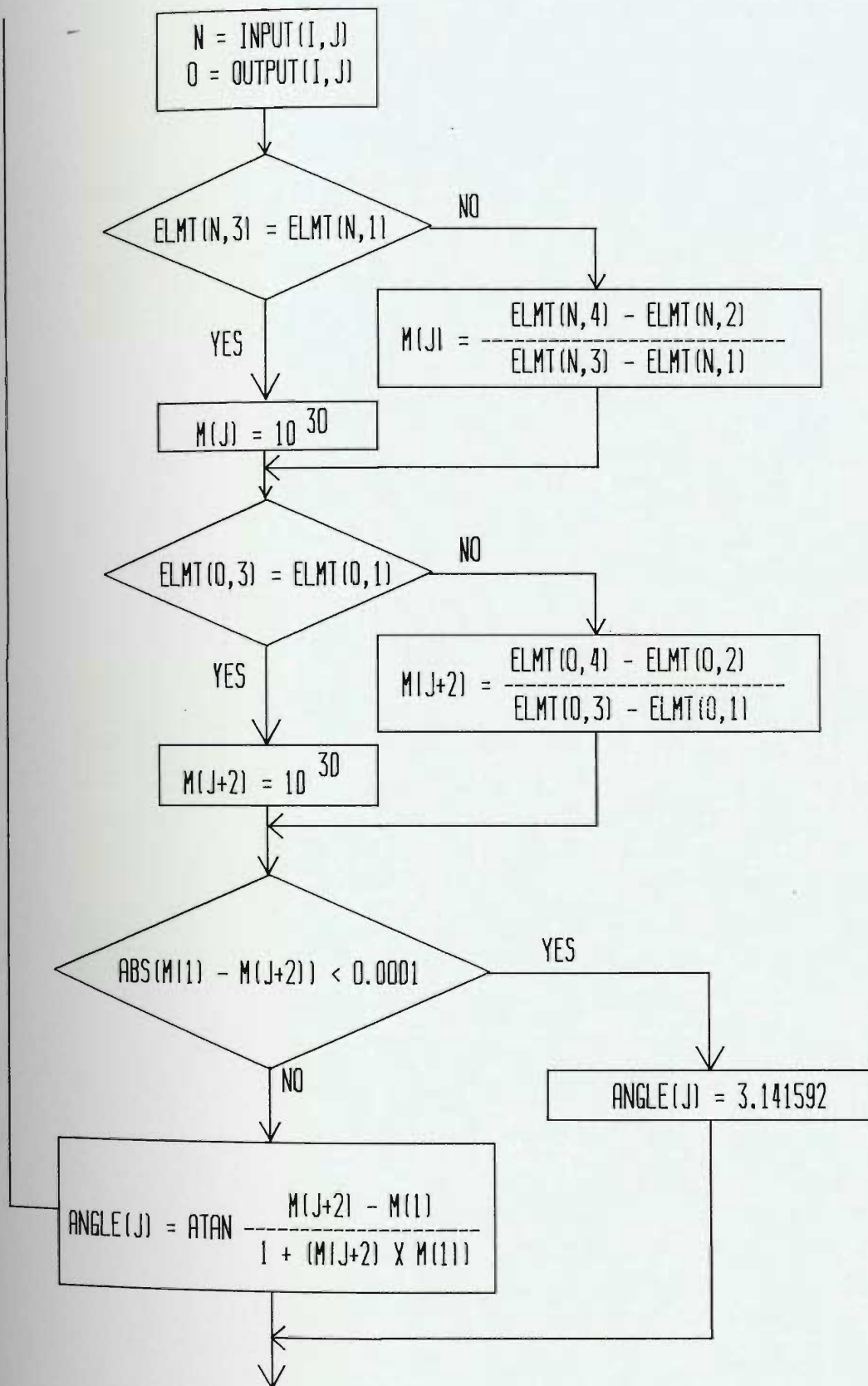


Figure 3.3 (continued) Flow chart of Subroutine BREAKUP

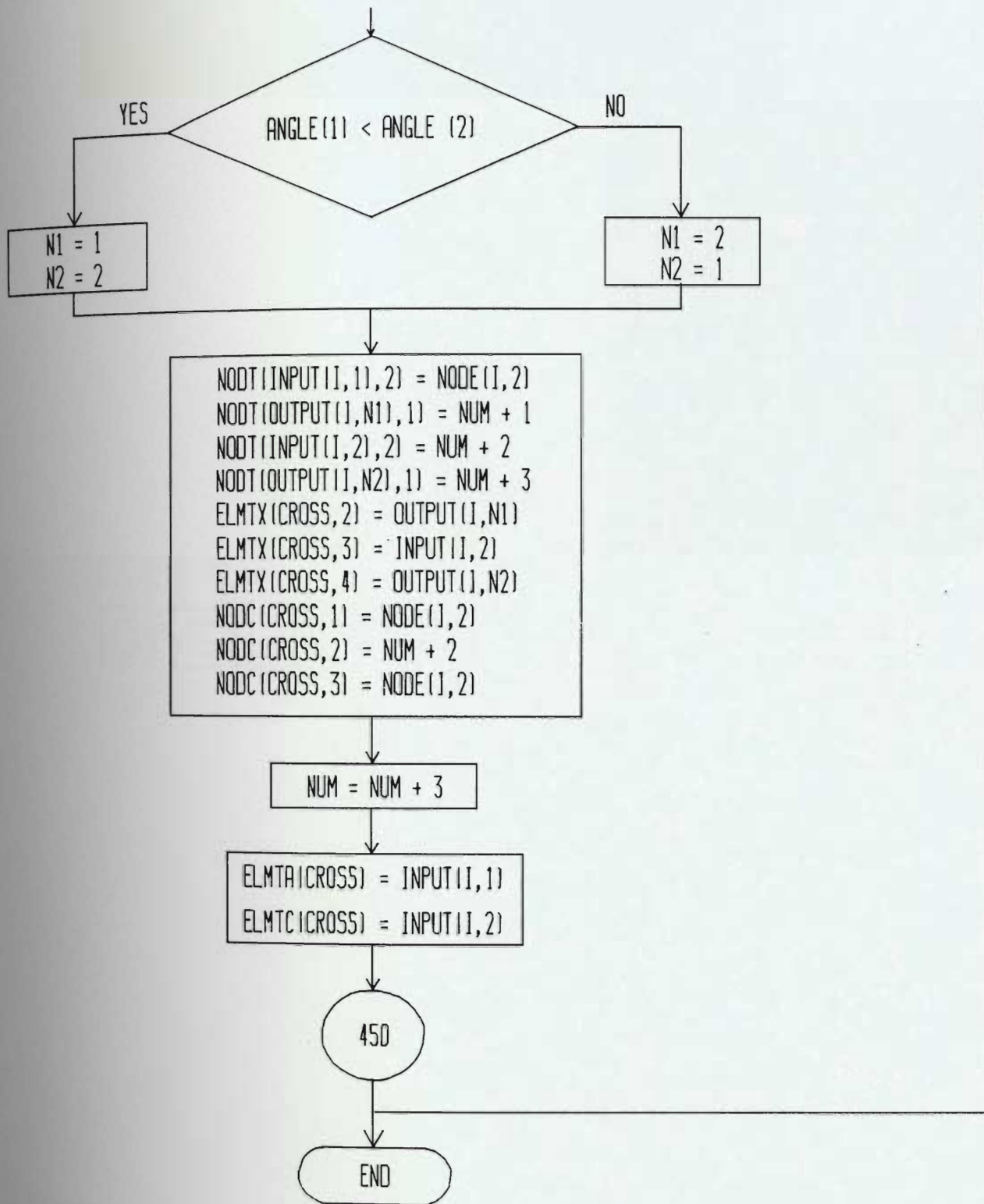


Figure 3.3 (continued) Flow chart of Subroutine BREAKUP

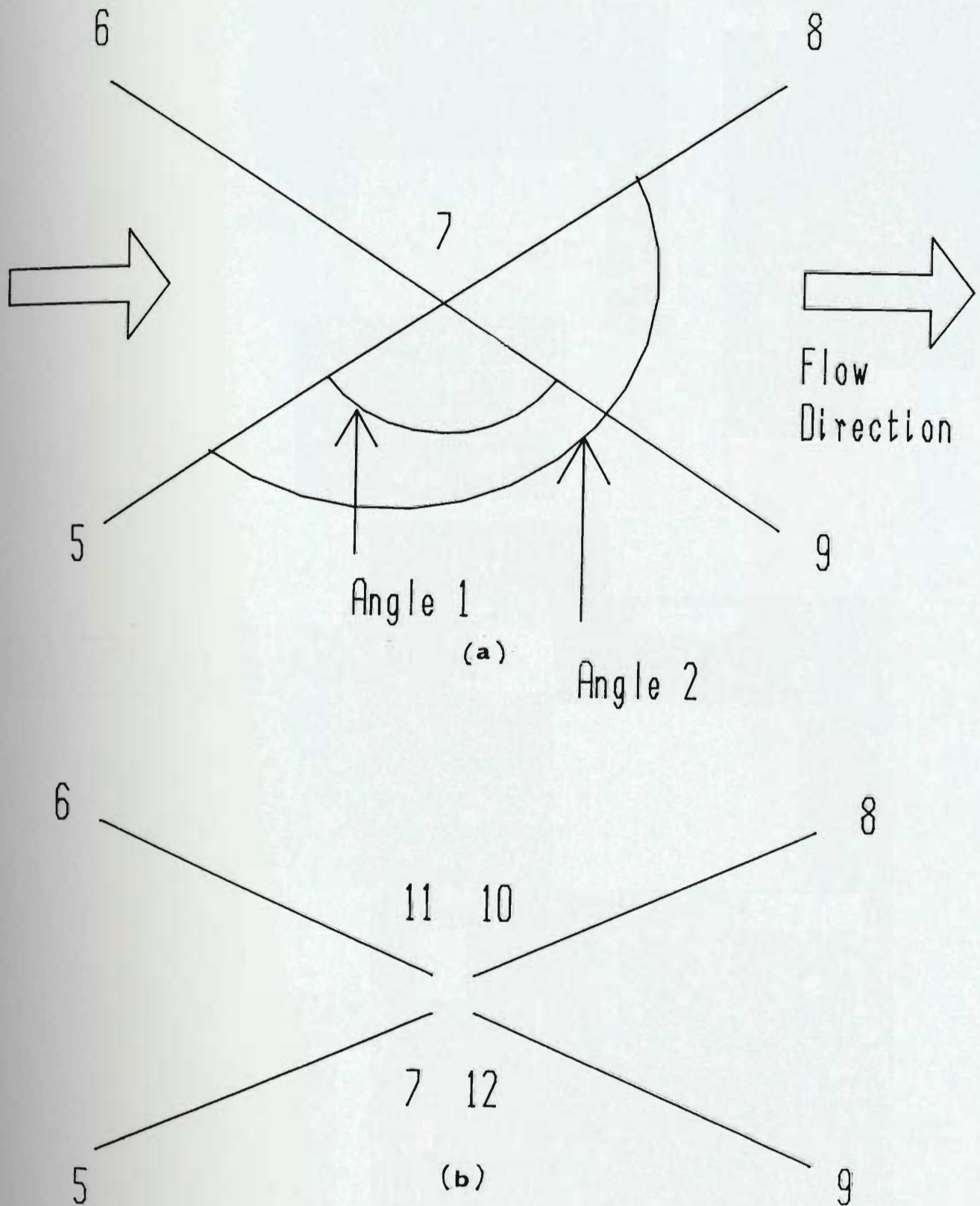


Figure 3.4 Four way fracture intersection showing (a) the angles that determine the direction of solute movement from inlet fractures to discharge fractures and (b) the renumbering of the intersection nodes.



#### 3.4.3 Subroutine CONCENTRATION

The initial values of concentration for each node are assigned by the subroutine CONCENTRATION and stored in (C). A value of one is assigned for each source node and a value of zero is assigned to all of the other nodes. The source nodes are specified by the control parameter CHOICE2. When CHOICE2 equals "b", all nodes lying on the left boundary are assigned a value of 1. When CHOICE2 equals "n" only the middle node on the left boundary is given a value of 1. The flow chart for CONCENTRATION is shown in Figure 3.5.

#### 3.4.4 Subroutines MATRICIES and PARTITION

The coefficients of the diffusion-advection and storage matrices are assigned by the subroutine MATRICIES. These values are stored in the [R] and [S] respectively. The routine uses Equations (3.19) and (3.20) to assemble the coefficients. Once they are assembled the coefficients of the [S] and [R] are added to make a new matrix [A]. When this has been done the subroutine PARTITION reduces the size of the arrays by partitioning all arrays according to the number of constrained nodes. The new reduced size of the partitioned matrices is assigned to the constant PSIZE.

The subroutine depends on the assigned value of concen

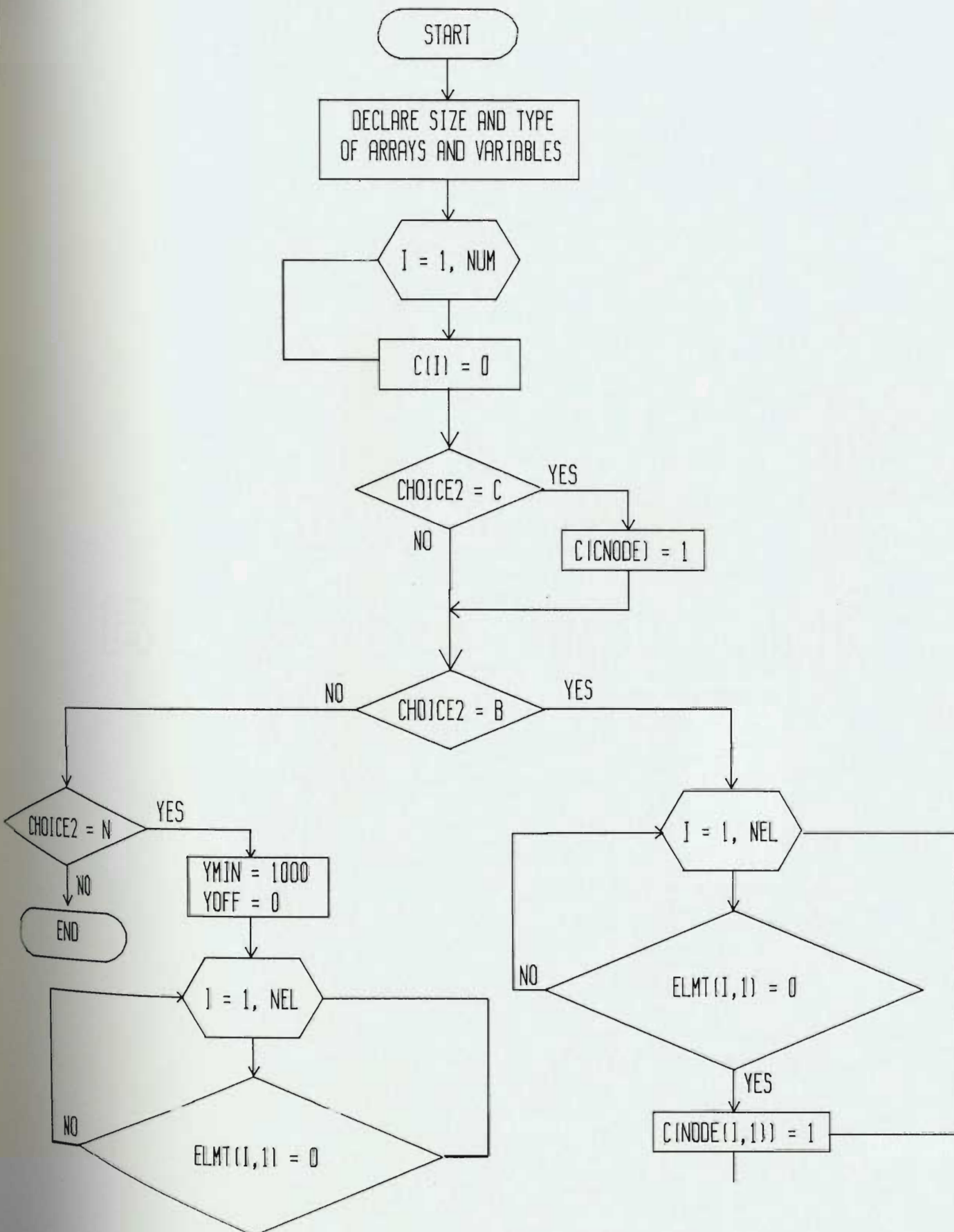


Figure 3.5 Flow chart of subroutine CONCENTRATION



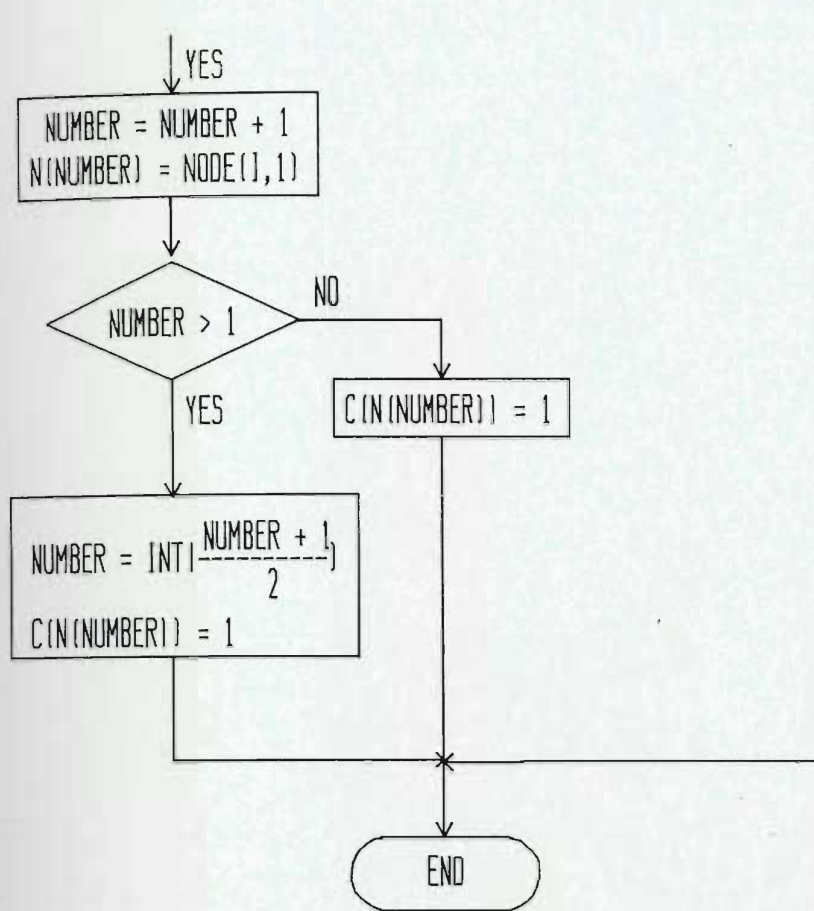


Figure 3.5 (continued) Flow chart of subroutine CONCENTRATION

tration (C) at each node, to determine if the node is free or not. Two arrays, KEEP and IGNORE, are used to store the node numbers of those nodes for which the corresponding value of C is 0 or 1 respectively. In addition to eliminating the constrained nodes from [R] and [S], the coefficients for the arrays [Afc] and [Sfc] are assembled and used in the solution of Equation (3.23). The flow chart for MATRICES is shown in Figure 3.6. The flow chart for PARTITION is shown in Figure 3.7.

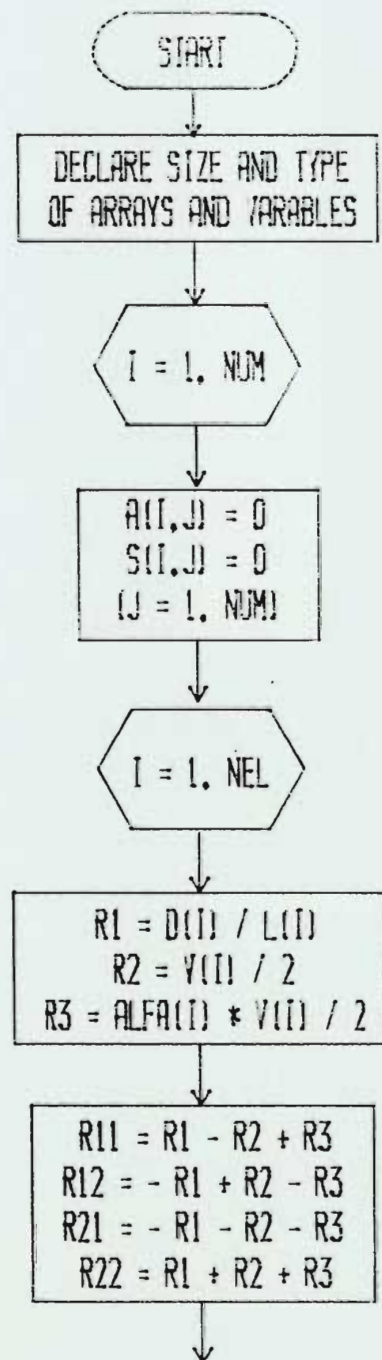


Figure 3.6 Flow chart for subroutine MATRICES

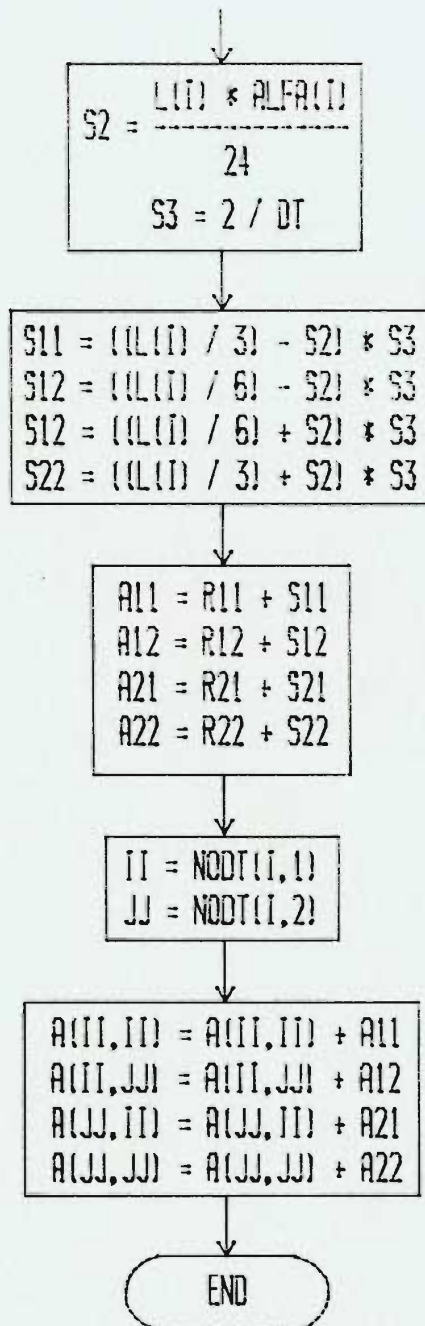


Figure 3.6 (continued) Flow chart for subroutine MATRICES

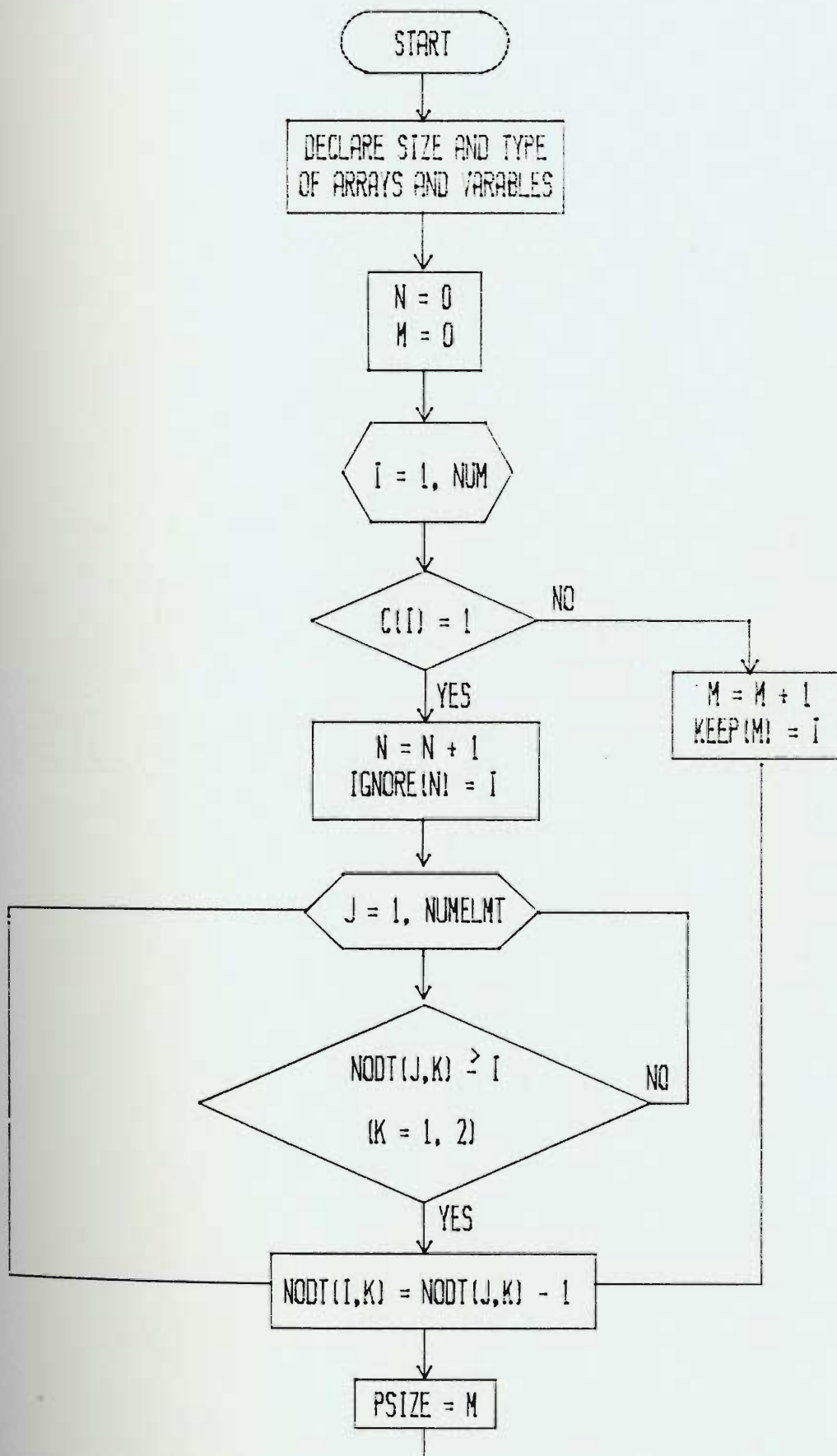


Figure 3.7 Flow chart for subroutine PARTITION

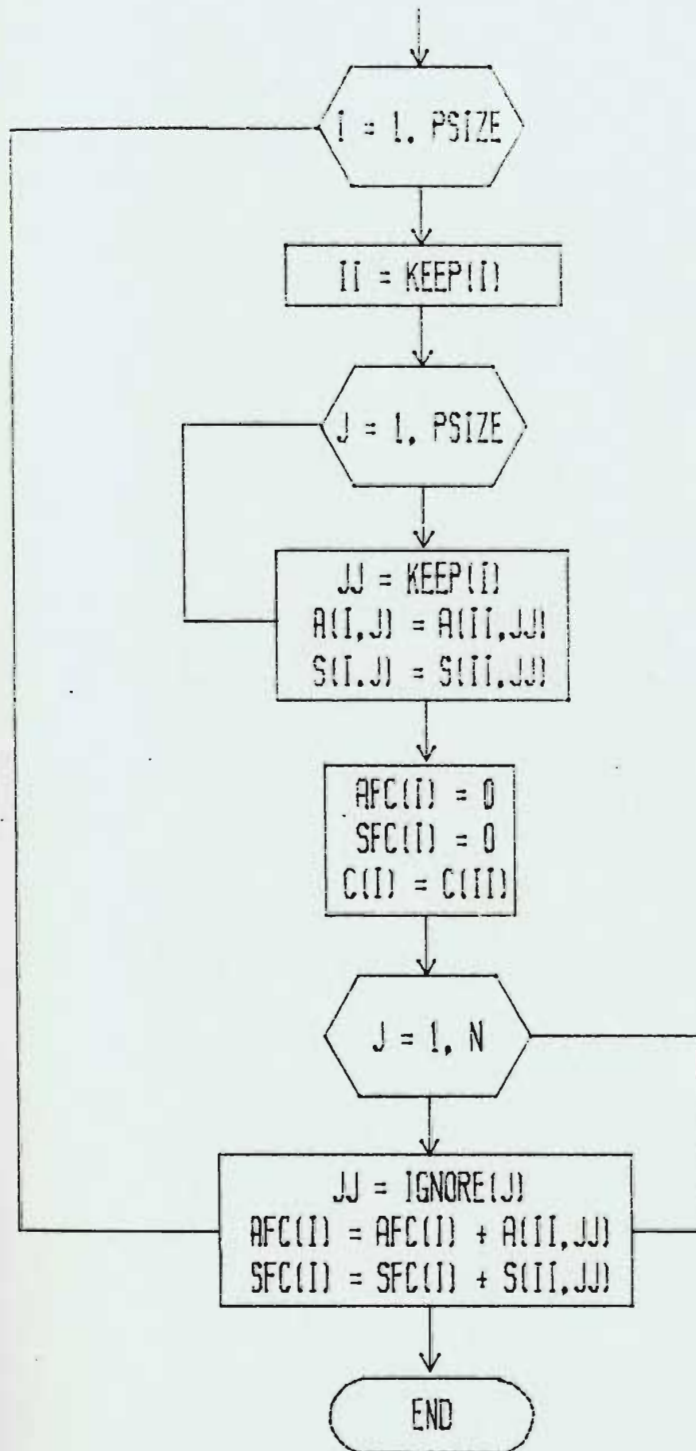


Figure 3.7 (continued) Flow chart for subroutine PARTITION

#### 3.4.5 Subroutines SOLVEC and RECONSTITUTE

The subroutine SOLVEC solves Equation (3.25) for the time as specified by the constant PARTIME. It does so in discreet steps as determined from the value of DT. For each time step, as the solution continues, the subroutine BRIDGIT is called to transfer the correct concentration of solute from the inlet fractures to the discharge fractures. This transfer takes into consideration the preferred route of solute movement as determined by subroutine BREAKUP and any forced mixing that takes place because of the variation in the size and flow rate of the fractures filling and draining the intersection.

In order to reduce the computation time, SOLVEC assembles [B] from the left hand side of Equation (3.23). It then calls the subroutine MULTIPLY which multiplies the [B] by the inverse of [A]. The number of times that this calculation is done is determined by the value of STEPS which equals PARTIME/DT. The flow chart for SOLVEC is shown in Figure 3.8. The flow charts for BRIDGIT and MULTIPLY are shown in Figures 3.9 and 3.10.

Before any concentration values can be output for plotting breakthrough curves and 3-D plots of the concentration distribution, a representative value must be determined

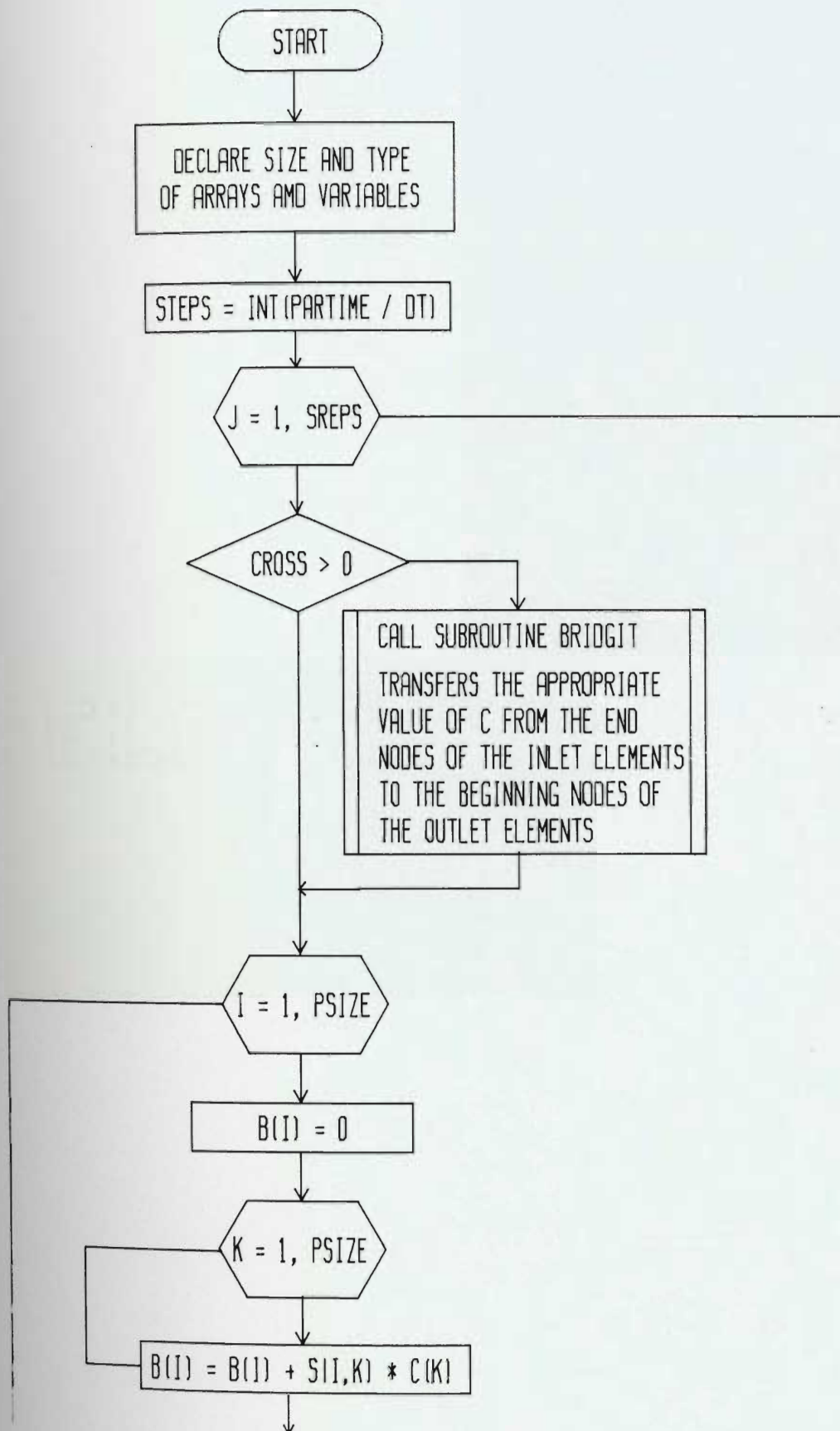


Figure 3.8 Flow chart for subroutine SOLVEC.



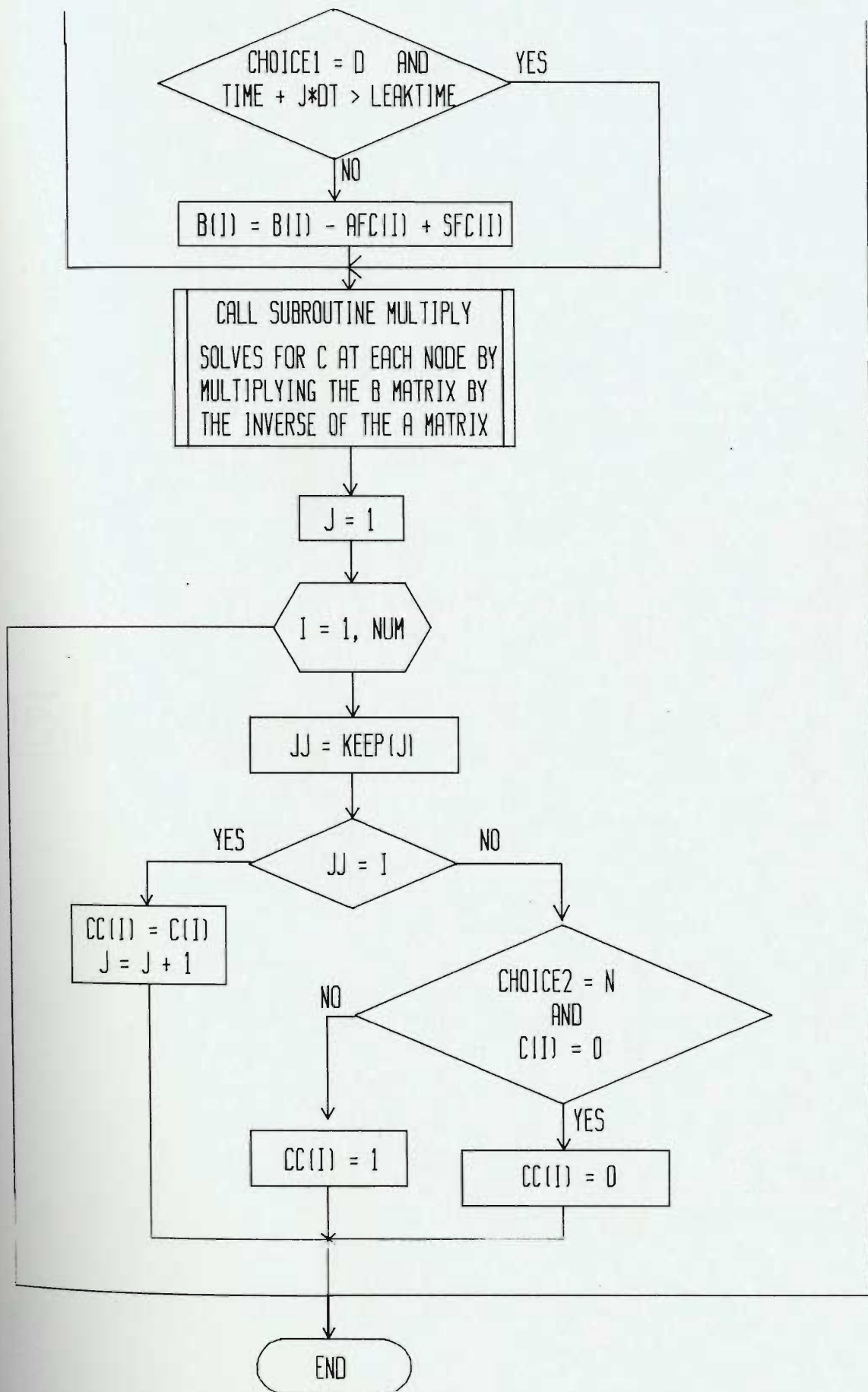


Figure 3.8 (continued) Flow chart for subroutine SOLVEC.



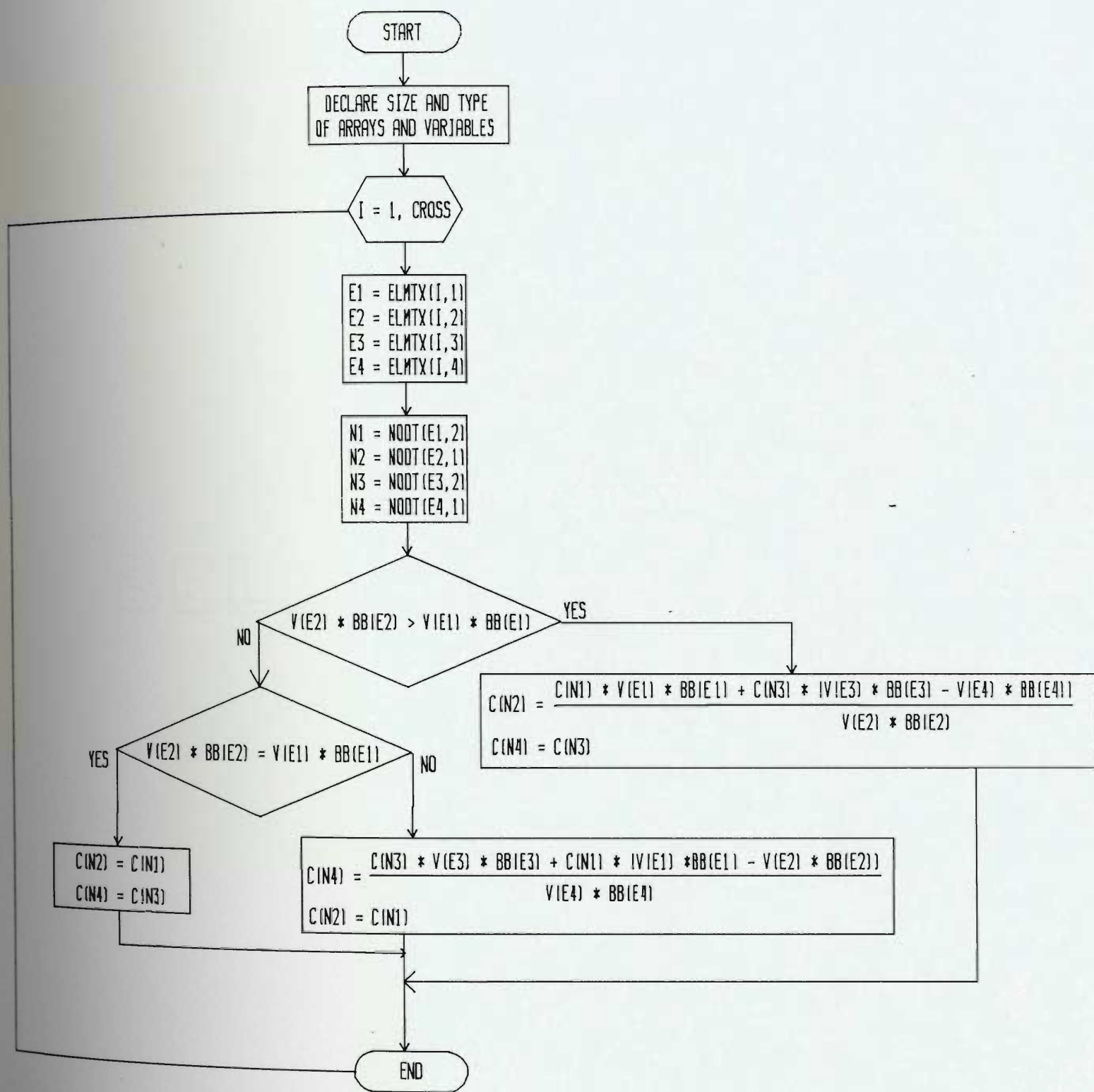


Figure 3.9 Flow chart for subroutine BRIDGIT.

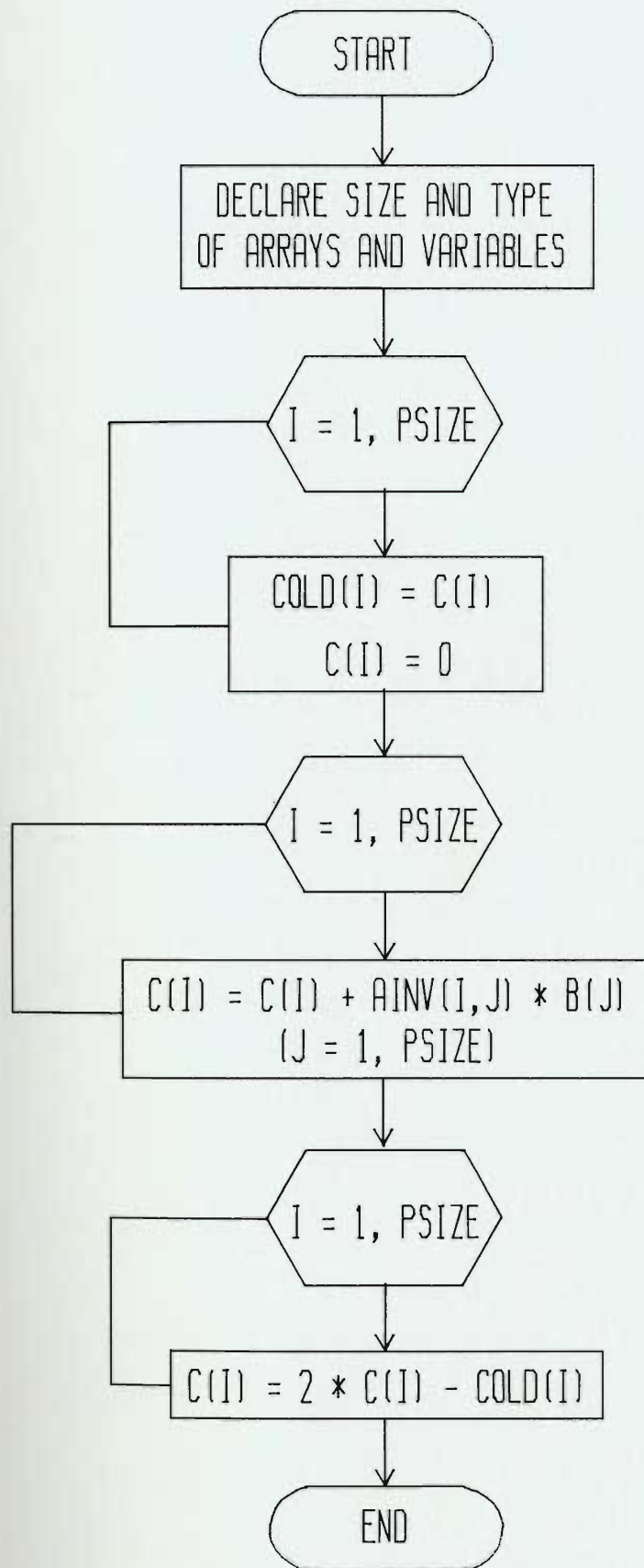


Figure 3.10 Flow chart for subroutine MULTIPLY.

for each of the original node numbers. The value of C at each node is determined by RECONSTITUTE from the values that are calculated for the end nodes of each contributing element. The correlation of the new node numbers with the original ones is done using the array NODC. The flow chart of RECONSTITUTE is shown in Figure 3.11.

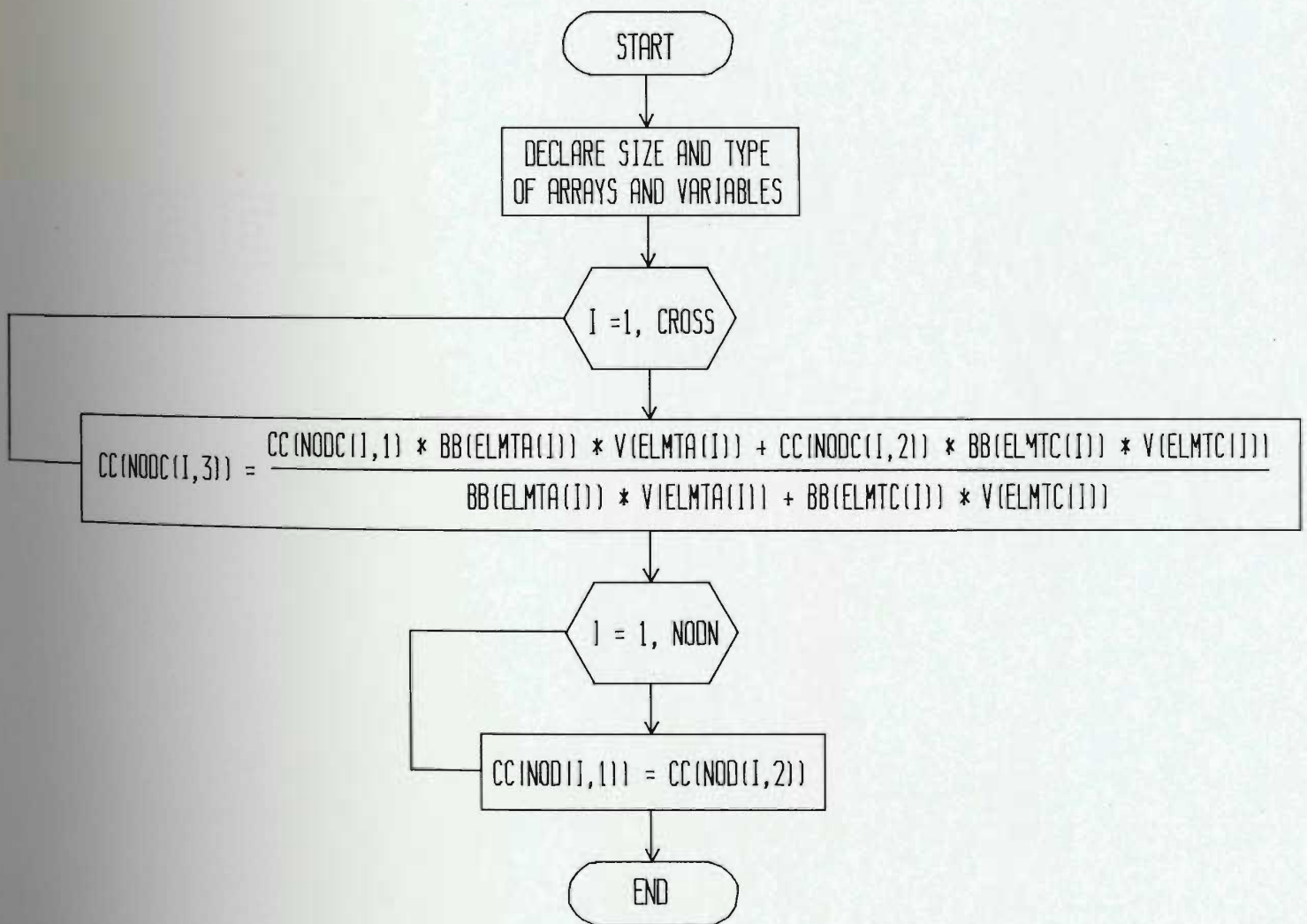


Figure 3.11 Flow chart for subroutine RECONSTITUTE

### 3.5 RESULTS OF NUMERICAL MODEL

The results of the numerical model were compared to those of Huyakorn and Nilkuha, (1979). This comparison was done using a single fracture of length 10 with consistent units, which was divided into 20 elements of length 0.5 as shown in Figure 3.12.

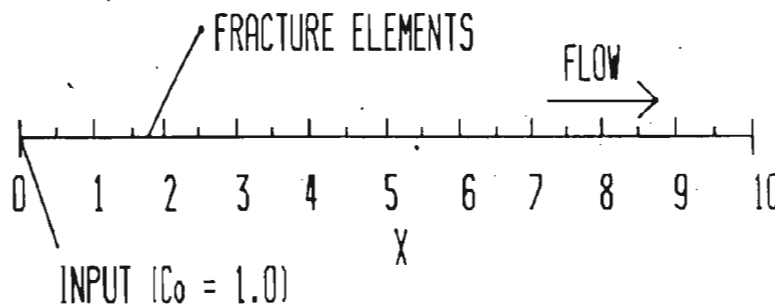


Figure 3.12 Fracture configuration used to test the numerical model.

Figure 3.13 shows the breakthrough curves for two of the cases considered by Huyakorn and Nilkuha. The first case, shown in (a), is a moderately convective-dominated transport condition where  $Pe$  equals 10. The second, shown in (b), is a highly convective-dominated transport condition where  $Pe$  equals 100. The concentration profiles shown in the figure were obtained using the analytical solution and a numerical solution where the values of  $dt$ ,  $t$ , and  $D$  in consistent units

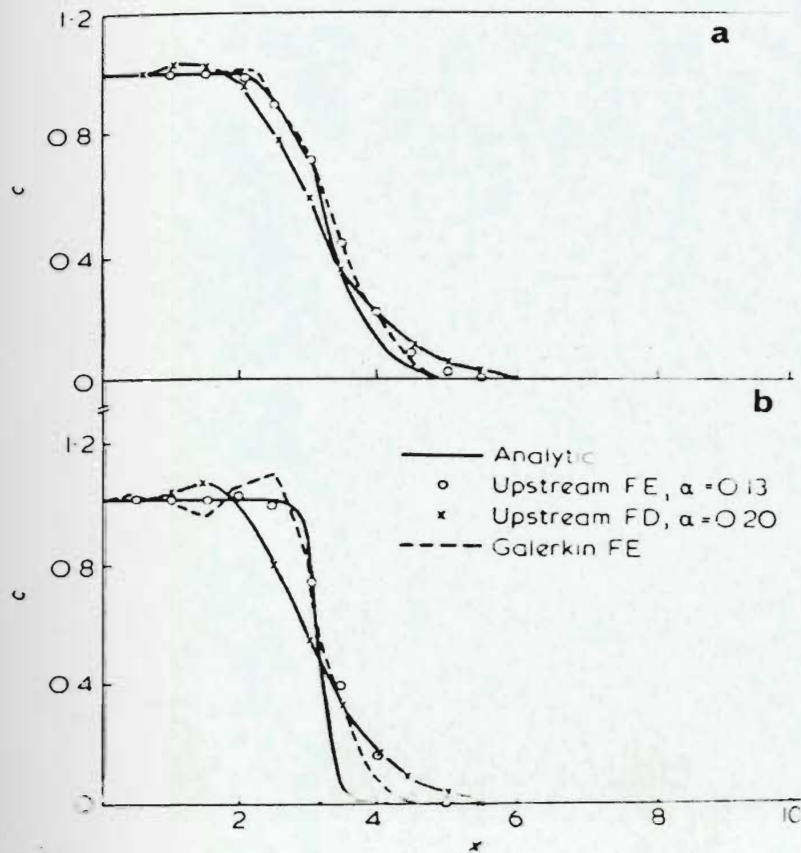


Figure 3.13 Concentration profiles using  $dt = 0.4$ ,  $t = 6.4$ ; (a)  $Pe = 10$ ; (b)  $Pe = 100$  (after Huyakorn and Nilkuha, 1979)

0.025 respectively. The numerical solution is shown for three values of the upstream element coefficient  $\alpha$ , 0.0, 0.13 and 0.2. When  $\alpha = 0.0$  the solution is equivalent to the Galerkin finite element scheme.

Figure 3.14 shows the results of the analytical solution of Ogata and Banks (1961) and the numerical model EXPORT, as written for this study. The value for each of the parameters are identical to those used by Huyakorn except that  $t$  equals 6. In this figure it is evident that the numerical solution lags somewhat behind that of the analytical solution. The



reason for this was not investigated fully but was thought to be due to small losses of mass from using too large a time step (ie,  $dt = 0.4$ ).

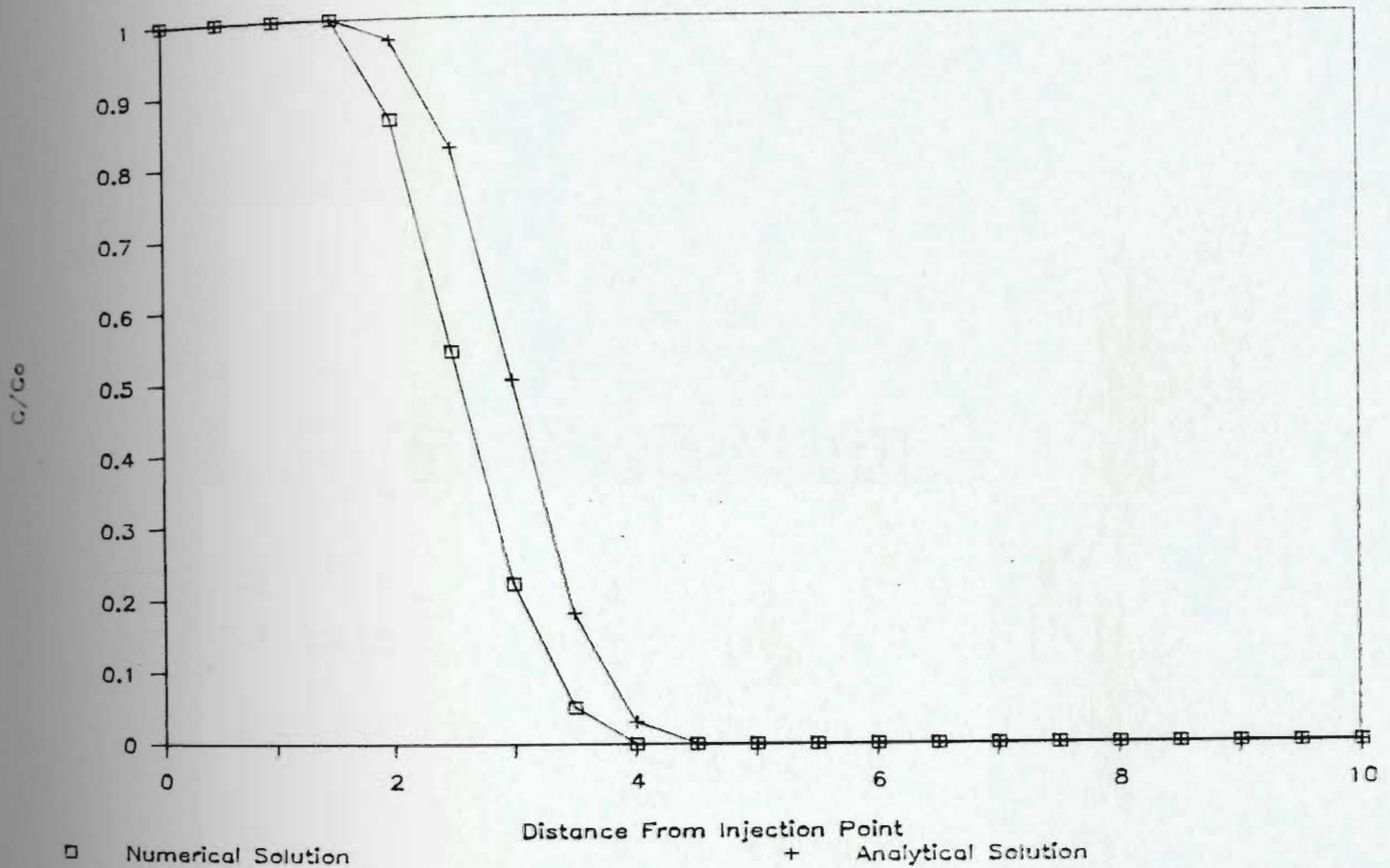


Figure 3.14 Concentration profiles using  $dt = 0.4$ ,  $t = 6.0$  and  $Pe = 10$  (Using the analytical solution and the numerical transport model EXPORT).

Two more simulations were run using time step values of 0.3 and 0.2. The results of these simulations are shown in Figures 3.15 and 3.16 respectively.

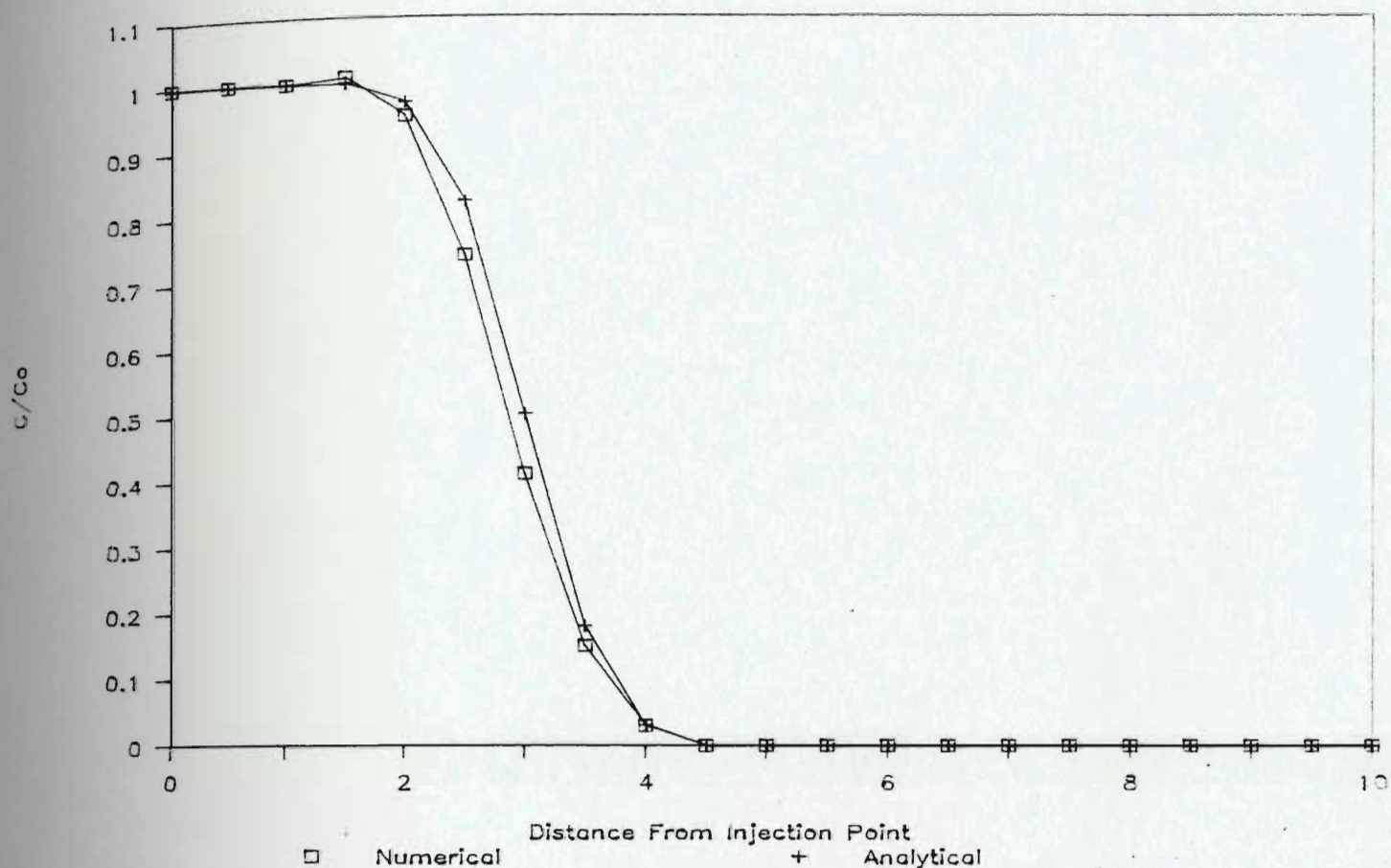


Figure 3.15 Concentration profiles using  $dt = 0.3$ ,  $t = 6.0$  and  $Pe = 10$  (Using the analytical solution and the numerical transport model EXPORT).

Figure 3.15 shows that when a time step of 0.3 is used, the breakthrough curve, as determined by the numerical solution, is much closer to that of the analytical solution, although still behind it in time. This forward movement is continued when a time step of 0.2 is used. Figure 3.16 shows the numerical solution is now ahead of the analytical solution. Further simulations were run using even smaller values of the time step, but no significant difference in the relative positions of the two curves, from those in Figure 3.16, was noted. It is probable that the forward movement of

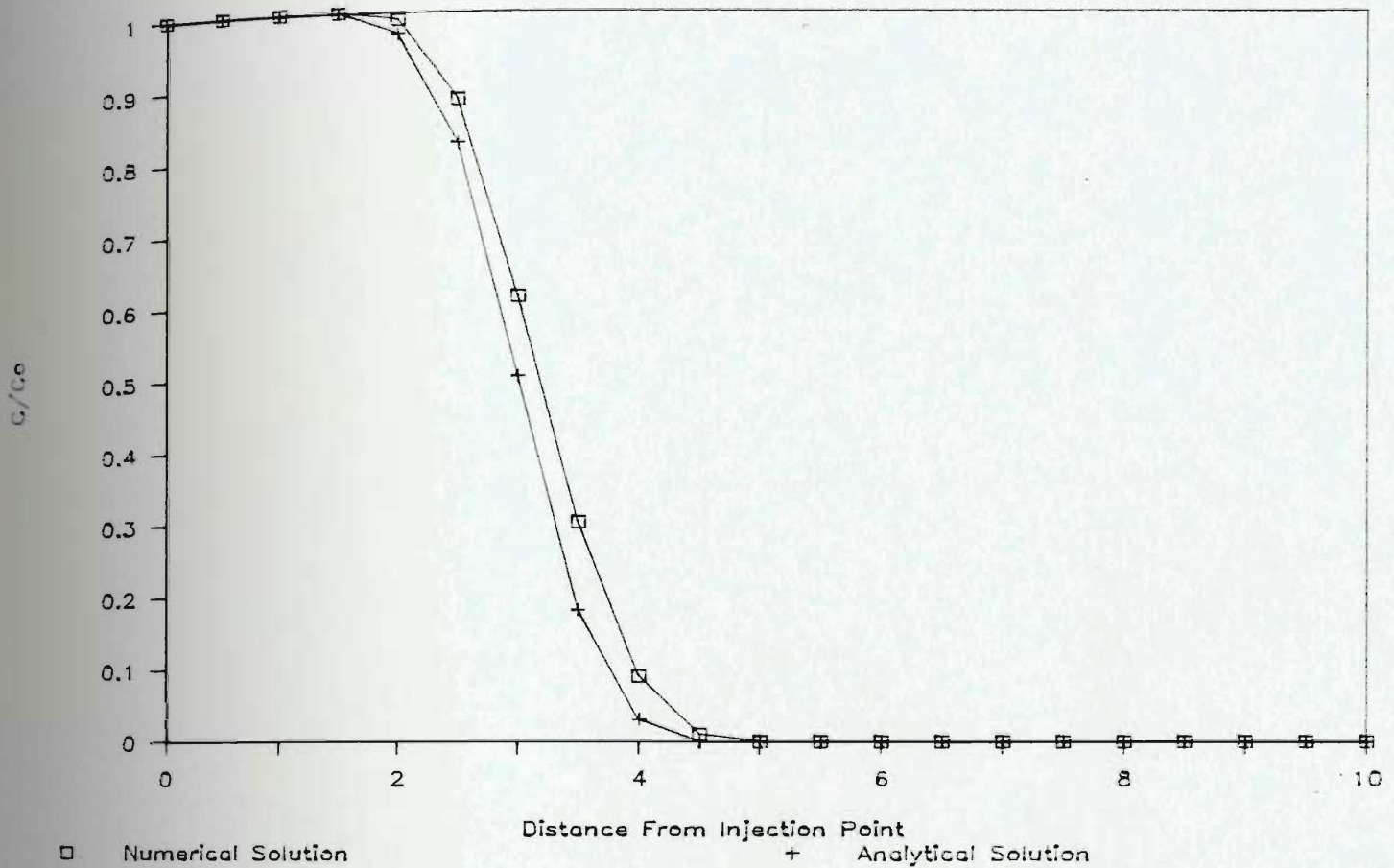


Figure 3.16 Concentration profiles using  $dt = 0.2$ ,  $t = 6.0$  and  $Pe = 10$  (Using the analytical solution and the numerical transport model EXPORT).

the curve as the time step decreases is due to the numerical errors that become more significant as the number of calculations increases. The effect of these errors appears to be compensating since time steps smaller than 0.2 do not significantly shift the breakthrough curve.

Two further simulations were done, using the fracture configuration shown in Figure 3.12, in order to compare the results of the upstream finite element formulation with those



of the Galerkin method. Figures 3.17 and 3.18 show the breakthrough curves that are produced using the upstream weighting functions at Peclet numbers of 10.0 and 100.0 respectively. Included also, for comparison, are the curves shown in Figure 3.13. It is evident from both of these figures that the results of the upstream finite element formulation are closely correlated with the analytical solution. The Galerkin solution however shows substantial

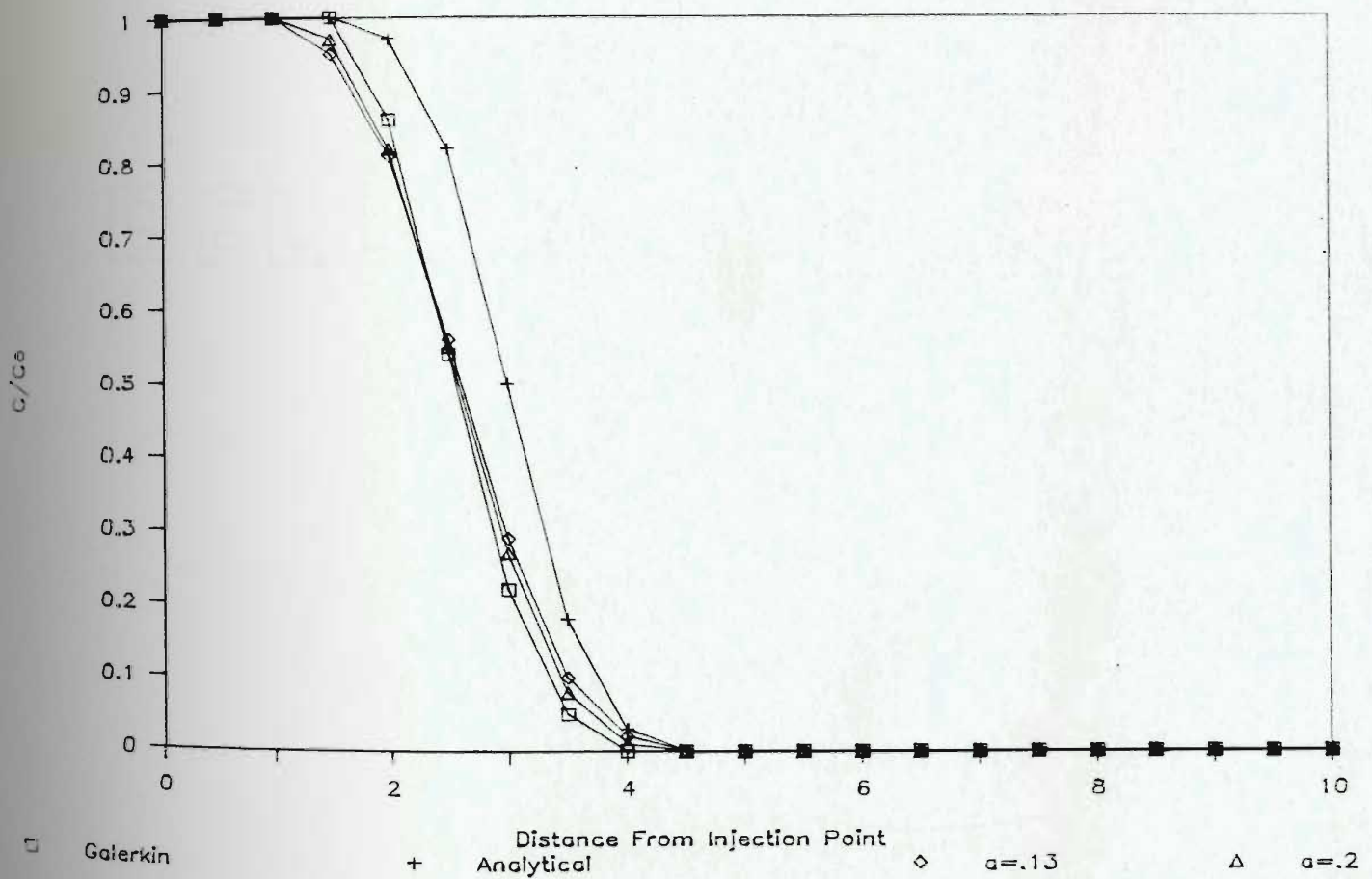


Figure 3.17 Concentration profiles using  $dt = 0.3$ ,  $t = 6.0$   
 $Pe = 10$ ,  $\alpha = 0.0$ ,  $\alpha = 0.13$  and  $\alpha = 0.2$  (Using  
the analytical solution and the numerical  
transport model EXPORT).

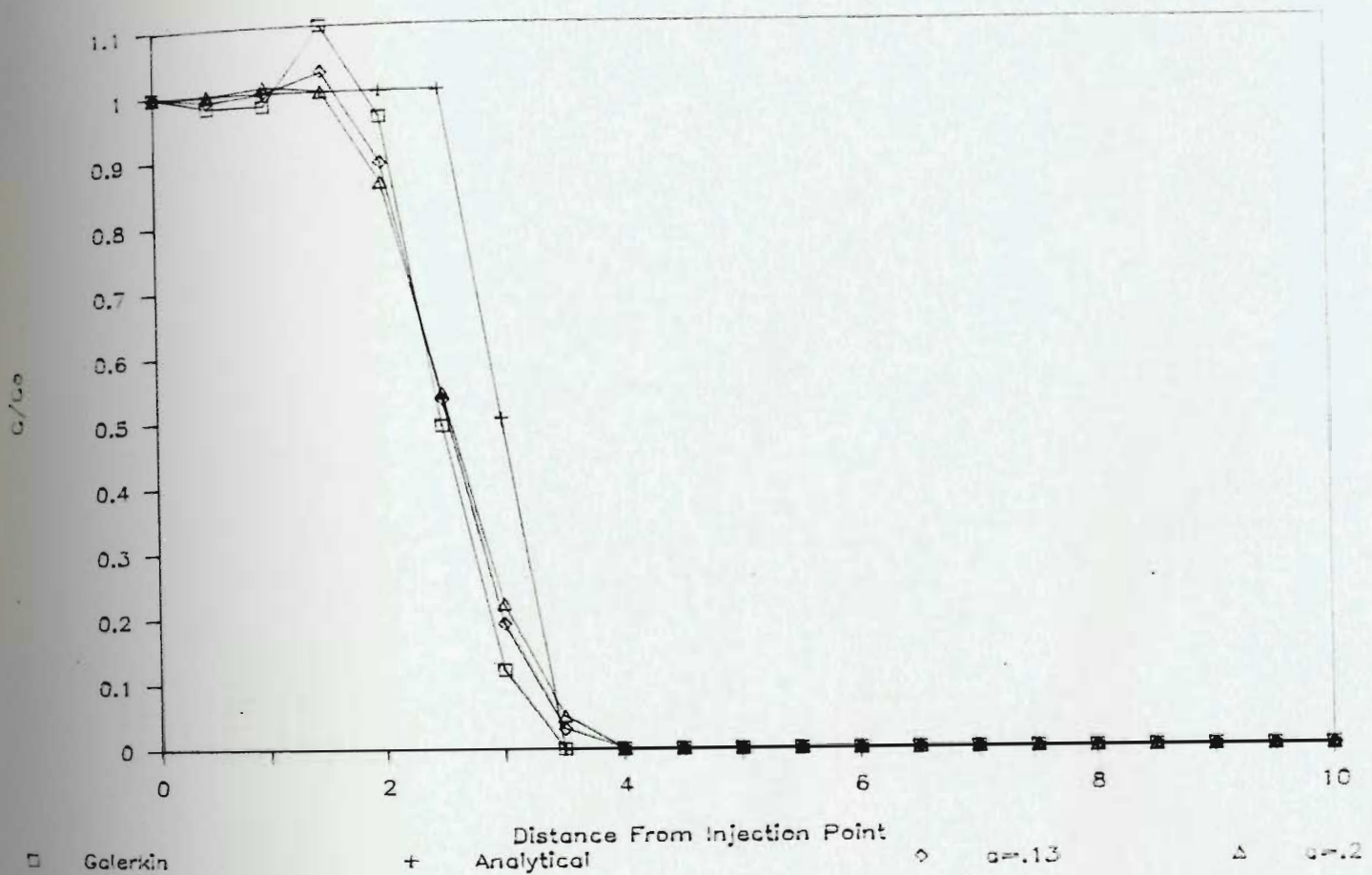


Figure 3.18 Concentration profiles using  $dt = 0.3$ ,  $t = 6.0$   
 $Pe = 100$ ,  $\alpha = 0.0$ ,  $\alpha = 0.13$  and  $\alpha = 0.2$  (Using  
the analytical solution and the numerical  
transport model EXPORT).

undershoot and overshoot which is not nearly as significant when the upstream weighing functions are used. This is especially so with the higher value of  $\alpha$ .

The above tests show that EXPORT gives essentially the

same results as those of Huyakorn and Nilkuha for a single continuous fracture. As described earlier in this chapter however, EXPORT incorporates into the finite element scheme a special algorithm which decouples the fracture mesh at intersections. The efficiency of this method was examined using the fracture configuration shown in Figure 3.19. This configuration is identical to the one in Figure 3.12 except that at every second node, up to number six there is an intersecting fracture. This fracture has flow into and out of the intersection. However, the flow is negligible (the velocity is specified as  $10^{-30}$  in consistent units) so that there is no loss of mass from the system.

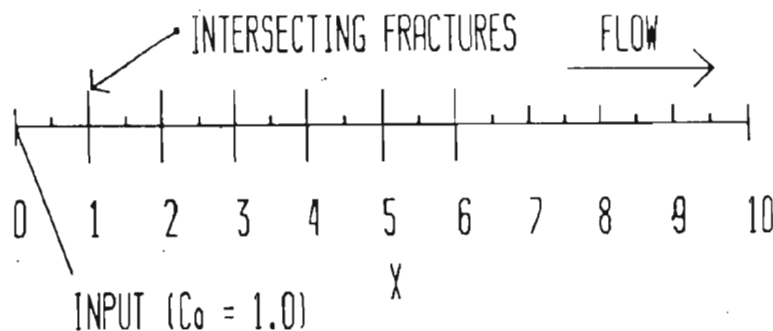


Figure 3.19 Fracture configuration used to examine the mixing algorithm used in EXPORT.

The concentration profile that was determined in this fracture is shown in Figure 3.20. Identical parameter

values were used as in Figure 3.13 and the results of the Galerkin and the analytical solution for the single fracture are plotted for comparison. It is apparent that the results agree quite closely with the single fracture Galerkin and analytical solutions. The slight discrepancies are probably due to the small numerical errors that result from the breakup of the intersections.

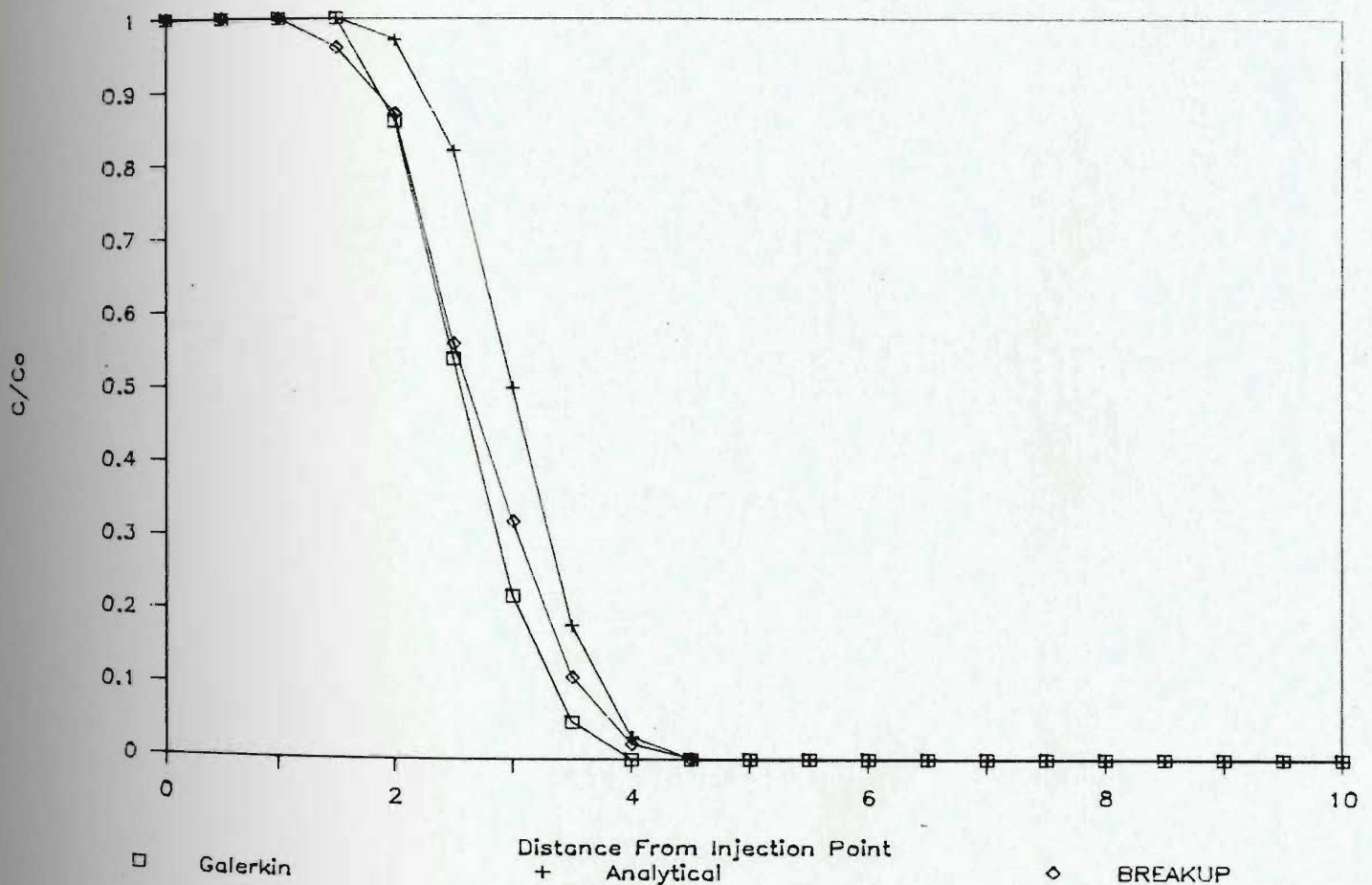


Figure 3.20 Concentration profiles using  $dt = 0.4$ ,  $t = 6.0$   
 $Pe = 10$ ,  $\alpha = 0.0$  and implementing the subrou-  
tine BREAKUP (Using the analytical solution and  
the numerical transport model EXPORT).

## CHAPTER FOUR

### NUMERICAL SIMULATION OF SOLUTE TRANSPORT IN FRACTURED SYSTEMS

#### 4.1 MODEL FOURTEEN

In order to compare the results of the numerical model to results measured under laboratory conditions, the fracture configuration in Model fourteen was generated by NETWORK and NETFLOW and EXPORT was used to simulate the transport of a solute through it. Figure 2.3 shows the pattern of fractures that were cut into model fourteen. In this figure the inlet and outlet ports are numbered for reference. The concentration of solute that was measured at the outlet ports of this model are listed in Table 5. The program NETWORK was altered slightly so that the same fracture network was generated and to be used by EXPORT for transport simulation.

Since the laboratory model was run under steady state conditions, a simulation time was used in EXPORT, which was of sufficient length to ensure that the same conditions were established in the numerical model. For comparison purposes one simulation was run without using the subroutine BREAKUP, thus perfect mixing at the fracture intersections was assumed. In contrast a second simulation was run using BREAKUP ie; imperfect mixing was assumed. The three dimensional plots of the solute concentration at each intersection, for these two simulations, are shown in Figures 4.1



and 4.2 respectively. The concentration of solute, in the form  $C/C_0$  for the two simulations are given, for comparison, in Table 5.

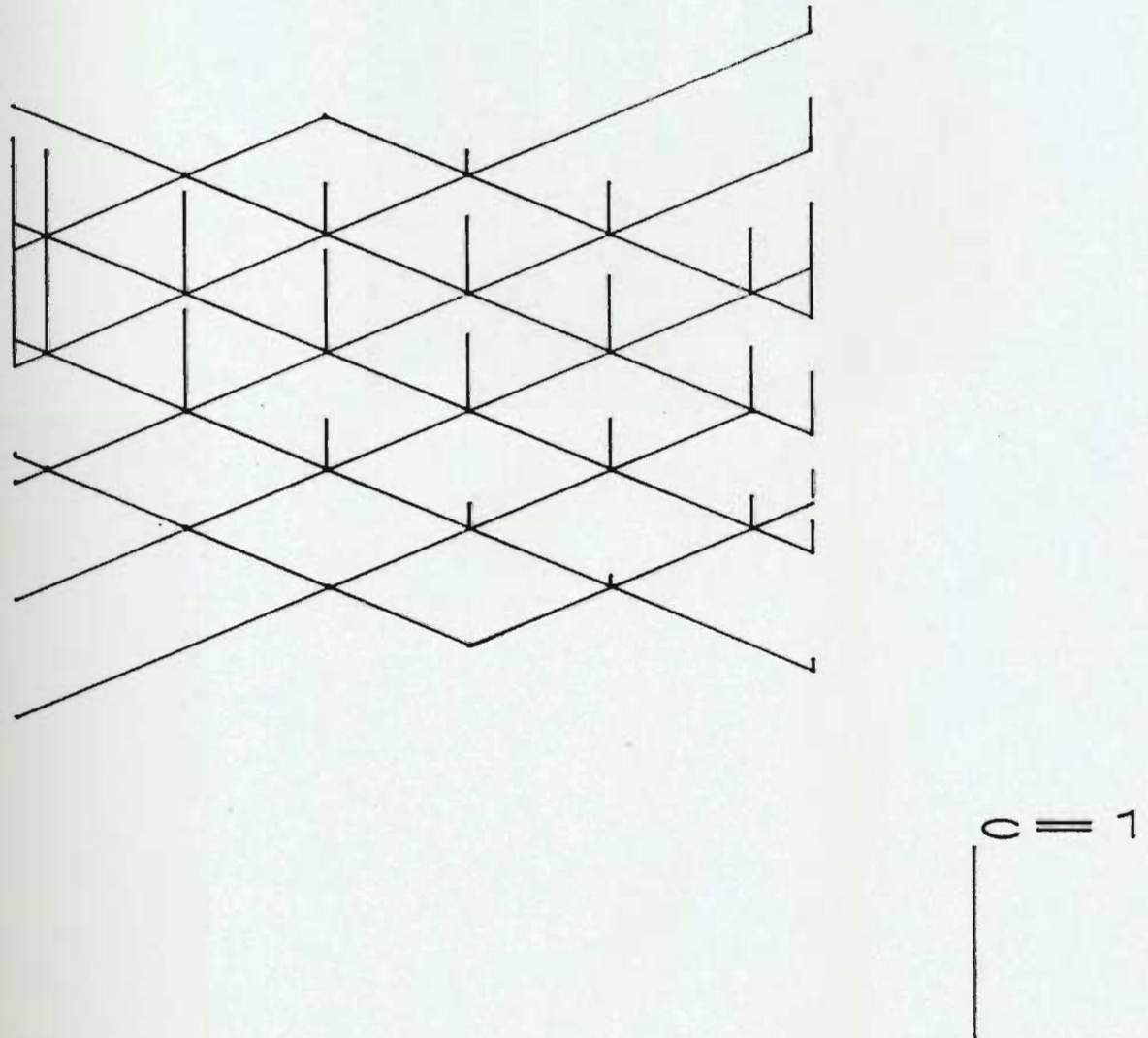


Figure 4.1 3-D plot of solute concentrations in model # 14 assuming perfect mixing at the fracture intersections.

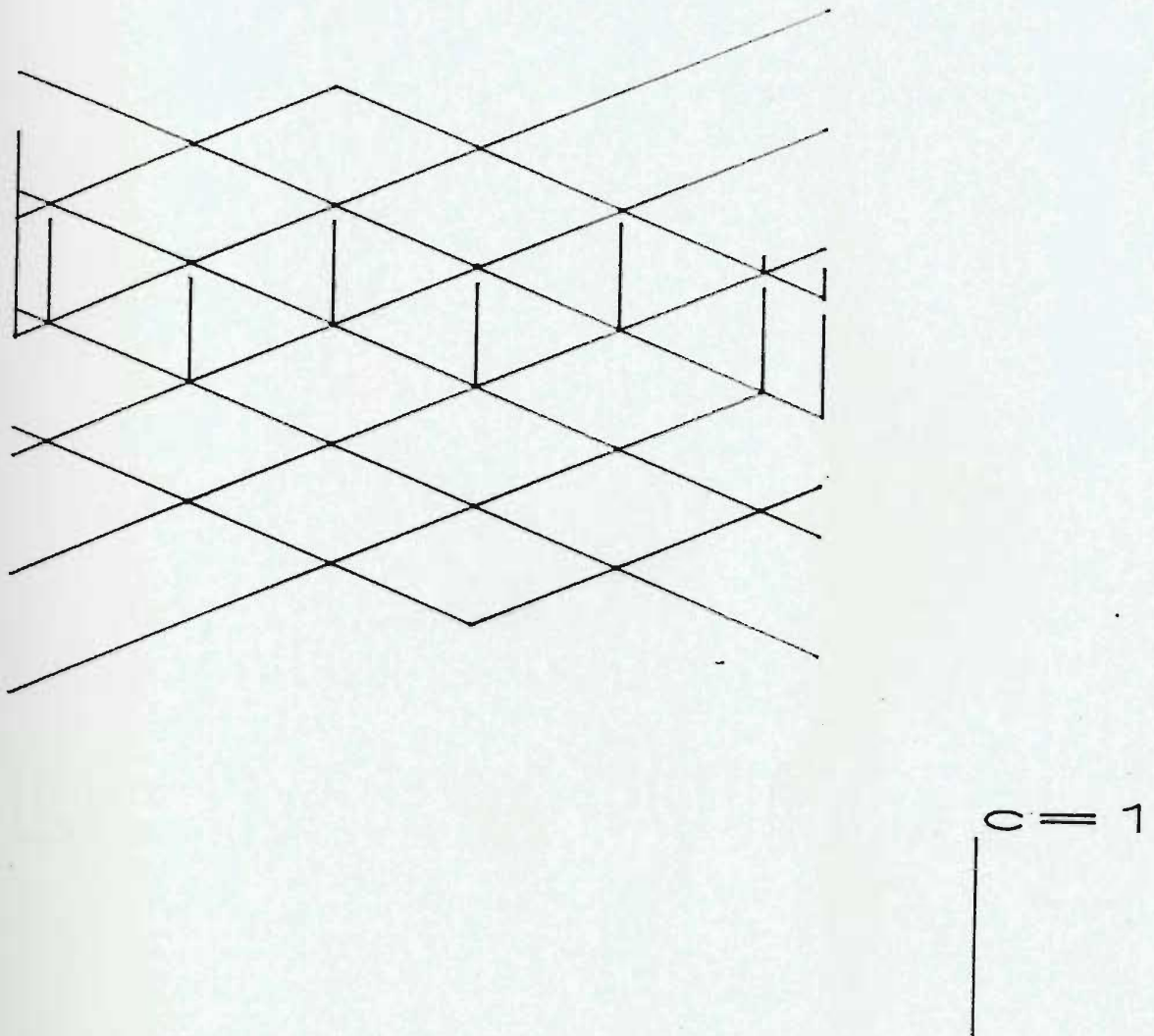


Figure 4.2 3-D plot of solute concentrations in model # 14 assuming no mixing at the fracture intersections.

A comparison of Figures 4.1 and 4.2 show the very marked difference in the spread of solute throughout the model. When mixing is assumed to be perfect at the intersections, the solute quickly spreads out over the whole model so that some concentration is determined at each of the outlet nodes and most of the internal nodes. When no mixing is allowed at

the fracture intersections, except that which is dictated by the variations in flow rate, the spread is very much less and only three of the outlet ports show significant concentrations of solute.

Table 5: Concentration Values ( $C/C_0$ ) Determined in Model # 14.

Port #	Measured	Determined by EXPORT	
		Not using BREAKUP	Using BREAKUP
5	1.0000	1.0000	1.0000
10	0.0001	0.1217	0.0000
11	0.0004	0.2486	0.0000
12	0.0471	0.3123	0.0065
13	0.3121	0.3123	0.1457
14	0.3005	0.3096	0.4991
15	0.0057	0.1582	0.0000
16	0.0006	0.1582	0.0000
17	0.0001	0.0613	0.0000

#### 4.2 RANDOM FRACTURE SYSTEMS

Three transport simulations were carried out using the numerical model EXPORT in order to determine the pattern of solute transport in artificially generated fracture systems with different hydrologic characteristics. Each system was generated using NETWORK and NETFLO. For each simulation the control parameters, used by EXPORT, were identical, as given in Table 6.



Table 6: Data File CHOICE.DAT

```
choice1 =      d
choice2 =      n
node     =      1
alltime  =     100
partime  =     100
dt       = 0.100000D+01
alpha    = 0.500000D-01
coef     = 0.100000D+01
leaktime = 0.100000D+01
options  = y    n    y    y    n    n    y
```

#### 4.2.1 Equivalent Fracture Sets

The first simulation was run in a fracture system with two sets of fractures which were generated with equal density, length and aperture. The data file used by NETWORK to generate the fracture system is listed in Appendix D. The fracture configuration is shown in Figure 4.3. The element data and the nodal concentrations, as determined by EXPORT, are listed in Appendix D to illustrate the general form of the file THRED.DAT. These nodal concentrations are shown in the 3-D plot in Figure 4.4.

It is evident, from this figure, that the solute is moderately dispersed throughout the fracture system downstream of the injection point. The flow path with the largest velocity is favoured, as would be expected.

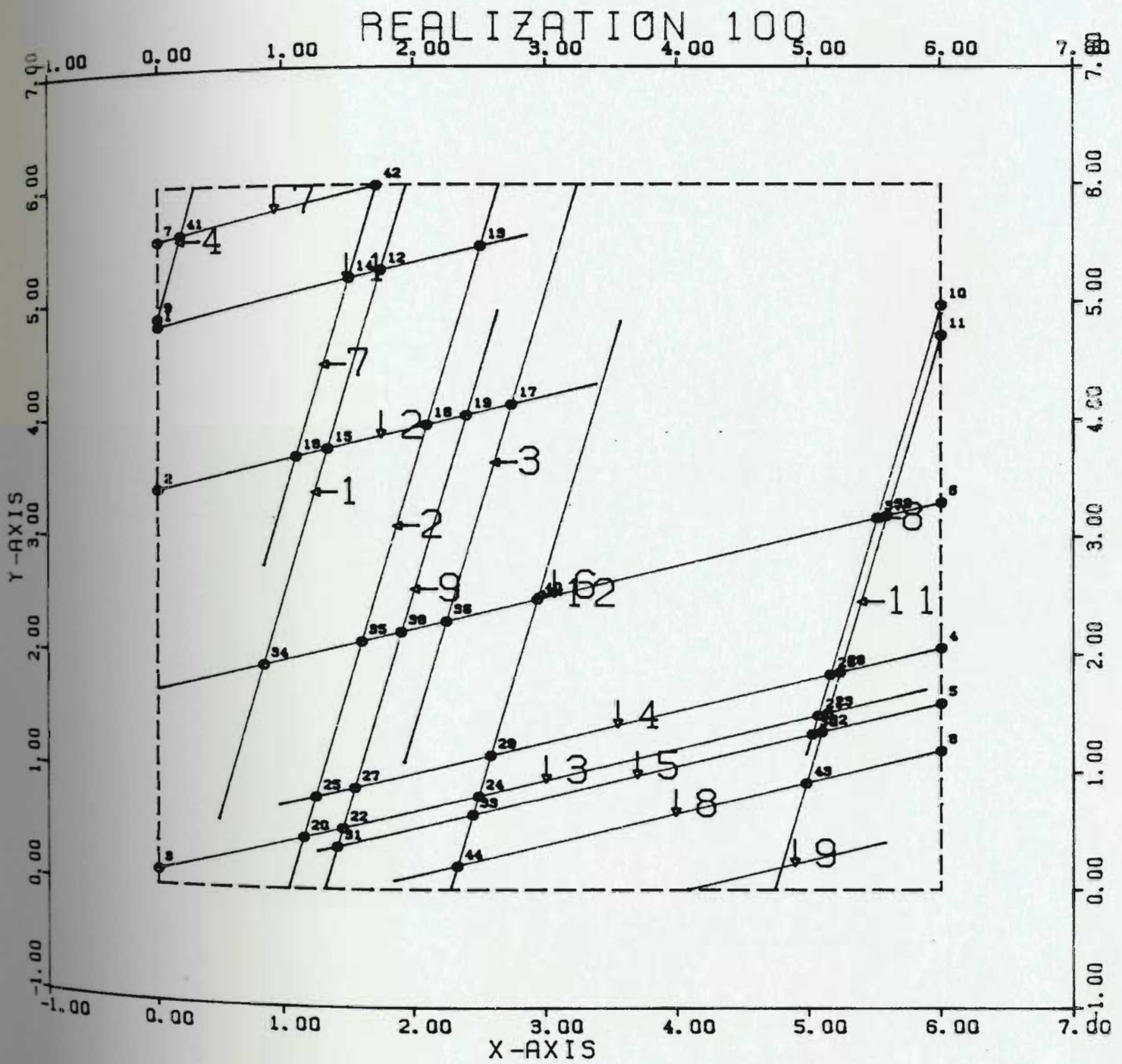
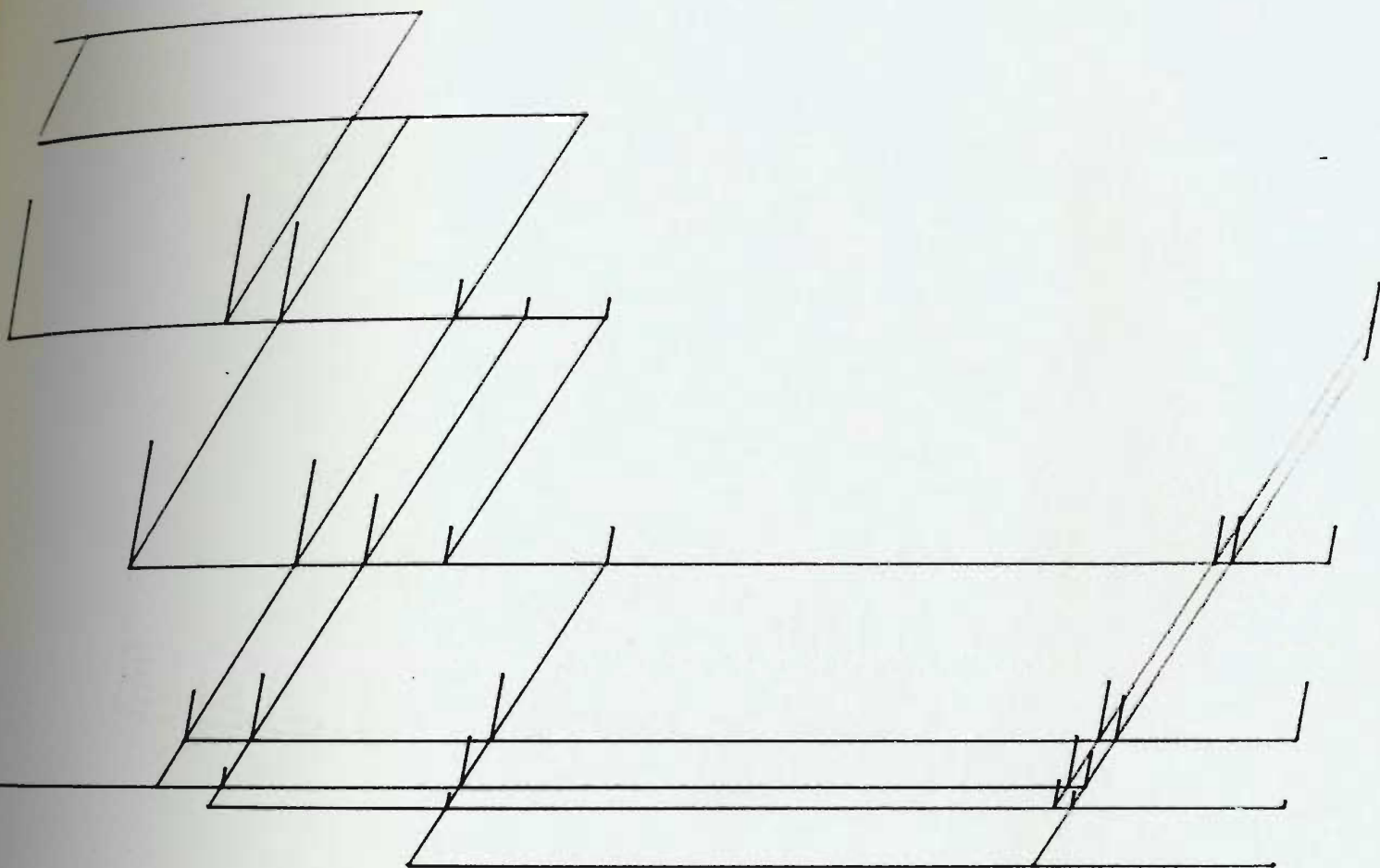


Figure 4.3 Configuration of equal density/equal aperture fracture model.



$C = 1$

Figure 4.4 3-D plot of nodal concentrations for equal density/equal aperture fracture model.

#### 4.2.2 Unequal Aperture Model

The second simulation was run using the same fracture configuration as depicted in Figure 4.4 but with fracture sets of unequal aperture. The set oriented 15 degrees from the horizontal had twice the aperture of the other set. The nodal concentrations determined by EXPORT are shown in the 3-D plot in Figure 4.5.

It is evident from Figure 4.5 that the solute is again moderately dispersed throughout the fracture system, downstream of the injection point. Once again the flow path with the largest velocity is favoured. The difference that the larger aperture fracture set makes is shown by the smaller concentrations of solute that are found in the three fractures that drain the lower portion of the system. Since the one central fracture is able to carry the main load (because it's aperture is twice as large as the earlier system) less solute is able to move into the lower portion of the system. It is also evident that a higher concentration of solute reaches the right side of the model.

#### 4.2.3 Equal Apertures and Unequal Spacing and Density

The third simulation was run in a fracture system with two sets of fractures which were generated with equal

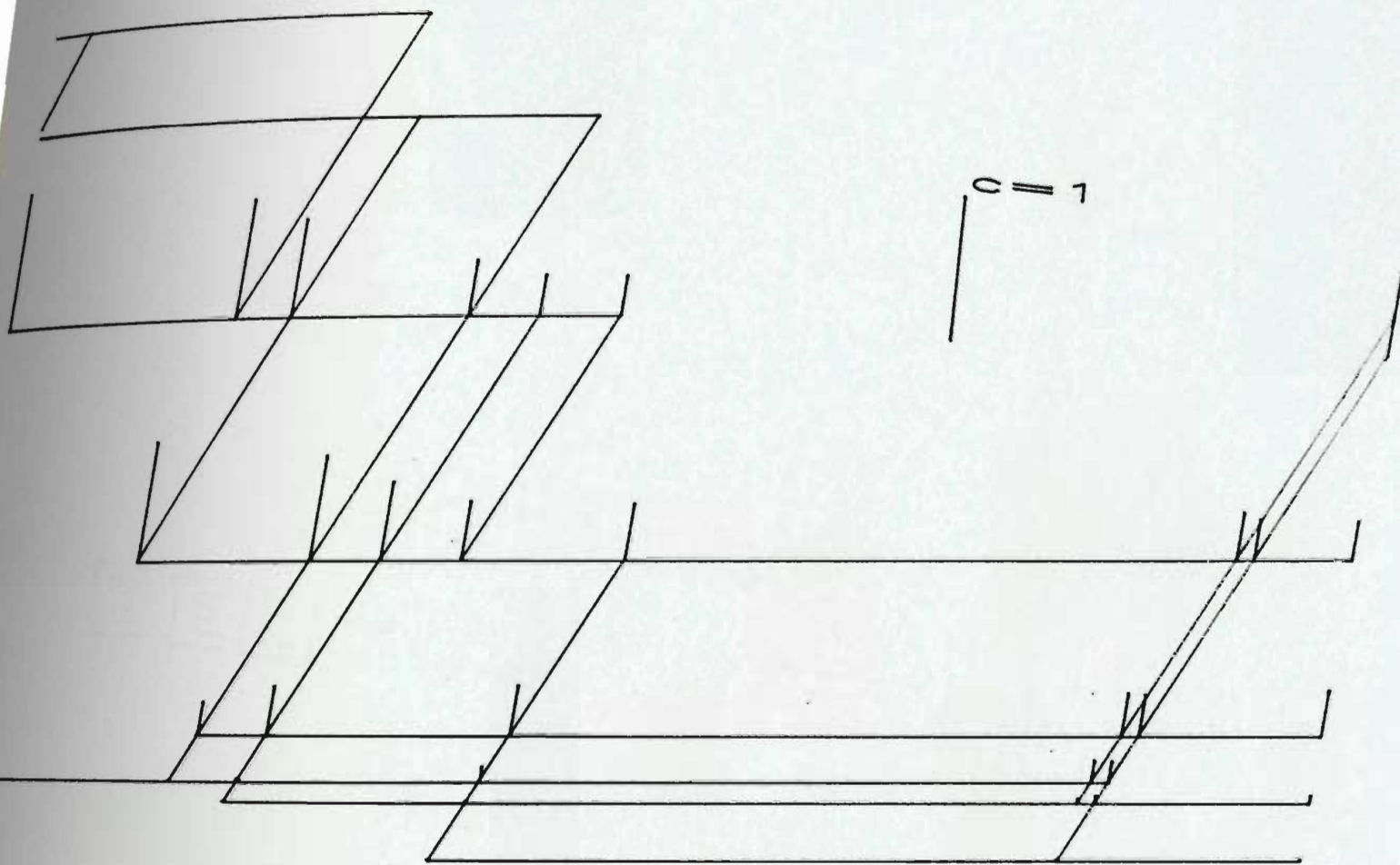


Figure 4.5 3-D plot of nodal concentrations for equal density-spacing fracture model in which the fracture set at 15 degrees from the horizontal has twice the aperture as the other set.

apertures but with unequal density and length. The set oriented 15 degrees from the horizontal has twice the density and length of the other set. The fracture configuration is shown in Figure 4.6.



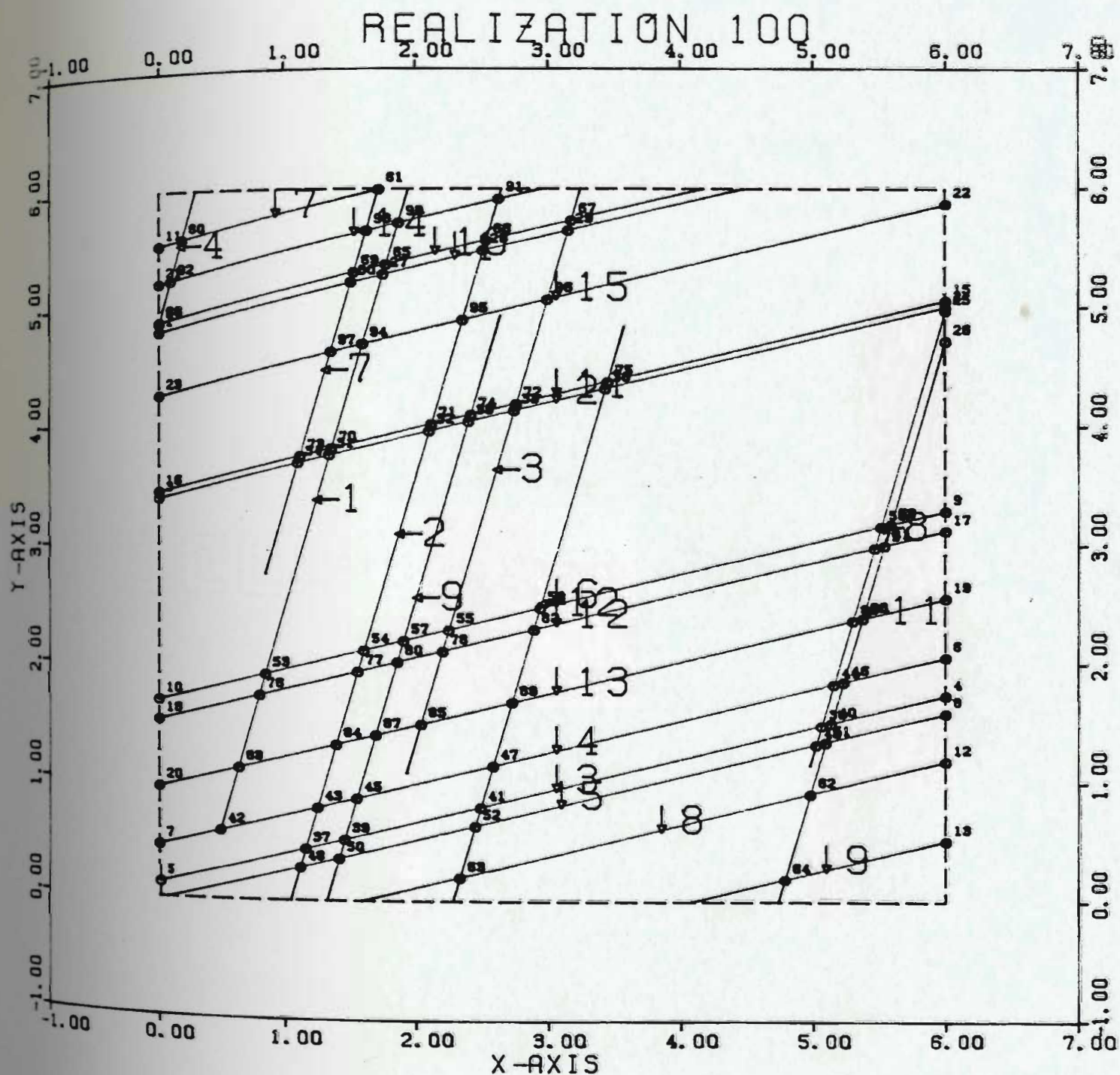


Figure 4.6 Configuration of equal aperture fracture model with unequal density and length (set one, 15 degrees from horizontal, has twice the length and twice the density of set two).

The fracture system that is generated this time is very much different than the earlier one. The number of fractures that traverse the model completely is more than doubled and consequently the number of nodes on the flow boundary is greater. The nodal concentrations generated by EXPORT are shown in the 3-D plot in Figure 4.7. The figure shows that very little solute is transferred to the other elements but that most of it is carried by the fracture into which it was injected.

#### 4.3 STRIPA FRACTURE MODEL

A final transport simulation was run on a fracture system generated from actual field measurements obtained from the Stripa study site in Stripa Sweden (Gale and Rouleau, 1986). The fracture system existing in a small section of the ventilation drift was simulated using NETWORK AND NETFLOW. The resulting network is depicted in Figure 4.9. This network contains 584 elements and 389 nodes or intersections. The direction of flow is from the outer boundary inward towards the center of the circular section.

Node 4 on the outer boundary of the network is shown in Figure 4.8. The continuous injection of solute, at this node, at a concentration of  $C/C_o = 1.0$ , for 1,000,000 seconds was simulated by EXPORT. Figure 4.9 shows the concentration

of solute at the element nodes when the subroutine BREAKUP was not used. Figure 4.10 shows the concentration of solute at the element nodes when the subroutine BREAKUP was used.

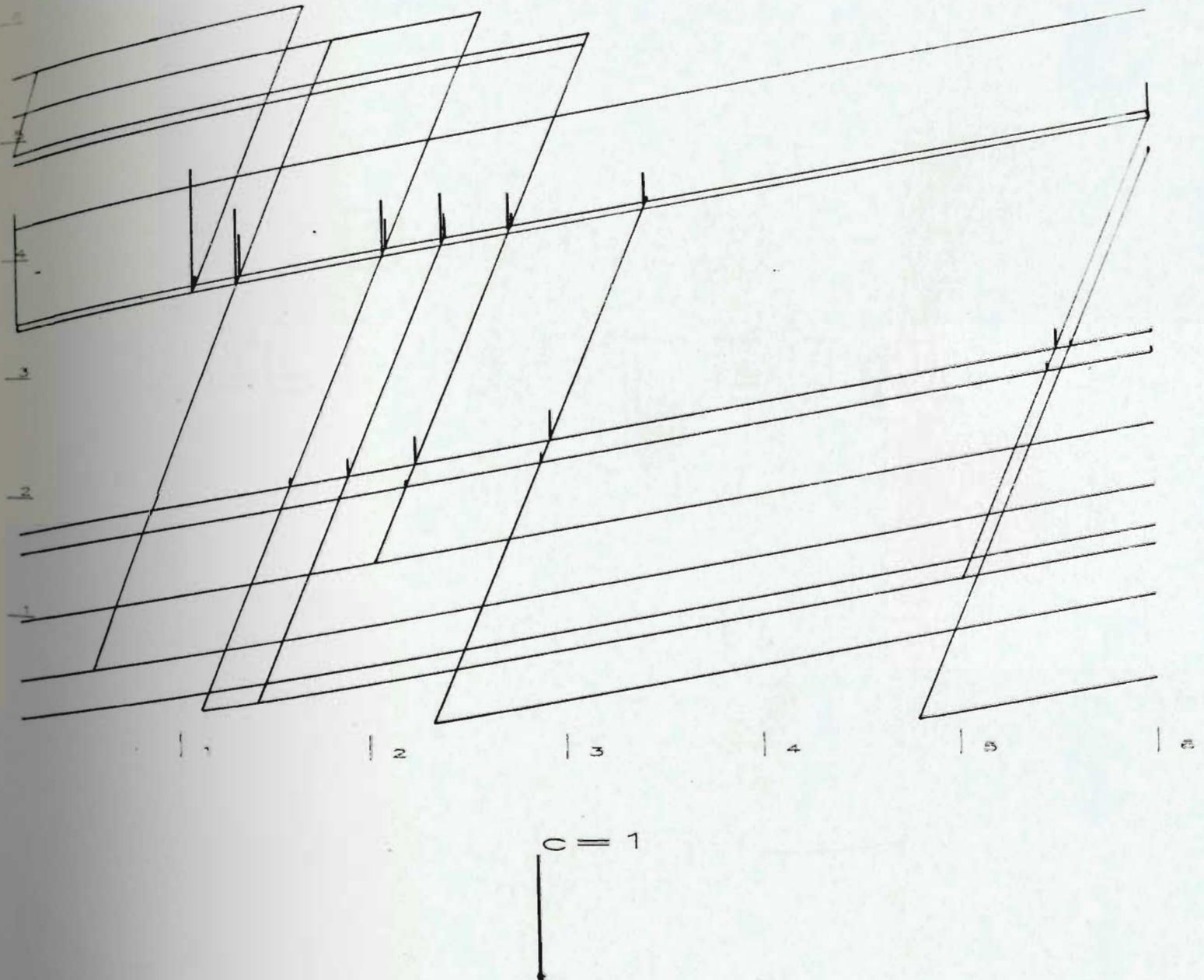


Figure 4.7 3-D plot of nodal concentrations for fracture model with equal aperture and unequal density and length.



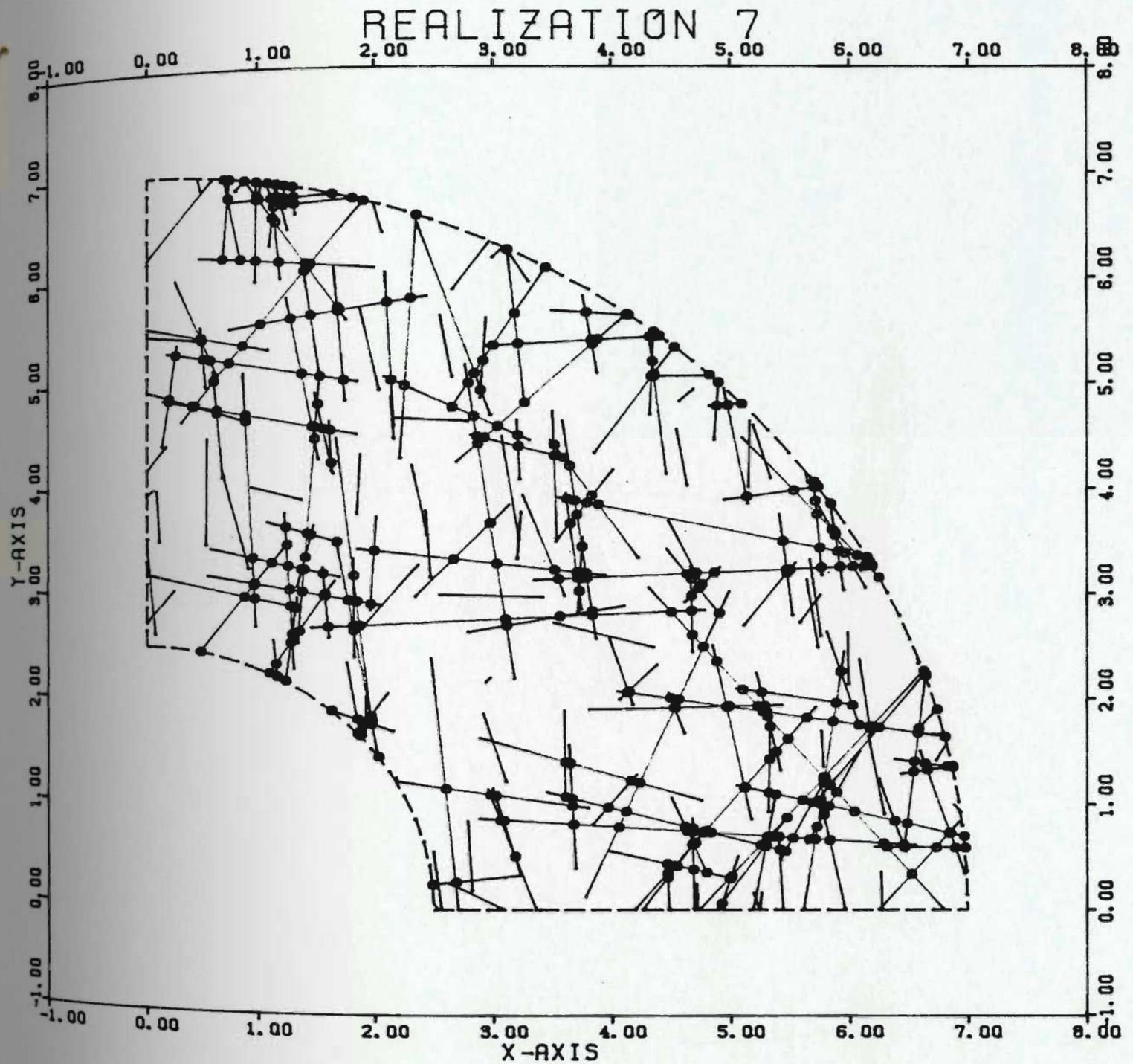


Figure 4.8 Fracture network configuration generated by NETWORK from data obtained in Stripa Sweden.

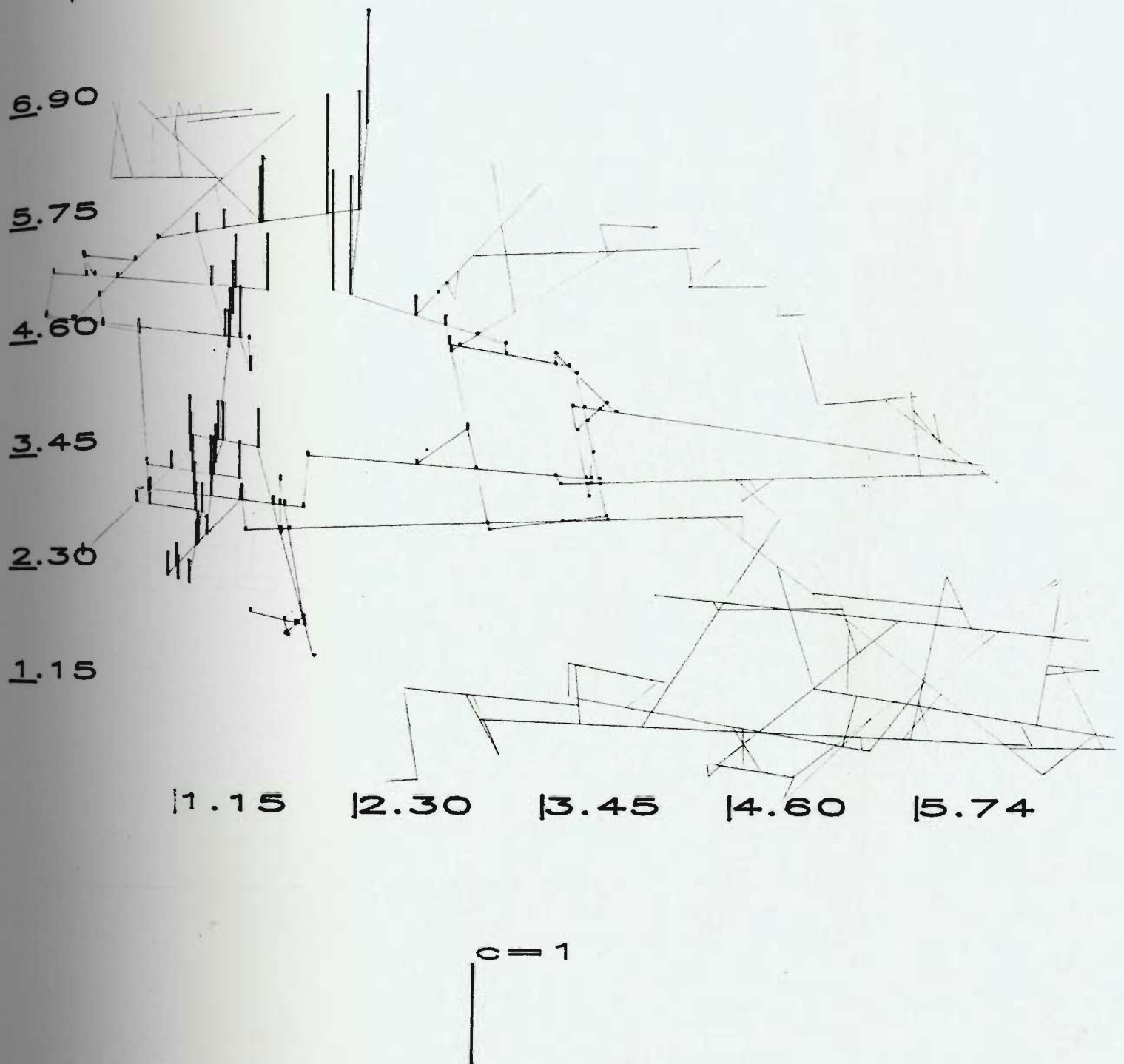


Figure 4.9 Concentration of solute at fracture intersections using EXPORT without BREAKUP

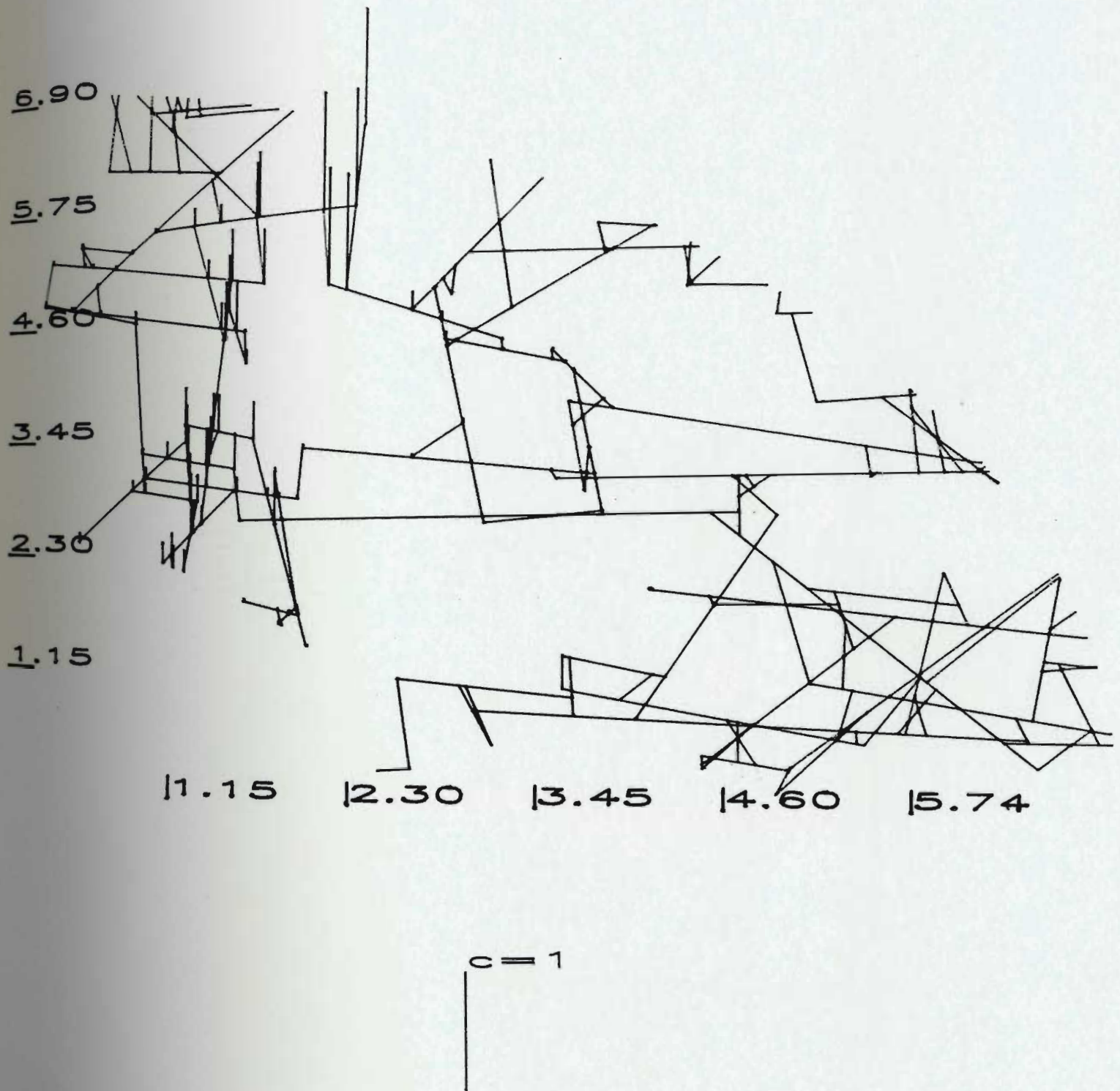


Figure 4.10 Concentration of solute at fracture intersections using EXPORT with BREAKUP

It is evident from both figures that the movement of a solute in a discontinuous fracture system is quite localized to the flow path from the area of injection to the discharge area under radially convergent flow conditions. It is noted that there is very little difference between the results of using BREAKUP and not using it. The reason for this is the virtual absence of four-way intersections in the fracture network. The program counted only 31 such intersections in the configuration that was used. In addition to this the flow in each element was very different. Under these radial flow and fracture geometry conditions the effects of using the correct mixing algorithm would be minimal for this number of fractures.

## CHAPTER FIVE

### CONCLUSIONS AND RECOMMENDATIONS FOR FURTHER WORK

The mixing algorithm in open fractures, used until recently, in most transport models for fractured rock systems is in error. This series of extensive laboratory tests has shown conclusively, that instead of perfect mixing at four-way intersections it is evident that, when the flow is equal in ~~each of the~~ fractures then, under laminar flow conditions, no mixing takes place. At intersections that are not four-way, perfect mixing is of course valid. When the flow is not equal in the intersecting fractures, mixing is forced to take place when the flow streams are redistributed to the outflow fractures. Hence it is important to establish the proportion of four-way intersections in a fracture network in order to determine which mixing algorithm is dominant. More research is required to determine how the physical attributes of the system such as spacing, trace length, and connectivity are related to the proportion of four-way intersections.

The numerical model assumes that parallel flow streams in one fracture mix perfectly, whereas the laboratory tests indicate that these streams do not mix. This means that each of the individual flow streams in open fractures must be traced throughout the model in order to correctly predict the concentration at any one point. It can be appreciated that

the available computer memory, in most systems, would soon be filled for even very small networks. Further, the computer requirements of tracing the transport of a solute in a three dimensional fracture network would severely limit the size of the network that could be modeled.

In its handling of matrices the numerical model EXPORT needs to be refined to make it more efficient. The present version stores all coefficients of all matrices. Since these matrices are sparse the use of a more efficient storage system would greatly increase the efficiency and capabilities of the model. The method of uncoupling each four-way intersection can lead to very large computer memory and computational time requirements. It may be possible to use a three dimensional fracture model at the intersections to reduce these requirements and achieve the same fracture modelling capability.

In its present form the model has demonstrated the effects of using the correct mixing algorithm for transport in open fracture networks of various geometries. Such effects can be quite significant when the networks consist of many four-way intersections. In these systems the simulations indicate that contaminants migrating through fractured media will not be dispersed and diluted to the extent that past numerical models have predicted and hence the contami-



nant will be discharged to the biosphere much more quickly and at a higher concentration than expected. It should be noted that when the discharge is a stream or lake, while the peak concentration will be higher, the total loading to the biosphere will be the same. However in the case of a well bore intersecting a fracture, along which contaminants are migrating, the toxicity levels will be much greater.

The simulations that were run using the real fracture network geometry obtained from Strepa show that when natural systems contain few four-way intersections then the effects of using the correct mixing algorithm are not as pronounced. Other natural features such as contacting surfaces, surface roughness, the geometry and roughness of the intersection and 3-dimensionality also contribute to the overall transport pattern. To some degree these features will determine the relative importance of forced mixing. Additional laboratory and field studies are needed to determine how dominant these characteristics are in the transport processes that operate in real fractured aquifers.

# REFERENCES

- Castillo, R.E., Dispersion of a Contaminant in Jointed Rock, Ph.D. Thesis, Northwestern University, Evanston, Ill. June 1972.
- Endo, H.K., Long, J.C.S., Wilson, C.R., Witherspoon, P.A., A Model for Investigating Mechanical Transport in Fracture Networks, Water Resources Research, Vol.20, No. 10, October 1984.
- Gale, J.E. and A. Rouleau, Hydrogeological characterization of the ventilation drift (buffer mass) area, Stripa, Sweden, OECD/NEA, Stripa Project, Internal Report 86-02, SKB Stockholm, Sweden, 1986.
- Grisak, G.E. and J.F. Pickens, Solute Transport Through Fractured Media 1. The Effect of Matrix Diffusion, Water Resources Research, Vol. 16, No. 4, pp 719-730, August 1980.
- Grisak, G.E. and J.F. Pickens, An Analytical Solution For Solute Transport Through Fractured Media With Matrix Diffusion, Journal of Hydrology, Vol. 52, pp 47-57, 1981
- Huyakorn, P.S. and K. Nilkuha, Solution of Transient Transport Equation Using an Upstream Finite Element Scheme, Appl. Math. Modelling, Vol. 3, pp 7-17, February 1979.
- Huyakorn, P.E. and G.F. Pinder, Computational Methods in Subsurface Flow, Academic Press, 473 pp, 1983.
- Hwang, J.C., C. Chen, M. Sheikholeslami, B.K. Panigrahi, Finite Analytic Numerical Solution for Two-Dimensional Groundwater Solute Transport, Water Resources Research, Vol 21, No. 9, pp 1354-1360, September 1985.
- Hwang, J.C., W.C. Cho, G.T. Yeh, An Eigenvalue Solution Continuous in Time to the Spatially Discretized Solute Transport Equation in Steady Groundwater Flow, Water Resources Research, Vol 20, No. 11, pp 1725-1732, November 1984.
- Josselin de Jong, G., Dispersion in Fissured Rock, 1969, unpublished.
- Krizek, R.J., Karadi, G.M. Socias, E., 1972. "Dispersion of a Contaminant in Fissured Rock". Proceedings - Symposium Percolation Through Fissured Rock. Stuttgart 1972.

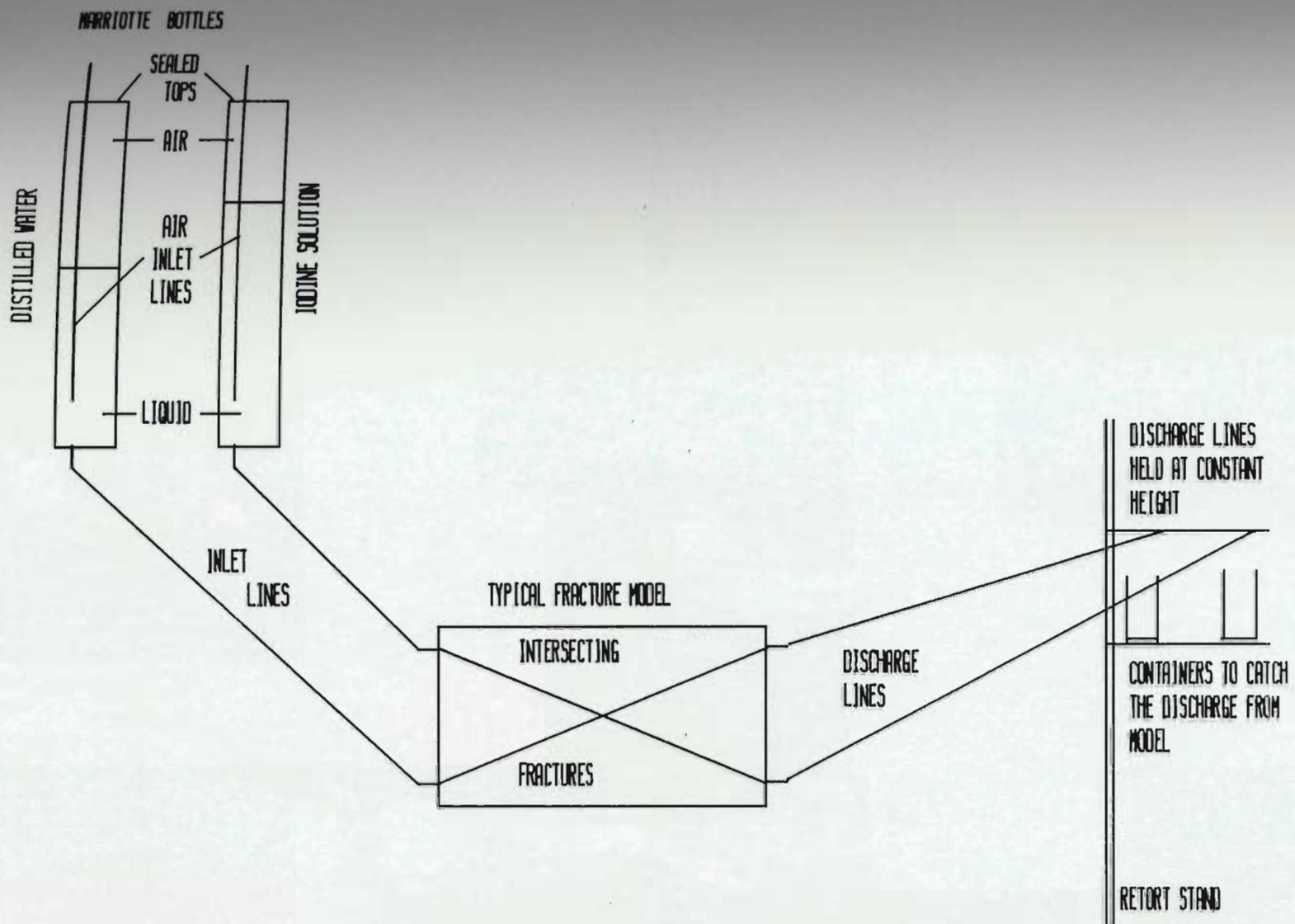


- Neretnieks, I., T. Eriksen, P. Tahtinen, Tracer Movement in a Single Fissure in Granitic Rock: Some Experimental Results and Their Interpretation, Water Resources Research, Vol. 18, No. 4, pp 849-858, August 1982.
- Noorishad, J. and M. Mehran, An Upstream Finite Element Method for Solution of Transient Transport Equation in Fractured Porous Media, Water Resources Research, Vol. 18, No.3, pp 588-596, June 1982.
- Ogata, A. and R.B. Banks, A Solution of the Differential Equation of Longitudinal Dispersion in Porous Media, U.S. Geological Survey Professional Paper 411-A, 7 pp, 1961.
- Rasmuson, A., Analysis of Hydrodynamic Dispersion in Discrete Fracture Networks Using the Method of Moments, Water Resources Research, Vol. 21, No. 11, pp 1677-1683, November 1985.
- Rasmuson, A., T.N. Narasimhan, I. Neretnieks, Chemical Transport in a Fissured Rock: Verification of a Numerical Model, Water Resources Research, Vol. 18, No. 5, pp 1479-1492, October 1982.
- Rouleau, A., Statistical Characterization and Numerical Simulation of a Fracture System - Application to Groundwater Flow in the Stripa Granite, Phd. Thesis, University of Waterloo, Ontario, Canada, 1984.
- Schwartz, F.W., L. Smith, and A.S. Crowe, A Stochastic Analysis of Macroscopic Dispersion in Fractured Media, Water Resources Research, Vol. 19, No. 5, pp 1253-1265, October, 1983.
- Smith, L., C.W. Mase, F.W. Schwartz, D. Chorley, A Numerical Model for Transport in Networks of Planar Fractures, International Association of Hydrogeologists Memoirs, Vol. XVII, Proceedings Hydrogeology of Rock of Low Permeability, Tucson Arizona, 1985.
- Sudicky, E.A. and E.O. Frind, Contaminant Transport in Fractured Porous Media: Analytical Solutions for a System of Parallel Fractures, Water Resources Research, Vol. 18, No. 6, pp 1634-1642, December 1982.
- Tsang, Y.W., The Effect of Tortuosity on Fluid Flow Through a Single Fracture, Water Resources Research, Vol. 20, No. 9, pp 1209-1215, September 1984.

Wilson, C.R. and P.A. Witherspoon, Flow Interference Effects  
at Fracture Intersections, Water Resources Research Vol.  
12, No. 1, Feb. 1976.

APPENDIX A  
TESTING RESULTS OF PLEXIGLASS FRACTURE MODELS

Figure A-1 Diagram of experimental setup.



### CALCULATION OF MIXING RESULTS FOR MODEL ONE

The mixing test results, that are listed in this appendix were calculated using the equations that are described in Chapter Two. The use of these equations is illustrated below. The test results from Model one (page \*\*\*) are used for this purpose. In the calculations that follow reference should be made to Figure 2.5 for the physical meaning of the terms. The terms are defined as follows:

- Vs The volume of iodide solution injected into the fracture intersection.
- Vw The volume of distilled water injected into the fracture intersection.
- Vi The volume of fluid discharged from fracture segment i.
- C The concentration of iodide in the injection solution.
- C2 The concentration of iodide in the distilled water.
- Ci The concentration of iodide in the discharge from fracture segment i.
- Vsi The volume of iodide solution found in the discharge from fracture segment i.
- Vsi' The volume of iodide solution forced into discharge fracture segment i.
- Vwi The volume of distilled water found in the discharge from fracture segment i.
- Vwi' The volume of distilled water forced into discharge fracture segment i.
- Mi The percent mixing that occurs in fracture segment i.
- Mi' The adjusted percent mixing that occurs in fracture segment i.

**T<sub>Mi</sub>** The total mixing that takes place in fracture segment i.

**F<sub>Mi</sub>** The forced mixing that takes place in fracture segment i.

In the calculations that follow the results are not exactly the same as listed on page \*\*\*. This is because more significant figures were used to produce the results on page 114.

### TEST RESULTS

The flow volumes and concentrations of Iodide for the various fracture segments are given on page \*\*\* as follows:

V <sub>s</sub> = 0.12857 L	C = 110.1 mg/L
V <sub>w</sub> = 0.73076 L	C <sub>2</sub> = 0.00 mg/L
V <sub>3</sub> = 0.12733 L	C <sub>3</sub> = 0.467 mg/L
V <sub>4</sub> = 0.73200 L	C <sub>4</sub> = 18.067 mg/L

### ERROR VALUES

The experimental error that occurred during the testing was determined from Equation (2.11) as follows:

$$\begin{aligned}
 E &= 100 \frac{\text{abs}[(V_s C) - (V_3 C_3) - (V_4 C_4)]}{V_s C} \\
 &= 100 \frac{\text{abs}[14.16 - 0.059 - 13.23]}{14.16} \\
 &= 6.15
 \end{aligned}$$

## MIXING RESULTS

### COMPONENT VOLUME OF IODINE SOLUTION

#### ACTUAL VALUES

The component volumes of distilled water and iodine solution that were contained in the discharge segments of the fracture intersection are calculated using Equation 2.5 as follows:

$$\begin{aligned}Vw3 &= \frac{V3 (C - C3)}{C} \\&= \frac{0.12733(110.1-0.467)}{110.1} \\&= 0.12679\end{aligned}$$

$$\begin{aligned}Vs3 &= V3 - Vw3 \\&= 0.12733-0.12679 \\&= 0.00054\end{aligned}$$

$$\begin{aligned}Vw4 &= \frac{V4 (C - C4)}{C} \\&= \frac{0.732(110.1-18.067)}{110.1} \\&= 0.61188\end{aligned}$$

$$\begin{aligned}Vs4 &= V4 - Vw4 \\&= 0.732-0.61188\end{aligned}$$



$$= 0.12012$$

#### ASSUMING 100% MIXING

When perfect or 100% mixing is assumed the component volumes of iodine solution and distilled water are determined from the ratio of the volumes of each that are injected into the two inlet fractures. The ratio  $V_s/V_w$  must be reflected in each of the discharge fractures. The determination is done as follows:

$$\begin{aligned} V_{w3} &= V_3 \frac{V_w}{V_w + V_s} \\ &= 0.12733 \frac{0.73076}{0.73076 + 0.12857} \\ &= 0.10828 \end{aligned}$$

$$\begin{aligned} V_{s3} &= V_3 - V_{w3} \\ &= 0.12733 - 0.10828 \\ &= 0.01905 \end{aligned}$$

$$\begin{aligned} V_{w4} &= V_4 \frac{V_w}{V_w + V_s} \\ &= 0.732 \frac{0.73076}{0.73076 + 0.12857} \\ &= 0.62248 \end{aligned}$$

$$\begin{aligned} V_{s4} &= V_4 - V_{w4} \\ &= 0.732 - 0.62248 \\ &= 0.10952 \end{aligned}$$

#### ACTUAL MIXING VALUES

The actual mixing values are determined from Equations (2.7) and (2.8) as follows:

$$\begin{aligned} M_3 &= 100 \frac{V_{s3}/V_{w3}}{V_s/V_w} \\ &= 100 \frac{0.00054/0.12679}{0.12857/0.73076} \\ &= 2.42 \end{aligned}$$

$$\begin{aligned} M_4 &= 100 \frac{V_{w4}/V_{s4}}{V_w/V_s} \\ &= 100 \frac{0.61188/0.12012}{0.73076/0.12857} \\ &= 89.62 \end{aligned}$$

#### ADJUSTED MIXING VALUES

The adjusted mixing values were calculated for Equation (2.9) as follows:

$$M_i' = T_{Mi} - F_{Mi}$$

$F_{Mi}$  is determined from Equation (2.10) as follows:

$$F_{Mi} = 100 \frac{V_{si}/V_{wi}'}{V_s/V_w}$$

For the test under consideration the values of  $V_{wi}'$  are determined as follows:

$$\begin{aligned} V_{w3}' &= V_3 - V_w \\ &= - 0.60343 \end{aligned}$$

The negative value means that no distilled water was forced into discharge Fracture Segment 3.

$$V_{w4}' = V_w - V_3 = 0.60343$$

These two equations are not mentioned in the text because they are not the same when distilled water is injected at one of the other nodes. The form of the equations must be determined from each new test set-up. These tests have determined that fluid flows preferentially into the adjacent fracture segment as illustrated in Figure 2.6. This fact must be used to determine the form of the appropriate equations.

Using the values determined above, the adjusted mixing

value is calculated as follows:

$$FM3 = 100 \frac{0.00054/0.0}{0.12857/0.73076}$$

This equation of course cannot be evaluated. The ratio terms must be inverted as follows:

$$\begin{aligned} FM3 &= 100 \frac{Vw3'/Vs3}{Vw/Vs} \\ &= 100 \frac{0.0/0.00054}{0.73076/0.12857} \\ &= 0.0 \end{aligned}$$

Therefore there is no forced mixing in Fracture Segment 3 and thus the adjusted mixing value is given by:

$$\begin{aligned} M3' &= 2.42 - 0.0 \\ &= 2.42 \end{aligned}$$

For Segment 4 the calculations are as follows:

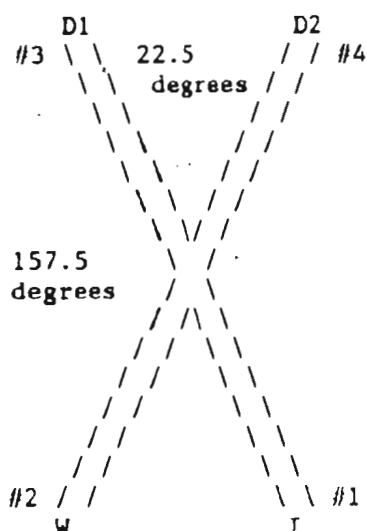
$$\begin{aligned} FM4 &= 100 \frac{Vs4/Vw4'}{Vs/Vw} \\ &= 100 \frac{0.12012/0.60343}{0.12857/0.73076} \\ &= 113.14 \end{aligned}$$

This value is clearly in error. The ratio terms must be inverted as for the other segment. This follows:

$$\begin{aligned} FM4 &= 100 \frac{Vw4'/Vs4}{Vw/Vs} \\ &= 100 \frac{0.60343/0.12012}{0.73076/0.12857} \\ &= 88.26 \end{aligned}$$

The adjusted mixing value is calculated as follows:

$$\begin{aligned} M4' &= TM4 - FM4 \\ &= 89.62 - 88.26 \\ &= 1.36 \end{aligned}$$



## FLOW CONFIGURATION

I solution inlet (I)	1
distilled water inlet (W)	2
discharge #1 (D1)	3
discharge #2 (D2)	4

## APERTURE/DEPTH CONFIGURATION

fracture #1-#3	0.28 mm
fracture #2-#4	0.5 mm

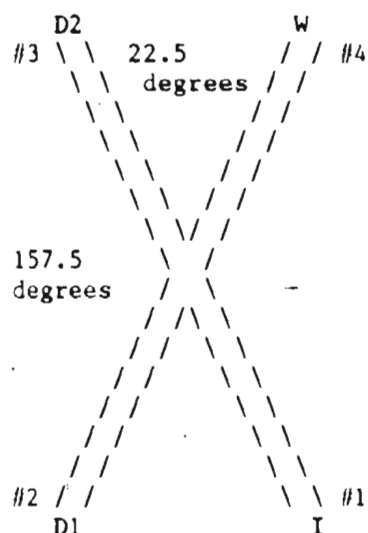
depth of f #1-3 = 15.0 mm  
 depth of f #2-4 = 14.0 mm

## TEST RESULTS (Average for 3 tests)

TEST CONDITIONS m, ,s,Z	FRACTURE NUMBER	FLOW VOLUME L	VELOCITY OF FLOW m/s	REYNOLDS NUMBER	IODINE CONCENTRATION mg/L
HEAD = 100.00	1	.129	.181	100.85	110.10
GRAD = 3.33	2	.731	.622	617.39	0.00
TIME = 156.92	3	.127	.207	115.24	.47
ERROR = 6.40	4	.732	.717	712.40	18.07
HEAD = 50.00	1	.086	.097	53.78	110.10
GRAD = 1.67	2	.479	.323	320.50	0.00
TIME = 197.87	3	.078	.100	55.69	0.00
ERROR = 7.98	4	.487	.379	376.02	17.83
HEAD = 10.00	1	.082	.021	11.78	110.10
GRAD = .33	2	.494	.076	75.48	0.00
TIME = 866.70	3	.081	.024	13.24	.03
ERROR = 12.95	4	.495	.088	87.33	15.90

## MIXING RESULTS (Average for 3 tests)

TEST CONDITIONS m, ,	DISCHARGE NUMBER	VOL. OF I SOL. 100% MIXING L	ACTUAL VALUES L	VOL. OF WATER 100% MIXING L	ACTUAL VALUES L	MIXING ACTUAL Z	MIXING ADJUSTED Z
HEAD = 100.0	1	.019	.001	.108	.127	2.30	2.30
GRAD = 3.3	2	.110	.120	.622	.612	90.02	1.31
HEAD = 50.0	1	.012	0.000	.066	.078	0.00	0.00
GRAD = 1.7	2	.074	.079	.413	.408	92.61	1.55
HEAD = 10.0	1	.012	0.000	.069	.081	.18	.18
GRAD = .3	2	.071	.071	.425	.424	98.58	2.48



## FLOW CONFIGURATION

I solution inlet (I) 1  
 distilled water inlet (W) 4  
 discharge #1 (D1) 2  
 discharge #2 (D2) 3

## APERTURE/DEPTH CONFIGURATION

fracture #1-#3 0.28 mm  
 fracture #2-#4 0.5 mm

depth of f #1-3 = 15.0 mm  
 depth of f #2-4 = 14.0 mm

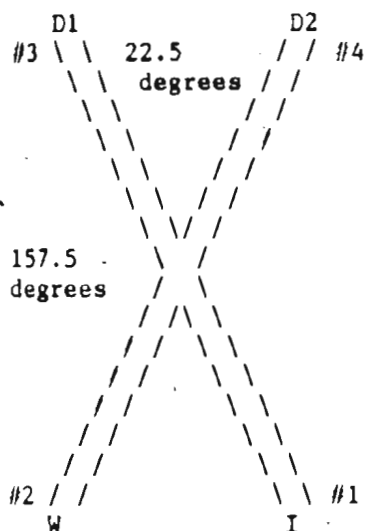
## TEST RESULTS (Average for 3 tests)

TEST CONDITIONS m, s, %	FRACTURE NUMBER	FLOW VOLUME L	VELOCITY OF FLOW m/s	REYNOLDS NUMBER	IODINE CONCENTRATION mg/L
HEAD = 100.00	1	.104	.201	111.74	104.10
GRAD = 3.33	4	.535	.717	711.77	0.00
TIME = 114.86	2	.553	.642	637.78	19.60
ERROR = 6.09	3	.085	.189	105.29	.30
HEAD = 50.00	1	.093	.101	56.31	104.10
GRAD = 1.67	4	.494	.371	368.80	0.00
TIME = 204.69	2	.510	.332	329.67	18.07
ERROR = 4.67	3	.077	.096	53.59	.03
HEAD = 10.00	1	.061	.022	12.13	104.10
GRAD = .33	4	.351	.087	86.06	0.00
TIME = 622.86	2	.358	.077	76.11	17.87
ERROR = 2.77	3	.054	.022	12.22	.03

## MIXING RESULTS (Average for 3 tests)

TEST CONDITIONS m, s	DISCHARGE NUMBER	VOL. OF I SOL.		VOL. OF WATER		MIXING	
		100% MIXING L	ACTUAL VALUES L	100% MIXING L	ACTUAL VALUES L	ACTUAL %	ADJUSTED %
HEAD = 100.0	1	.090	.104	.464	.450	83.81	0.00
GRAD = 3.3	2	.014	0.000	.071	.085	1.64	1.64
HEAD = 50.0	1	.081	.088	.429	.421	89.46	.93
GRAD = 1.7	2	.012	0.000	.065	.077	.17	.17
HEAD = 10.0	1	.053	.061	.305	.297	83.82	0.00
GRAD = .3	2	.008	0.000	.046	.054	.18	.18





## FLOW CONFIGURATION

I solution inlet (I) 1  
 distilled water inlet (W) 2  
 discharge #1 (D1) 3  
 discharge #2 (D2) 4

## APERTURE/DEPTH CONFIGURATION

fracture #1-#3 0.5 mm  
 fracture #2-#4 0.5 mm

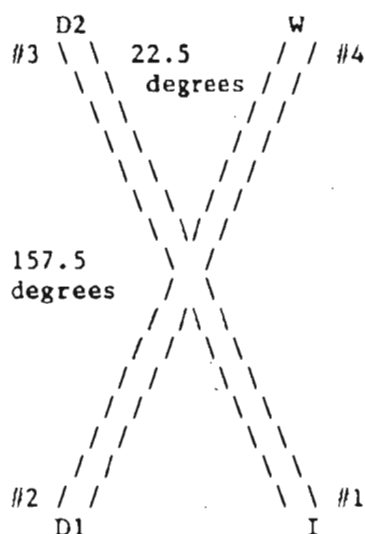
depth of f #1-3 = 13.75 mm  
 depth of f #2-4 = 14.5 mm

## TEST RESULTS (Average for 3 tests)

TEST CONDITIONS m, s, %	FRACTURE NUMBER	FLOW VOLUME L	VELOCITY OF FLOW m/s	REYNOLDS NUMBER	IODINE CONCENTRATION mg/L
HEAD = 100.00	1	.171	.659	654.01	102.00
GRAD = 3.33	2	.163	.583	578.53	0.00
TIME = 38.57	3	.164	.609	604.63	4.40
ERROR = 1.61	4	.170	.608	603.66	96.97
HEAD = 50.00	1	.083	.344	341.28	102.00
GRAD = 1.67	2	.079	.304	301.52	0.00
TIME = 35.92	3	.079	.316	313.55	2.47
ERROR = 2.35	4	.083	.319	316.53	99.47
HEAD = 10.00	1	.071	.087	86.14	102.00
GRAD = .33	2	.060	.068	67.58	0.00
TIME = 121.68	3	.065	.076	75.78	6.47
ERROR = 3.63	4	.066	.075	74.62	102.00

## MIXING RESULTS (Average for 3 tests)

TEST CONDITIONS m, s	DISCHARGE NUMBER	VOL. OF I SOL.		VOL. OF WATER		MIXING	
		100% MIXING L	ACTUAL VALUES L	100% MIXING L	ACTUAL VALUES L	ACTUAL %	ADJUSTED %
HEAD = 100.0	1	.084	.007	.080	.157	4.30	3.44
GRAD = 3.3	2	.087	.161	.083	.009	5.55	5.55
HEAD = 50.0	1	.041	.002	.039	.077	2.35	1.94
GRAD = 1.7	2	.043	.081	.040	.002	2.75	2.75
HEAD = 10.0	1	.035	.004	.030	.061	5.67	0.00
GRAD = .3	2	.036	.066	.030	0.000	0.00	0.00



## FLOW CONFIGURATION

I solution inlet (I)	1
distilled water inlet (W)	4
discharge #1 (D1)	2
discharge #2 (D2)	3

## APERTURE/DEPTH CONFIGURATION

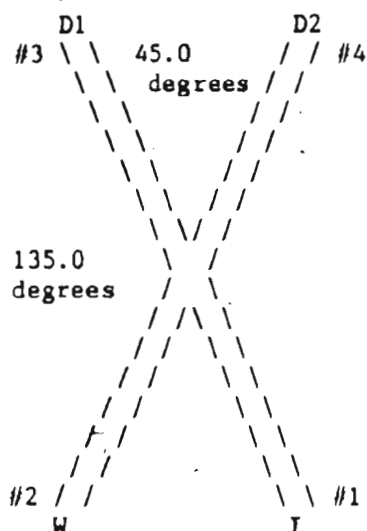
fracture #1-#3	0.5 mm
fracture #2-#4	0.5 mm
depth of f #1-3	= 13.75 mm
depth of f #2-4	= 14.5 mm

## TEST RESULTS (Average for 3 tests)

TEST CONDITIONS m, s, %	FRACTURE NUMBER	FLOW VOLUME L	VELOCITY OF FLOW m/s	REYNOLDS NUMBER	IODINE CONCENTRATION mg/L
HEAD = 100.00	1	.136	.605	600.40	103.80
GRAD = 3.33	4	.138	.572	567.86	0.00
TIME = 33.27	2	.137	.568	564.01	102.27
ERROR = 1.09	3	.137	.587	582.94	.97
HEAD = 50.00	1	.083	.319	316.81	103.80
GRAD = 1.67	4	.086	.304	301.76	0.00
TIME = 38.75	2	.084	.300	297.66	101.00
ERROR = 1.31	3	.085	.312	309.74	.70
HEAD = 10.00	1	.068	.078	77.29	103.80
GRAD = .33	4	.064	.069	68.14	0.00
TIME = 129.19	2	.068	.072	71.85	103.00
ERROR = 1.25	3	.064	.071	70.69	.40

## MIXING RESULTS (Average for 3 tests)

TEST CONDITIONS m, ,	DISCHARGE NUMBER	VOL. OF I SOL.		VOL. OF WATER		MIXING	
		100% MIXING L	ACTUAL VALUES L	100% MIXING L	ACTUAL VALUES L	ACTUAL %	ADJUSTED %
HEAD = 100.0	1	.068	.135	.069	.002	1.48	.54
GRAD = 3.3	2	.068	.001	.069	.135	.96	.96
HEAD = 50.0	1	.042	.082	.043	.002	2.77	1.70
GRAD = 1.7	2	.042	.001	.043	.084	.70	.70
HEAD = 10.0	1	.035	.067	.033	.001	.82	.82
GRAD = .3	2	.033	0.000	.031	.064	.37	.23



## FLOW CONFIGURATION

I solution inlet (I)	1
distilled water inlet (W)	2
discharge #1 (D1)	3
discharge #2 (D2)	4

## APERTURE/DEPTH CONFIGURATION

fracture #1-#3	0.28 mm
fracture #2-#4	0.5 mm

depth of f #1-3 = 14.25 mm

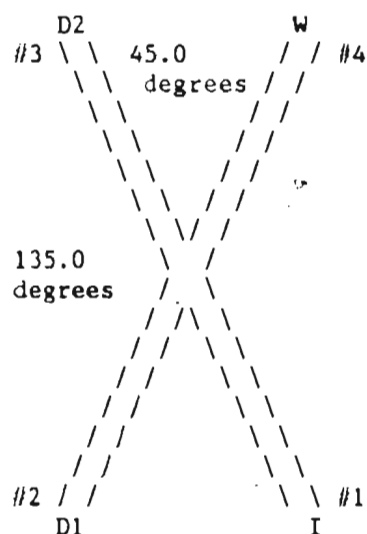
depth of f #2-4 = 15.0 mm

## TEST RESULTS (Average for 3 tests)

TEST CONDITIONS m, ,s,Z	FRACTURE NUMBER	FLOW VOLUME L	VELOCITY OF FLOW m/s	REYNOLDS NUMBER	IODINE CONCENTRATION mg/L
HEAD = 100.00	1	.048	.260	144.86	103.80
GRAD = 3.33	2	.216	.639	635.00	0.00
TIME = 48.33	3	.045	.219	121.89	.27
ERROR = 2.78	4	.219	.568	563.58	23.07
HEAD = 50.00	1	.060	.130	72.02	103.80
GRAD = 1.67	2	.283	.336	333.82	0.00
TIME = 120.70	3	.057	.112	62.44	.10
ERROR = 3.79	4	.286	.296	294.33	21.33
HEAD = 10.00	1	.055	.031	17.03	103.80
GRAD = .33	2	.289	.087	86.03	0.00
TIME = 476.92	3	.056	.028	15.60	.03
ERROR = 3.00	4	.288	.076	75.03	19.33

## MIXING RESULTS (Average for 3 tests)

TEST CONDITIONS m, ,	DISCHARGE NUMBER	VOL. OF I SOL.		VOL. OF WATER		MIXING	
		100% MIXING L	ACTUAL VALUES L	100% MIXING L	ACTUAL VALUES L	ACTUAL Z	ADJUSTED Z
HEAD = 100.0	1	.008	0.000	.036	.044	1.16	1.16
GRAD = 3.3	2	.040	.049	.180	.171	77.10	0.00
HEAD = 50.0	1	.010	0.000	.047	.057	.46	.46
GRAD = 1.7	2	.050	.059	.236	.227	80.75	.17
HEAD = 10.0	1	.009	0.000	.047	.056	.16	.16
GRAD = .3	2	.046	.054	.242	.235	83.53	.57



## FLOW CONFIGURATION

I solution inlet (I)	1
distilled water inlet (W)	4
discharge #1 (D1)	2
discharge #2 (D2)	3

## APERTURE/DEPTH CONFIGURATION

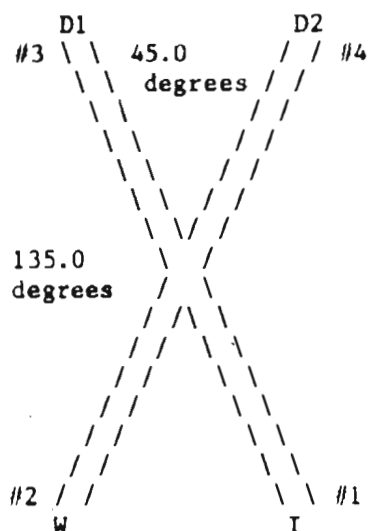
fracture #1-#3	0.28 mm
fracture #2-#4	0.5 mm
depth of f #1-3	= 14.25 mm
depth of f #2-4	= 15.0 mm

## TEST RESULTS (Average for 3 tests)

TEST CONDITIONS m, s, %	FRACTURE NUMBER	FLOW VOLUME L	VELOCITY OF FLOW m/s	REYNOLDS NUMBER	IODINE CONCENTRATION mg/L
HEAD = 100.00	1	.119	.243	135.24	105.70
GRAD = 3.33	4	.611	.589	585.06	0.00
TIME = 129.31	2	.611	.672	667.62	18.93
ERROR = 7.72	3	.120	.221	122.67	.57
HEAD = 72.70	1	.100	.168	93.35	105.73
GRAD = 2.42	4	.526	.417	414.15	0.00
TIME = 157.66	2	.519	.470	467.03	19.33
ERROR = 4.90	3	.107	.162	89.87	.23
HEAD = 10.00	1	.057	.023	12.58	105.80
GRAD = .33	4	.333	.062	61.43	0.00
TIME = 650.47	2	.315	.066	65.53	18.23
ERROR = 7.64	3	.076	.028	15.68	.03

## MIXING RESULTS (Average for 3 tests)

TEST CONDITIONS m, ,	DISCHARGE NUMBER	VOL. OF I SOL.		VOL. OF WATER		MIXING	
		100% MIXING L	ACTUAL VALUES L	100% MIXING L	ACTUAL VALUES L	ACTUAL %	ADJUSTED %
HEAD = 100.0	1	.100	.110	.511	.501	88.95	1.66
GRAD = 3.3	2	.020	.001	.100	.119	2.60	2.60
HEAD = 72.7	1	.083	.095	.436	.424	85.00	1.03
GRAD = 2.4	2	.017	0.000	.090	.107	1.16	1.16
HEAD = 10.0	1	.046	.053	.268	.261	83.93	1.23
GRAD = .3	2	.011	0.000	.065	.076	.13	.13



## FLOW CONFIGURATION

I solution inlet (I)	1
distilled water inlet (W)	2
discharge #1 (D1)	3
discharge #2 (D2)	4

## APERTURE/DEPTH CONFIGURATION

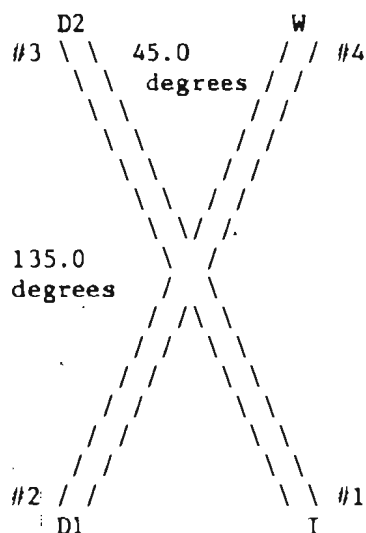
fracture #1-#3	0.36 mm
fracture #2-#4	0.5 mm
depth of f #1-3 =	14.25 mm
depth of f #2-4 =	14.25 mm

## TEST RESULTS (Average for 3 tests)

TEST CONDITIONS m, , s, %	FRACTURE NUMBER	FLOW VOLUME L	VELOCITY OF FLOW m/s	REYNOLDS NUMBER	IODINE CONCENTRATION mg/L
HEAD = 100.00	1	.189	.360	257.51	105.00
GRAD = 3.33	2	.500	.709	703.94	0.00
TIME = 100.69	3	.175	.344	246.08	.17
ERROR = 7.92	4	.515	.704	699.59	35.60
HEAD = 50.00	1	.100	.175	125.19	105.00
GRAD = 1.67	2	.276	.361	358.37	0.00
TIME = 109.39	3	.098	.178	127.09	.20
ERROR = 8.06	4	.278	.351	348.50	34.60
HEAD = 10.00	1	.081	.042	30.30	105.00
GRAD = .33	2	.222	.087	86.04	0.00
TIME = 365.81	3	.078	.042	30.15	.10
ERROR = 3.74	4	.225	.085	84.26	37.13

## MIXING RESULTS (Average for 3 tests)

TEST CONDITIONS m, ,	DISCHARGE NUMBER	VOL. OF I SOL. 100% MIXING L	ACTUAL VALUES L	VOL. OF WATER 100% MIXING L	ACTUAL VALUES L	MIXING ACTUAL %	ADJUSTED %
HEAD = 100.0	1	.048	0.000	.127	.174	.42	.42
GRAD = 3.3	2	.141	.174	.374	.341	73.95	3.29
HEAD = 50.0	1	.026	0.000	.072	.098	.53	.53
GRAD = 1.7	2	.074	.092	.204	.187	73.68	3.29
HEAD = 10.0	1	.021	0.000	.057	.078	.26	.26
GRAD = .3	2	.060	.080	.165	.145	66.15	.43



## FLOW CONFIGURATION

I solution inlet (I) 1  
 distilled water inlet (W) 4  
 discharge #1 (D1) 2  
 discharge #2 (D2) 3

## APERTURE/DEPTH CONFIGURATION

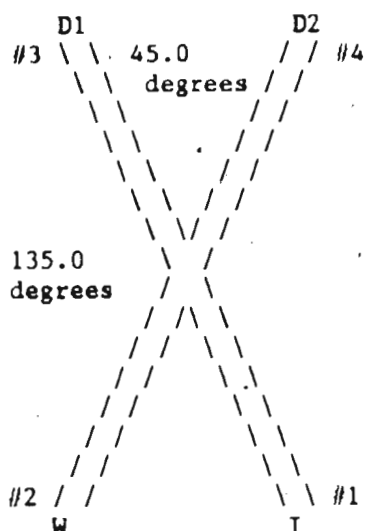
fracture #1-#3 0.36 mm  
 fracture #2-#4 0.5 mm  
 depth of f #1-3 = 14.25 mm  
 depth of f #2-4 = 14.25 mm

## TEST RESULTS (Average for 3 tests)

TEST CONDITIONS m, s, %	FRACTURE NUMBER	FLOW VOLUME L	VELOCITY OF FLOW m/s	REYNOLDS NUMBER	IODINE CONCENTRATION mg/L
HEAD = 100.00	1	.133	.342	244.85	110.30
GRAD = 3.33	4	.349	.646	641.37	0.00
TIME = 74.50	2	.357	.684	679.65	38.90
ERROR = 5.00	3	.125	.333	238.23	.57
HEAD = 50.00	1	.152	.170	121.61	105.10
GRAD = 1.67	4	.423	.341	338.17	0.00
TIME = 171.28	2	.430	.358	355.83	34.43
ERROR = 7.10	3	.145	.168	120.36	.37
HEAD = 10.00	1	.098	.040	28.65	105.10
GRAD = .33	4	.260	.077	76.49	0.00
TIME = 465.87	2	.275	.084	83.65	35.90
ERROR = 7.30	3	.083	.035	25.26	.13

## MIXING RESULTS (Average for 3 tests)

TEST CONDITIONS m, ,	DISCHARGE NUMBER	VOL. OF I SOL. 100% MIXING L	ACTUAL VALUES L	VOL. OF WATER 100% MIXING L	ACTUAL VALUES L	MIXING ACTUAL %	ADJUSTED %
HEAD = 100.0	1	.099	.126	.258	.231	70.05	2.22
GRAD = 3.3	2	.035	.001	.091	.125	1.36	1.36
HEAD = 50.0	1	.114	.141	.316	.289	73.82	2.91
GRAD = 1.7	2	.039	.001	.107	.145	.98	.98
HEAD = 10.0	1	.075	.094	.200	.181	72.36	1.51
GRAD = .3	2	.023	0.000	.060	.083	.34	.34



## FLOW CONFIGURATION

I solution inlet (I)	1
distilled water inlet (W)	2
discharge #1 (D1)	3
discharge #2 (D2)	4

## APERTURE/DEPTH CONFIGURATION

fracture #1-#3	0.5 mm
fracture #2-#4	0.5 mm
depth of f #1-3	= 14.25 mm
depth of f #2-4	= 14.25 mm

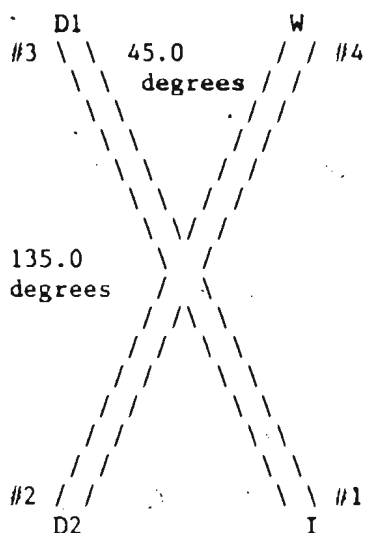
## TEST RESULTS (Average for 3 tests)

TEST CONDITIONS m, , s, %	FRACTURE NUMBER	FLOW VOLUME L	VELOCITY OF FLOW m/s	REYNOLDS NUMBER	IODINE CONCENTRATION mg/L
HEAD = 100.00	1	.210	.646	641.62	102.40
GRAD = 3.33	2	.199	.635	630.74	0.00
TIME = 44.76	3	.205	.654	649.33	4.73
ERROR = 3.03	4	.204	.628	623.66	101.73
HEAD = 54.00	1	.219	.378	374.98	104.60
GRAD = 1.80	2	.203	.361	358.96	0.00
TIME = 80.04	3	.211	.377	374.04	12.30
ERROR = 3.16	4	.211	.363	360.42	95.50
HEAD = 10.00	1	.067	.076	75.30	102.40
GRAD = .33	2	.067	.079	78.11	0.00
TIME = 121.29	3	.069	.081	80.19	8.73
ERROR = 3.07	4	.065	.074	73.29	99.10

## MIXING RESULTS (Average for 3 tests)

TEST CONDITIONS m, ,	DISCHARGE NUMBER	VOL. OF I SOL.		VOL. OF WATER		MIXING	
		100% MIXING L	ACTUAL VALUES L	100% MIXING L	ACTUAL VALUES L	ACTUAL %	ADJUSTED %
HEAD = 100.0	1	.105	.009	.100	.196	4.59	1.90
GRAD = 3.3	2	.105	.204	.099	0.000	.13	.13
HEAD = 54.0	1	.110	.025	.101	.186	12.33	8.16
GRAD = 1.8	2	.109	.193	.101	.018	10.18	10.18
HEAD = 10.0	1	.034	.006	.034	.063	9.35	6.52
GRAD = .3	2	.032	.063	.032	.002	3.35	3.35





## FLOW CONFIGURATION

I solution inlet (I) 1  
 distilled water inlet (W) 4  
 discharge #1 (D1) -3  
 discharge #2 (D2) 2

## APERTURE/DEPTH CONFIGURATION

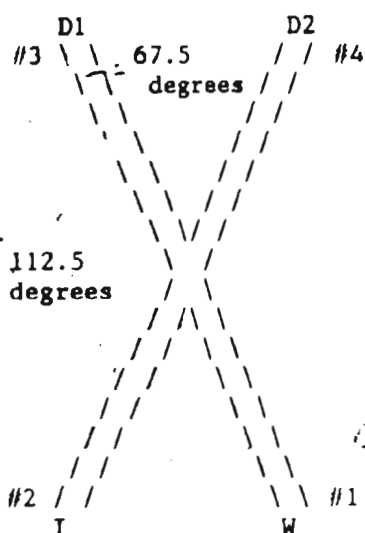
fracture #1-#3 0.5 mm  
 fracture #2-#4 0.5 mm  
 depth of f #1-3 = 14.25 mm  
 depth of f #2-4 = 14.25 mm

## TEST RESULTS (Average for 3 tests)

TEST CONDITIONS m, s, %	FRACTURE NUMBER	FLOW VOLUME L	VELOCITY OF FLOW m/s	REYNOLDS NUMBER	IODINE CONCENTRATION mg/L
HEAD = 100.00	1	.200	.583	578.83	104.50
GRAD = 3.33	4	.191	.545	541.16	0.00
TIME = 47.89	3	.198	.593	588.93	3.77
ERROR = 5.50	2	.193	.575	571.06	102.70
HEAD = 50.00	1	.114	.316	313.93	102.40
GRAD = 1.67	4	.113	.312	310.30	0.00
TIME = 49.90	3	.115	.329	327.17	3.53
ERROR = 2.11	2	.112	.322	319.35	102.40
HEAD = 10.00	1	.067	.084	83.63	102.40
GRAD = .33	4	.055	.070	69.21	0.00
TIME = 108.81	3	.061	.080	84.46	9.33
ERROR = 7.95	2	.060	.080	78.95	99.77

## MIXING RESULTS (Average for 3 tests)

TEST CONDITIONS m, ,	DISCHARGE NUMBER	VOL. OF I SOL.		VOL. OF WATER		MIXING	
		100% MIXING L	ACTUAL VALUES L	100% MIXING L	ACTUAL VALUES L	ACTUAL %	ADJUSTED %
HEAD = 100.0	1	.101	.007	.097	.191	3.58	0.00
GRAD = 3.3	2	.099	.189	.094	.003	1.93	1.93
HEAD = 50.0	1	.058	.004	.057	.111	3.53	1.80
GRAD = 1.7	2	.056	.112	.056	0.000	0.00	0.00
HEAD = 10.0	1	.034	.006	.027	.055	8.39	0.00
GRAD = .3	2	.033	.059	.027	.002	3.40	3.40



## FLOW CONFIGURATION

I solution inlet (I)	2
distilled water inlet (W)	1
discharge #1 (D1)	3
discharge #2 (D2)	4

## APERTURE/DEPTH CONFIGURATION

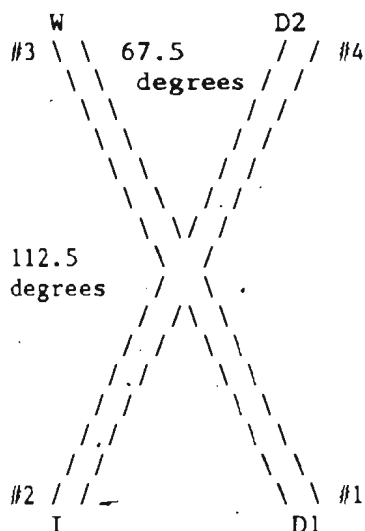
fracture #1-#3	0.28 mm
fracture #2-#4	0.5 mm
depth of f #1-3 =	14.25 mm
depth of f #2-4 =	14.25 mm

## TEST RESULTS (Average for 3 tests)

TEST CONDITIONS m, s, %	FRACTURE NUMBER	FLOW VOLUME L	VELOCITY OF FLOW m/s	REYNOLDS NUMBER	IODINE CONCENTRATION mg/L
HEAD = 100.00	2	.064	.088	87.63	102.10
GRAD = 3.33	1	.514	1.215	675.91	0.00
TIME = 104.08	3	.489	1.198	666.09	12.73
ERROR = 1.14	4	.089	.118	117.40	4.67
HEAD = 50.00	2	.058	.043	42.68	102.10
GRAD = 1.67	1	.498	.634	352.34	0.00
TIME = 193.72	3	.471	.620	344.92	12.07
ERROR = 4.50	4	.086	.061	60.53	.53
HEAD = 10.00	2	.039	.009	9.04	102.10
GRAD = .33	1	.366	.148	82.31	0.00
TIME = 609.23	3	.346	.145	80.39	11.47
ERROR = 5.28	4	.060	.014	13.42	.13

## MIXING RESULTS (Average for 3 tests)

TEST CONDITIONS m, s	DISCHARGE NUMBER	VOL. OF I SOL. 100% MIXING L	ACTUAL VALUES L	VOL. OF WATER 100% MIXING L	ACTUAL VALUES L	MIXING ACTUAL %	ADJUSTED %
HEAD = 100.0	1	.054	.061	.434	.428	87.85	.69
GRAD = 3.3	2	.010	.004	.079	.085	38.24	38.24
HEAD = 50.0	1	.049	.056	.422	.415	87.35	.56
GRAD = 1.7	2	.009	0.000	.077	.085	4.47	4.47
HEAD = 10.0	1	.033	.039	.312	.307	84.51	.10
GRAD = .3	2	.006	0.000	.054	.060	1.28	1.28



## FLOW CONFIGURATION

I solution inlet (I)	2
distilled water inlet (W)	3
discharge #1 (D1)	1
discharge #2 (D2)	4

## APERTURE/DEPTH CONFIGURATION

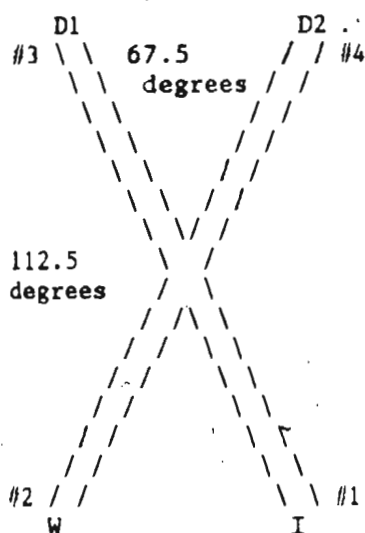
fracture #1-#3	0.28 mm
fracture #2-#4	0.5 mm
depth of f #1-3 =	14.25 mm
depth of f #2-4 =	14.25 mm

## TEST RESULTS (Average for 3 tests)

TEST CONDITIONS m, s, %	FRACTURE NUMBER	FLOW VOLUME L	VELOCITY OF FLOW m/s	REYNOLDS NUMBER	IODINE CONCENTRATION mg/L
HEAD = 100.00	2	.060	.085	84.44	100.60
GRAD = 3.33	3	.500	1.279	711.15	0.00
TIME = 99.68	1	.478	1.181	656.62	11.30
ERROR = 3.92	4	.081	.112	111.54	9.57
HEAD = 50.00	2	.060	.052	51.55	105.50
GRAD = 1.67	3	.428	.657	365.33	0.00
TIME = 165.93	1	.410	.609	338.65	10.17
ERROR = 30.34	4	.077	.064	63.85	3.00
HEAD = 10.00	2	.049	.010	9.95	100.60
GRAD = .33	3	.420	.154	85.59	0.00
TIME = 695.99	1	.399	.141	78.58	12.07
ERROR = 3.89	4	.069	.014	13.67	.40

## MIXING RESULTS (Average for 3 tests)

TEST CONDITIONS m, ,	DISCHARGE NUMBER	VOL. OF I SOL.		VOL. OF WATER		MIXING	
		100% MIXING L	ACTUAL VALUES L	100% MIXING L	ACTUAL VALUES L	ACTUAL %	ADJUSTED %
HEAD = 100.0	1	.051	.054	.427	.424	94.15	1.29
GRAD = 3.3	2	.009	.008	.073	.073	88.16	88.16
HEAD = 50.0	1	.050	.039	.360	.371	76.52	0.00
GRAD = 1.7	2	.009	.002	.068	.075	20.76	20.76
HEAD = 10.0	1	.042	.048	.358	.352	85.40	.24
GRAD = .3	2	.007	0.000	.062	.069	3.32	3.32



## FLOW CONFIGURATION

I solution inlet (I) 1  
 distilled water inlet (W) 2  
 discharge #1 (D1) 3  
 discharge #2 (D2) 4

## APERTURE/DEPTH CONFIGURATION

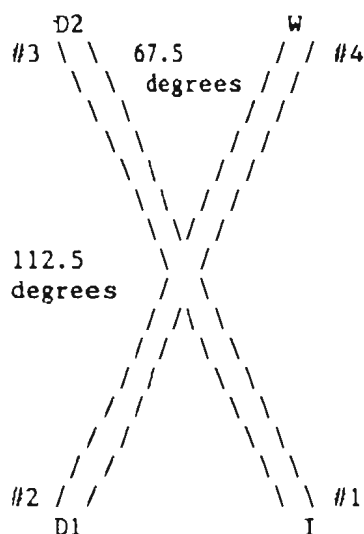
fracture #1-#3 0.36 mm  
 fracture #2-#4 0.5 mm  
 depth of f #1-3 = 13.75 mm  
 depth of f #2-4 = 14.25 mm

## TEST RESULTS (Average for 3 tests)

TEST CONDITIONS m, s, %	FRACTURE NUMBER	FLOW VOLUME L	VELOCITY OF FLOW m/s	REYNOLDS NUMBER	IODINE CONCENTRATION mg/L
HEAD = 100.00	1	.160	.325	232.72	102.80
GRAD = 3.33	2	.418	.612	607.46	0.00
TIME = 97.55	3	.137	.288	206.22	.77
ERROR = 7.87	4	.441	.624	619.21	34.13
HEAD = 50.00	1	.136	.163	116.34	102.80
GRAD = 1.67	2	.373	.323	320.47	0.00
TIME = 165.33	3	.125	.155	110.99	.23
ERROR = 8.61	4	.384	.321	318.41	33.07
HEAD = 10.00	1	.093	.038	26.88	102.80
GRAD = .33	2	.266	.078	76.96	0.00
TIME = 490.28	3	.084	.035	25.25	.07
ERROR = 5.75	4	.275	.077	76.76	32.73

## MIXING RESULTS (Average for 3 tests)

TEST CONDITIONS m, ,	DISCHARGE NUMBER	VOL. OF I SOL.		VOL. OF WATER		MIXING	
		100% MIXING L	ACTUAL VALUES L	100% MIXING L	ACTUAL VALUES L	ACTUAL %	ADJUSTED %
HEAD = 100.0	1	.038	.001	.099	.136	2.04	2.04
GRAD = 3.3	2	.122	.146	.320	.295	76.97	3.48
HEAD = 50.0	1	.033	0.000	.091	.124	.61	.61
GRAD = 1.7	2	.102	.124	.282	.261	76.62	3.54
HEAD = 10.0	1	.022	0.000	.062	.084	.18	.18
GRAD = .3	2	.071	.088	.204	.187	74.54	2.08



## FLOW CONFIGURATION

I solution inlet (I)	1
distilled water inlet (W)	4
discharge #1 (D1)	2
discharge #2 (D2)	3

## APERTURE/DEPTH CONFIGURATION

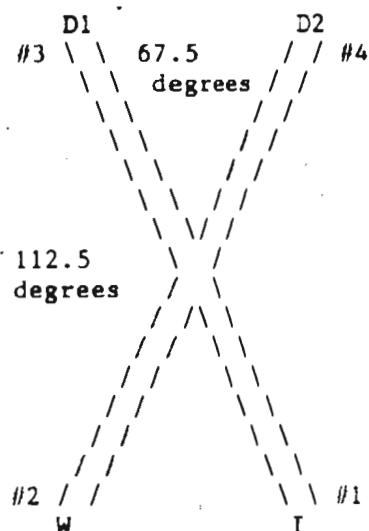
fracture #1-#3	0.36 mm
fracture #2-#4	0.5 mm
depth of f #1-3	= 13.75 mm
depth of f #2-4	= 14.25 mm

## TEST RESULTS (Average for 3 tests)

TEST CONDITIONS m, ,s,%	FRACTURE NUMBER	FLOW VOLUME L	VELOCITY OF FLOW m/s	REYNOLDS NUMBER	IODINE CONCENTRATION mg/L
HEAD = 100.00	1	.195	.322	230.52	103.40
GRAD = 3.33	4	.521	.596	592.33	0.00
TIME = 120.31	2	.541	.642	637.43	36.27
ERROR = 3.58	3	.175	.300	214.23	.87
HEAD = 50.00	1	.158	.166	118.94	103.40
GRAD = 1.67	4	.423	.310	307.43	0.00
TIME = 188.34	2	.439	.333	330.60	36.27
ERROR = 2.42	3	.142	.155	110.70	.37
HEAD = 10.00	1	.089	.038	27.39	103.40
GRAD = .33	4	.245	.073	72.72	0.00
TIME = 462.27	2	.251	.078	77.03	35.80
ERROR = 2.48	3	.084	.037	26.63	.17

## MIXING RESULTS (Average for 3 tests)

TEST CONDITIONS m, ,	DISCHARGE NUMBER	VOL. OF I SOL.		VOL. OF WATER		MIXING	
		100% MIXING L	ACTUAL VALUES L	100% MIXING L	ACTUAL VALUES L	ACTUAL %	ADJUSTED %
HEAD = 100.0	1	.147	.189	.393	.351	69.58	1.16
GRAD = 3.3	2	.048	.001	.127	.174	2.21	2.21
HEAD = 50.0	1	.120	.154	.319	.285	69.20	1.00
GRAD = 1.7	2	.039	0.000	.103	.141	.90	.90
HEAD = 10.0	1	.067	.087	.184	.164	68.71	1.00
GRAD = .3	2	.022	0.000	.061	.084	.44	.44



## FLOW CONFIGURATION

I solution inlet (I)	1
distilled water inlet (W)	2
discharge #1 (D1)	3
discharge #2 (D2)	4

## APERTURE/DEPTH CONFIGURATION

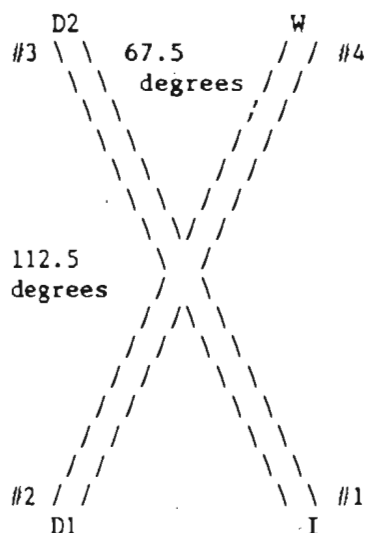
fracture #1-#3	0.5 mm
fracture #2-#4	0.5 mm
depth of f #1-3	= 14.1 mm
depth of f #2-4	= 13.9 mm

## TEST RESULTS (Average for 3 tests)

TEST CONDITIONS m, , s, %	FRACTURE NUMBER	FLOW VOLUME L	VELOCITY OF FLOW m/s	REYNOLDS NUMBER	IODINE CONCENTRATION mg/L
HEAD = 100.00	1	.274	.622	617.42	106.70
GRAD = 3.33	2	.270	.625	620.85	0.00
TIME = 61.79	3	.273	.630	625.51	3.80
ERROR = 6.85	4	.272	.640	635.13	96.30
HEAD = 50.00	1	.207	.330	327.57	106.70
GRAD = 1.67	2	.202	.327	324.78	0.00
TIME = 88.22	3	.205	.332	329.54	3.43
ERROR = 5.49	4	.205	.337	334.63	98.83
HEAD = 10.00	1	.125	.082	80.99	106.70
GRAD = .33	2	.114	.075	74.67	0.00
TIME = 215.91	3	.120	.079	78.92	5.40
ERROR = 2.91	4	.119	.080	79.60	104.07

## MIXING RESULTS (Average for 3 tests)

TEST CONDITIONS m, ,	DISCHARGE NUMBER	VOL. OF I SOL. 100% MIXING L	ACTUAL VALUES L	VOL. OF WATER 100% MIXING L	ACTUAL VALUES L	MIXING ACTUAL %	ADJUSTED %
HEAD = 100.0	1	.137	.010	.135	.263	3.66	2.86
GRAD = 3.3	2	.137	.245	.135	.026	10.94	10.94
HEAD = 50.0	1	.104	.007	.101	.198	3.26	1.99
GRAD = 1.7	2	.103	.189	.101	.016	8.49	8.49
HEAD = 10.0	1	.063	.006	.057	.114	4.87	.06
GRAD = .3	2	.062	.116	.057	.003	2.78	2.78



## FLOW CONFIGURATION

I solution inlet (I) 1  
 distilled water inlet (W) 4  
 discharge #1 (D1) 2  
 discharge #2 (D2) 3

## APERTURE/DEPTH CONFIGURATION

fracture #1-#3 0.5 mm  
 fracture #2-#4 0.5 mm

depth of f #1-3 = 14.1 mm  
 depth of f #2-4 = 13.9 mm

## TEST RESULTS (Average for 3 tests)

TEST CONDITIONS m, s, %	FRACTURE NUMBER	FLOW VOLUME L	VELOCITY OF FLOW m/s	REYNOLDS NUMBER	IODINE CONCENTRATION <sup>a</sup> mg/L
HEAD = 100.00	1	.269	.622	617.57	106.70
GRAD = 3.33	4	.262	.626	621.74	0.00
TIME = 60.74	2	.261	.614	609.62	98.83
ERROR = 4.72	3	.270	.634	629.61	5.77
HEAD = 50.00	1	.190	.327	324.84	106.70
GRAD = 1.67	4	.191	.341	338.35	0.00
TIME = 81.72	2	.188	.329	326.75	98.83
ERROR = 3.04	3	.194	.339	336.20	5.70
HEAD = 10.00	1	.144	.084	83.65	106.70
GRAD = .33	4	.131	.079	78.70	0.00
TIME = 240.01	2	.135	.080	79.74	104.10
ERROR = 1.28	3	.140	.083	82.69	8.07

## MIXING RESULTS (Average for 3 tests)

TEST CONDITIONS m, s	DISCHARGE NUMBER	VOL. OF I SOL.		VOL. OF WATER		MIXING	
		100% MIXING L	ACTUAL VALUES L	100% MIXING L	ACTUAL VALUES L	ACTUAL %	ADJUSTED %
HEAD = 100.0	1	.132	.242	.129	.019	7.94	7.94
GRAD = 3.3	2	.137	.015	.133	.255	5.58	2.51
HEAD = 50.0	1	.094	.175	.094	.014	7.74	7.74
GRAD = 1.7	2	.097	.010	.097	.183	5.68	4.42
HEAD = 10.0	1	.071	.132	.064	.003	2.75	2.75
GRAD = .3	2	.073	.011	.066	.129	7.43	.96

D2

#3 : :		FLOW CONFIGURATION
: :		-----
90.0 : :		I solution inlet (I) 2
degrees : :		distilled water inlet (W) 1
: :		discharge #1 (D1) 4
: :		discharge #2 (D2) 3
#2 : :	#4	.....
.....		
I	D1	
.....		
: :		APERTURE/DEPTH CONFIGURATION
: :		-----
90.0 : :		fracture #1-#3 0.5 mm
degrees : :		fracture #2-#4 0.28 mm
: :		
#1 : :		depth of f 1-3 = 12.8 mm
W		depth of f 2-4 = 13.5 mm
		.....

TEST RESULTS (Average for 3 tests)

TEST CONDITIONS m, ,s,Z	FRACTURE NUMBER	FLOW VOLUME L	VELOCITY OF FLOW m/s	REYNOLDS NUMBER	IODINE CONCENTRATION mg/L
HEAD = 100.00	2	.085	.203	112.83	104.00
GRAD = 3.33	1	.556	.746	741.07	0.00
TIME = 119.09	4	.086	.177	98.39	4.67
ERROR = 6.95	3	.555	.716	711.31	14.03
HEAD = 50.00	2	.073	.100	55.67	104.00
GRAD = 1.67	1	.505	.387	384.04	0.00
TIME = 208.86	4	.078	.092	51.02	1.83
ERROR = 7.96	3	.500	.368	365.90	13.70
HEAD = 10.00	2	.066	.023	12.67	104.00
GRAD = .33	1	.465	.090	89.60	0.00
TIME = 824.24	4	.070	.021	11.62	.97
ERROR = 6.64	3	.461	.086	85.38	13.70

MIXING RESULTS (Average for 3 tests)

TEST CONDITIONS m, ,	DISCHARGE NUMBER	VOL. OF I SOL.		VOL. OF WATER		MIXING	
		100Z MIXING L	ACTUAL VALUES L	100Z MIXING L	ACTUAL VALUES L	ACTUAL Z	ADJUSTED Z
HEAD = 100.0	1	.011	.004	.074	.082	30.85	30.85
GRAD = 3.3	2	.073	.075	.481	.480	97.69	1.99
HEAD = 50.0	1	.010	.001	.068	.076	12.44	12.44
GRAD = 1.7	2	.063	.066	.437	.434	95.42	1.58
HEAD = 10.0	1	.009	.001	.061	.069	6.62	6.62
GRAD = .3	2	.057	.061	.404	.400	92.98	1.14



D1  
 #3 : :  
 : :  
 : :  
 90.0 : :  
 degrees : :  
 : :  
 #2 : : #4  
 .....  
 W D2  
 .....

## FLOW CONFIGURATION

-----  
 I solution inlet (I) 1  
 distilled water inlet (W) 2  
 discharge #1 (D1) 3  
 discharge #2 (D2) 4  
 .....

## APERTURE/DEPTH CONFIGURATION

-----  
 : :  
 : : fracture #1-#3 0.5 mm  
 90.0 : : fracture #2-#4 0.36 mm  
 degrees : :  
 : :  
 #1 : : depth of f 1-3 = 13.8 mm  
 I depth of f 2-4 = 13.1 mm  
 .....

## TEST RESULTS (Average for 3 tests)

TEST CONDITIONS m, ,s,Z	FRACTURE NUMBER	FLOW VOLUME L	VELOCITY OF FLOW m/s	REYNOLDS NUMBER	IODINE CONCENTRATION mg/L
HEAD = 100.00	1	.215	.588	584.27	102.00
GRAD = 3.33	2	.095	.402	287.26	0.00
TIME = 50.32	3	.227	.694	688.78	62.97
ERROR = 6.86	4	.084	.358	255.69	100.73
HEAD = 50.00	1	.092	.312	309.75	102.00
GRAD = 1.67	2	.038	.197	140.60	0.00
TIME = 40.50	3	.094	.358	355.65	67.93
ERROR = 7.09	4	.035	.186	133.14	102.00
HEAD = 10.00	1	.176	.077	76.37	102.00
GRAD = .33	2	.054	.036	25.84	0.00
TIME = 316.03	3	.174	.085	84.12	70.50
ERROR = 2.07	4	.057	.038	27.40	102.00

## MIXING RESULTS (Average for 3 tests)

TEST CONDITIONS m, ,	DISCHARGE NUMBER	VOL. OF I SOL.		VOL. OF WATER		MIXING	
		100% MIXING L	ACTUAL VALUES L	100% MIXING L	ACTUAL VALUES L	ACTUAL %	ADJUSTED %
HEAD = 100.0	1	.157	.139	.070	.088	70.40	3.99
GRAD = 3.3	2	.058	.083	.026	.001	3.48	3.48
HEAD = 50.0	1	.067	.063	.028	.032	81.65	8.14
GRAD = 1.7	2	.025	.035	.010	0.000	0.00	0.00
HEAD = 10.0	1	.133	.120	.041	.054	69.17	.42
GRAD = .3	2	.043	.057	.013	0.000	0.00	0.00

W  
#3 : :  
: :  
: :  
90.0 : :  
degrees : :  
: :  
#2 : : #4  
.....  
I D1  
.....

## FLOW CONFIGURATION

I solution inlet (I) 2  
distilled water inlet (W) 3  
discharge #1 (D1) 4  
discharge #2 (D2) 1  
.....

## APERTURE/DEPTH CONFIGURATION

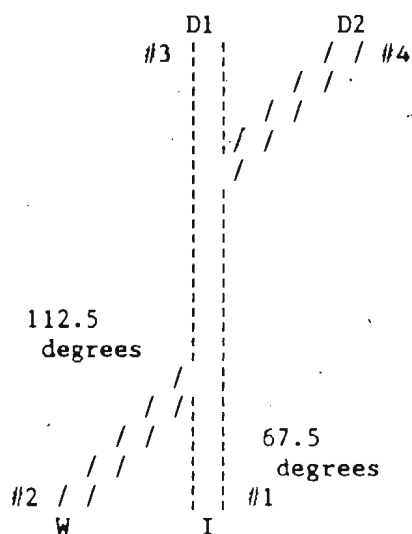
90.0 : :  
degrees : :  
: :  
#1 : :  
D2  
.....  
fracture #1-#3 0.5 mm  
fracture #2-#4 0.5 mm  
depth of f 1-3 = 14.25 mm  
depth of f 2-4 = 14.25 mm  
.....

## TEST RESULTS (Average for 3 tests)

TEST CONDITIONS m, s, %	FRACTURE NUMBER	FLOW VOLUME L	VELOCITY OF FLOW m/s	REYNOLDS NUMBER	IODINE CONCENTRATION mg/L
HEAD = 109.00	2	.245	.570	566.18	106.90
GRAD = 3.63	3	.247	.592	587.67	0.00
TIME = 61.03	4	.248	.596	592.02	6.00
ERROR = 3.33	1	.244	.566	561.99	100.03
HEAD = 54.00	2	.152	.350	347.63	106.90
GRAD = 1.80	3	.153	.365	362.09	0.00
TIME = 60.04	4	.157	.373	370.06	6.20
ERROR = 2.52	1	.149	.342	339.93	101.37
HEAD = 10.00	2	.126	.082	81.49	105.10
GRAD = .33	3	.117	.079	78.18	0.00
TIME = 212.07	1	.118	.077	76.43	100.80
ERROR = 4.14	4	.125	.084	83.42	6.27

## MIXING RESULTS (Average for 3 tests)

TEST CONDITIONS m, ,	DISCHARGE NUMBER	VOL. OF I SOL.		VOL. OF WATER		MIXING	
		100% MIXING L	ACTUAL VALUES L	100% MIXING L	ACTUAL VALUES L	ACTUAL %	ADJUSTED %
HEAD = 109.0	1	.124	.013	.125	.235	5.52	5.13
GRAD = 3.6	2	.122	.230	.123	.015	6.31	6.31
HEAD = 54.0	1	.078	.009	.079	.148	6.21	3.90
GRAD = 1.8	2	.074	.141	.075	.008	5.44	5.44
HEAD = 10.0	1	.061	.113	.057	.005	4.61	4.61
GRAD = .3	2	.065	.007	.060	.117	5.88	0.00



## FLOW CONFIGURATION

I solution inlet (I)	1
distilled water inlet (W)	2
discharge #1 (D1)	3
discharge #2 (D2)	4
.....	

## APERTURE/DEPTH CONFIGURATION

fracture #1-#3	0.5 mm
fracture #2-#4	0.5 mm
depth of f 1-3	= 14.0 mm
depth of f 2-4	= 14.0 mm
.....	

## TEST RESULTS (Average for 3 tests)

TEST CONDITIONS m, s, %	FRACTURE NUMBER	FLOW VOLUME L	VELOCITY OF FLOW m/s	REYNOLDS NUMBER	IODINE CONCENTRATION mg/L
HEAD = 100.00	1	.250	.424	421.54	108.10
GRAD = 3.33	2	.250	.425	421.87	0.00
TIME = 83.78	3	.254	.430	427.50	9.27
ERROR = 6.08	4	.246	.419	415.91	93.27
HEAD = 50.00	1	.208	.239	237.59	103.20
GRAD = 1.67	2	.204	.237	235.07	0.00
TIME = 123.93	3	.203	.235	233.22	11.17
ERROR = 7.05	4	.209	.241	239.44	94.40
HEAD = 10.00	1	.081	.042	41.72	103.20
GRAD = .33	2	.081	.042	41.86	0.00
TIME = 275.25	3	.080	.041	41.06	16.20
ERROR = 3.74	4	.082	.043	42.52	85.93

## MIXING RESULTS (Average for 3 tests)

TEST CONDITIONS m, ,	DISCHARGE NUMBER	VOL. OF I SOL. 100% MIXING L	ACTUAL VALUES L	VOL. OF WATER 100% MIXING L <sub>j</sub>	ACTUAL VALUES L	MIXING ACTUAL %	ADJUSTED %
HEAD = 100.0	1	.127	.022	.127	.231	9.63	8.05
GRAD = 3.3	2	.123	.212	.123	.034	15.98	15.98
HEAD = 50.0	1	.103	.022	.101	.181	11.77	11.77
GRAD = 1.7	2	.106	.195	.103	.014	7.13	6.95
HEAD = 10.0	1	.040	.013	.040	.067	18.68	18.68
GRAD = .3	2	.041	.069	.041	.014	20.04	17.79

APPENDIX B

LONG HAND DETERMINATION OF TRANSPORT IN A FRACTURE SYSTEM

### LONG HAND DETERMINATION OF TRANSPORT IN A FRACTURE SYSTEM

In order to illustrate the mathematical operations that are used in the numerical transport model, EXPORT, the long hand calculations are presented here. For this purpose, a simple example fracture system was used. The element configuration and the nodal numbers for each element are shown in Figure A-1. The numerical description of this fracture system is listed in Table A-1.

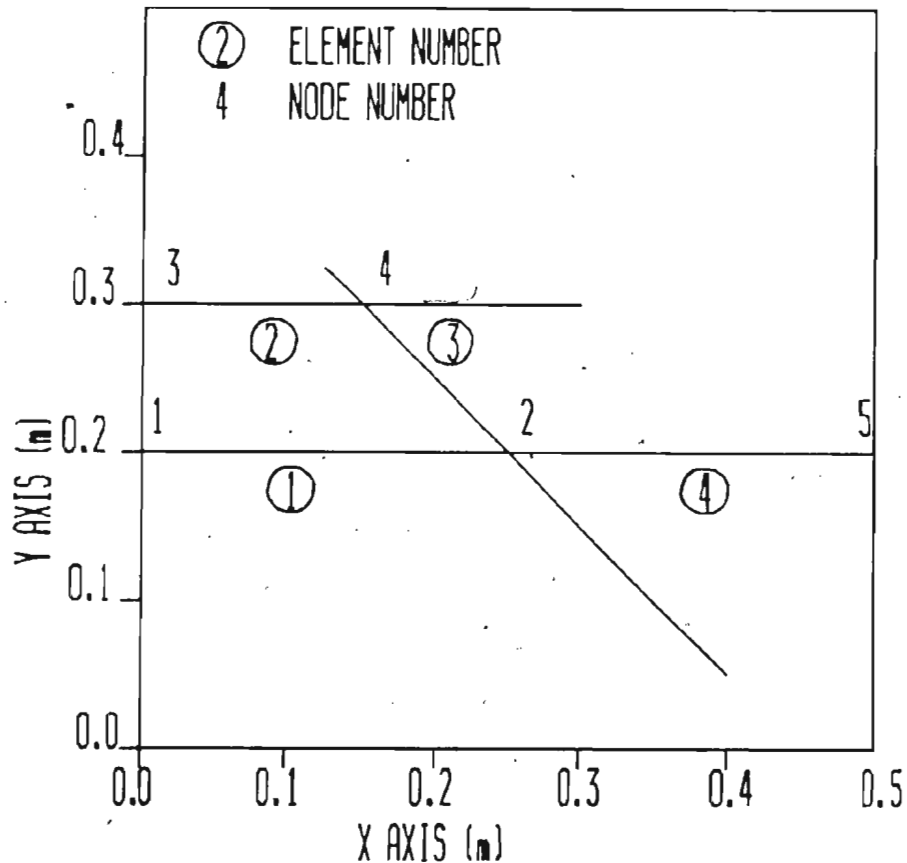


Figure B-1 Fracture configuration and element numbering

Table A-1

Co-ordinates

Element	x1	y1	x2	y2	Velocity	Length
1	0.0	0.2	0.25	0.2	0.5	0.2500
2	0.0	0.3	0.15	0.3	0.3	0.1500
3	0.15	0.3	0.25	0.2	0.3	0.1414
4	0.25	0.2	0.50	0.2	0.8	0.2500

Element	Peclet Number	Alfa	Dispersion Coefficient
1	0.50D+01	0.62D+00	0.25D-01
2	0.30D+01	0.44D+00	0.15D-01
3	0.28D+01	0.42D+00	0.15D-01
4	0.50D+01	0.61D+00	0.40D-01

Initial Concentration Data

Concentration at node	1 is	0.0
Concentration at node	2 is	0.0
Concentration at node	3 is	1.0
Concentration at node	4 is	0.0
Concentration at node	5 is	0.0

Equation 3.9 is the matrix equation that must be solved for  $\{C\}_{t+dt}$ . In this equation  $[R]$ ,  $[S]$  and  $[F]$  are the diffusion-advection, storage, and source matrices respectively. Each is of the order  $n$ , which is the number of nodes in the fracture system. The nodal coefficients of these matrices are calculated using equations 3.19, 3.20, and 3.21 respectively. For these equations the value of  $D$  for each element is calculated using the equation  $D=0.05*v$ . The value of  $\alpha$  is calculated using equation 3.18. The values of  $D$  and  $\alpha$  are listed in Table A-1. The coefficient matrix for  $[R]$  is thus:

$$[R] = \begin{bmatrix} 0.003 & -.003 & 0.000 & 0.000 & 0.000 \\ -.503 & 0.828 & 0.000 & -.319 & -.005 \\ 0.000 & 0.000 & 0.016 & -.016 & 0.000 \\ 0.000 & -.019 & -.316 & 0.335 & 0.000 \\ 0.000 & -.805 & 0.000 & 0.000 & 0.805 \end{bmatrix}$$

The coefficient matrix for [S] is given as:

$$[S] = \begin{bmatrix} 0.154 & 0.071 & 0.000 & 0.000 & 0.000 \\ 0.096 & 0.433 & 0.000 & 0.052 & 0.071 \\ 0.000 & 0.000 & 0.095 & 0.045 & 0.000 \\ 0.000 & 0.042 & 0.055 & 0.195 & 0.000 \\ 0.000 & 0.096 & 0.000 & 0.000 & 0.179 \end{bmatrix}$$

Now letting  $[A] = [S] + [R]$  we have the coefficient matrix of [A] as follows:

$$[A] = \begin{bmatrix} 0.157 & 0.067 & 0.000 & 0.000 & 0.000 \\ -.407 & 1.260 & 0.000 & -.267 & 0.065 \\ 0.000 & 0.000 & 0.110 & 0.029 & 0.000 \\ 0.000 & 0.023 & -.260 & 0.529 & 0.000 \\ 0.000 & -.709 & 0.000 & 0.000 & 0.985 \end{bmatrix}$$

If the solute is injected at node 3 on the Y-axis this node will have a constant concentration value (really  $C/C_0$ , where  $C_0$  is the initial concentration) of 1.0. Since this node is constrained the matrices can be partitioned as shown below:

$$[S] = \begin{bmatrix} 0.154 & 0.071 & 0.000 & 0.000 & 0.000 \\ 0.096 & 0.433 & 0.000 & 0.052 & 0.071 \\ \hline 0.000 & 0.000 & 0.095 & 0.045 & 0.000 \\ \hline 0.000 & 0.042 & 0.055 & 0.195 & 0.000 \\ 0.000 & 0.096 & 0.000 & 0.000 & 0.179 \end{bmatrix}$$

and

$$[A] = \begin{bmatrix} 0.157 & 0.067 & 0.000 & 0.000 & 0.000 \\ -0.407 & 1.260 & 0.000 & -0.267 & 0.065 \\ \hline 0.000 & 0.000 & 0.110 & 0.029 & 0.000 \\ \hline 0.000 & 0.023 & -0.260 & 0.529 & 0.000 \\ 0.000 & -0.709 & 0.000 & 0.000 & 0.985 \end{bmatrix}$$

Now moving column 3 and row 3 to the right hand side and the top respectively we partition the matrices according to the constrained nodes as in equation (3.22). Thus we have:

$$[S] = \begin{bmatrix} 0.095 & 0.000 & 0.000 & 0.045 & 0.000 \\ \hline 0.000 & 0.154 & 0.071 & 0.000 & 0.000 \\ 0.000 & 0.096 & 0.433 & 0.052 & 0.071 \\ 0.055 & 0.000 & 0.042 & 0.195 & 0.000 \\ 0.000 & 0.000 & 0.096 & 0.000 & 0.179 \end{bmatrix}$$

and

$$[A] = \begin{bmatrix} 0.110 & 0.000 & 0.000 & 0.029 & 0.000 \\ \hline 0.000 & 0.157 & 0.067 & 0.000 & 0.000 \\ 0.000 & -0.407 & 1.260 & -0.267 & 0.065 \\ -0.260 & 0.000 & 0.023 & 0.529 & 0.000 \\ 0.000 & 0.000 & -0.709 & 0.000 & 0.985 \end{bmatrix}$$

In order to assemble the vector  $\{B\}$ , as defined on the right hand side of equation (3.23) the appropriate parts of the partitioned matrices are added together. First it is noted that all of the values of  $\{C_f\}_t$  are equal to 0.0 at the beginning of the simulation and thus no contribution to  $\{B\}$  is obtained from  $[A_{ff}]$  for the first time step. As the value



of C rises at the individual nodes, with time, more terms from the product of  $[S_{ff}]$  and  $\{C_f\}$  contribute to  $\{B\}$ . For the first time step  $\{B\}$  is given as follows:

$$\{B\} = \begin{bmatrix} 0 \\ 0 \\ .0555 \\ 0 \end{bmatrix} - \begin{bmatrix} 0 \\ 0 \\ -.2602 \\ 0 \end{bmatrix} = \begin{bmatrix} 0 \\ 0 \\ .3157 \\ 0 \end{bmatrix}$$

The solution to equation (3.25) is:

$$\{C_f\}_{t+dt/2} = [A_{ff}]^{-1} \{BC_f\}_t$$

The inverse of  $[A_{ff}]$  is determined using the adjoint of the matrix since:

$$[A]^{-1} = \text{adj}[A] / |A|$$

where  $\text{adj}[A]$  is the adjunct of  $[A]$  and is assembled from the cofactors of  $[A]$ . The cofactors of  $[A]$  are individually listed and determined as follows:

$$a_{11} = (-1)^2 \begin{vmatrix} 1.260 & -.267 & 0.065 \\ 0.023 & 0.529 & 0.000 \\ -.709 & 0.000 & 0.985 \end{vmatrix} = 0.687$$

$$a_{12} = (-1)^3 \begin{vmatrix} -.407 & -.267 & 0.065 \\ 0.000 & 0.529 & 0.000 \\ 0.000 & 0.000 & 0.985 \end{vmatrix} = 0.212$$

$$a_{13} = (-1)^4 \begin{vmatrix} -.407 & 1.260 & 0.065 \\ 0.000 & 0.023 & 0.000 \\ 0.000 & -.709 & 0.985 \end{vmatrix} = -.009$$

$$a_{14} = (-1)^5 \begin{vmatrix} -.407 & 1.260 & -.267 \\ 0.000 & 0.023 & 0.529 \\ 0.000 & -.709 & 0.000 \end{vmatrix} = 0.153$$

$$\alpha_{21} = (-1)^3 \begin{vmatrix} 0.067 & 0.000 & 0.000 \\ 0.023 & 0.529 & 0.000 \\ -0.709 & 0.000 & 0.985 \end{vmatrix} = -.035$$

$$\alpha_{22} = (-1)^4 \begin{vmatrix} 0.157 & 0.000 & 0.000 \\ 0.000 & 0.529 & 0.000 \\ 0.000 & 0.000 & 0.985 \end{vmatrix} = 0.082$$

$$\alpha_{23} = (-1)^5 \begin{vmatrix} 0.157 & 0.067 & 0.000 \\ 0.000 & 0.023 & 0.000 \\ 0.000 & -0.709 & 0.985 \end{vmatrix} = -.004$$

$$\alpha_{24} = (-1)^6 \begin{vmatrix} 0.157 & 0.067 & 0.000 \\ 0.000 & 0.023 & 0.529 \\ 0.000 & -0.709 & 0.000 \end{vmatrix} = 0.059$$

$$\alpha_{31} = (-1)^4 \begin{vmatrix} 0.067 & 0.000 & 0.000 \\ 1.260 & -0.267 & 0.065 \\ -0.709 & 0.000 & 0.985 \end{vmatrix} = -.018$$

$$\alpha_{32} = (-1)^5 \begin{vmatrix} 0.157 & 0.000 & 0.000 \\ -0.407 & -0.267 & 0.065 \\ 0.000 & 0.000 & 0.985 \end{vmatrix} = 0.041$$

$$\alpha_{33} = (-1)^6 \begin{vmatrix} 0.157 & 0.067 & 0.000 \\ -0.407 & 1.260 & 0.065 \\ 0.000 & -0.709 & 0.985 \end{vmatrix} = 0.229$$

$$\alpha_{34} = (-1)^7 \begin{vmatrix} 0.157 & 0.067 & 0.000 \\ -0.407 & 1.260 & -0.267 \\ 0.000 & -0.709 & 0.000 \end{vmatrix} = 0.030$$

$$\alpha_{41} = (-1)^5 \begin{vmatrix} 0.067 & 0.000 & 0.000 \\ 1.260 & -0.267 & 0.065 \\ 0.023 & 0.529 & 0.000 \end{vmatrix} = 0.002$$

$$\alpha_{42} = (-1)^6 \begin{vmatrix} 0.157 & 0.000 & 0.000 \\ -0.407 & -0.267 & 0.065 \\ 0.000 & 0.529 & 0.000 \end{vmatrix} = -.005$$

$$a_{43} = (-1)^7 \begin{vmatrix} 0.157 & 0.067 & 0.000 \\ -0.407 & 1.260 & 0.065 \\ 0.000 & 0.023 & 0.000 \end{vmatrix} = 2.35 \cdot 10^{-4}$$

$$a_{44} = (-1)^8 \begin{vmatrix} 0.157 & 0.067 & 0.000 \\ -0.407 & 1.260 & -0.267 \\ 0.000 & 0.023 & 0.529 \end{vmatrix} = 0.120$$

where  $a_{ij}$  is the cofactor.

Since  $|A| = 0.122$  therefore  $[A]^{-1}$  is given as:

$$[A]^{-1} = \begin{bmatrix} 5.628 & 1.737 & -0.074 & 1.253 \\ -0.287 & 0.672 & -0.033 & 0.483 \\ -0.147 & 0.336 & 1.876 & 0.246 \\ 0.016 & -0.041 & 0.002 & 0.983 \end{bmatrix}$$

Thus  $Co/C$  is determined by:

$$\{C_f\}_{t+dt/2} = \{B\}_t / [A]^{-1} \text{ or:}$$

$$\{C_f\}_{t+dt/2} = \begin{bmatrix} 0.046 \\ 0.107 \\ 0.592 \\ 0.077 \end{bmatrix}$$

where  $\{C_f\}_{t+dt} = 2\{C\}_{t+dt/2} - \{C\}_t$ . Thus:

$$\begin{aligned} Co/C \text{ at node 1} &= 0.091 \\ Co/C \text{ at node 2} &= 0.213 \\ Co/C \text{ at node 3} &= 1.000 \\ Co/C \text{ at node 4} &= 1.183 \\ Co/C \text{ at node 5} &= 0.153 \end{aligned}$$

To get  $\{C\}$  at the next time step  $\{B\}$  is reassembled using the right hand side of equation (3.24) and again it is multiplied by  $[A]^{-1}$ . This can be continued until the desired time has elapsed.

APPENDIX C

FORTRAN LISTING OF NUMERICAL MODEL EXPORT AND ALL SUBROUTINES

program EXPORT  
\*\*\*\*\*

VERSION 1.0

This program is controlled by the control parameters found in the file "CHOICE.DAT" and the element data in "ELEMENT.DAT" to simulate the transport of a non reactive solute through a system of discrete fractures. A finite element procedure is used to solve the differential equation which describes conservative, advective-dispersive transport.

The program solves the matrix equations that result from the upstream finite element formulation as defined by Noorishad and Mehran as referenced below:

Jahan Noorishad and Mohsen Mehran, An upstream finite element method for solution of transient transport equation in fractured porous media, Water Resources Research, Vo. 18, No. 3, Pages 588 - 596, June 1982.

The matrix equation is:

$$[R]\{C\} + [S] \frac{d\{C\}}{dt} + [F] = 0 \quad (1)$$

where [R], [S] and [F] are the diffusion-advection, storage and source matrices respectively.

When some of these variables are constrained then partitioning is done by the program as indicated below:

$$\begin{array}{c|c|c} \text{---} & | & \text{---} \\ R_{cc} & | & R_{fc} \\ \text{---} & | & \text{---} \\ R_{fc} & | & R_{ff} \\ \text{---} & | & \text{---} \end{array} \quad \begin{array}{l} \text{for a} \\ \text{matrix} \end{array} \quad \begin{array}{c} (C_c) \\ \text{---} \\ (C_f) \end{array} \quad \begin{array}{l} \text{for a} \\ \text{vector} \end{array}$$

where c refers to a constrained condition  
and f refers to a free condition.

The program solves the equation derived from equation (1).

In terms of the variables in this program this equation  
can be written as follows:

$$[a]\{c\}time+dt = [b]\{c\}time$$

This program solves for  $\{c\}time+dt$

\*\*\*\*\*

\*\*\*\*\*

# DEFINITIONS OF PARAMETERS USED

SYMBOL	DIM	DEFINITION
--------	-----	------------

## R\*8 VARIABLES

alpha		coefficient for determining dispersion
coef		specifies the method of determining the
		upstream weighting function coefficient
dt		time step
leaktime		length of injection for discontinuous sources
r11,r12,r21,r22		elemental components of [R]
rb11		elemental component of {RB}
s11,s22		elemental components of {S}
time		time that has elapsed so far
x,y		element end point coordinates used temporarily for negative velocity check

## R\*8 ARRAYS

a	(599,599)	[a]=RHS matrix of knowns ie: [R]+[Rb]+[S]*t
afc	(599)	{afc}=the partitioned part of [a] with subscr- ipts f=free and c=constrained
ainv	(599,599)	the invert of [A]
alfa	(599)	the upstream weighting function coefficient
b	(599)	[b]=LHS matrix of knowns ie: [S]{C}-{Rfc}
bb	(599)	the fracture aperture
c	(599)	{c}=nodal concentrations
cc	(599)	{cc}=a temporary matrix used to hold the partitioned and constrained values of nodal concentration
d	(599)	coefficient of dispersion (v*alpha)
elmt	(599,5)	[elmt]=co-ordinates of elements and velocity data
l	(599)	{l}=element lengths
pe	(599)	peclet number for each element
s	(599,599)	the storage matrix in

c	sfc	(599)	the partitioned part of [S] with
c			subscripts f=free and c= constrained
c	v	(599)	{v}=velocity of flow in each element
c	wkarea	(370000)	the work area needed by linv2f to invert
c			[A]
c	z	(599)	used to store the x coordinates of the
c			element ends for printing to THRED.DAT
c	R*4 ARRAYS		
c	angle	(2)	the angles of intersection of the four-way
c			fracture intersection under consideration
c	m	(4)	the slope of the elements in a four-way
c			intersection
c	I*4 VARIABLES		
c	alltime		the total time for which transport is calculated
c	chnode		the injection node specified for circular
c			boundaries
c	cross		the number of four-way fracture intersections
c	i		counting variable
c	ia		variable needed for subroutine linv2f
c	idgt		variable needed for subroutine linv2f
c	ier		variable needed for subroutine linv2f
c	in		number of first element flowing into four-way
c			intersection
c	iterations		number of times the program must solve for [C]
c			is equal to alltime/partime
c	j		counting variable
c	n		counting variable
c	num		number of nodes used if BREAKUP finds some
c			four-way intersections
c	numelmt		number of elements
c	numin		stores node number at begining of element
c			temporally for negative velocity check
c	numnode		initial number of nodes used if BREAKUP is not
c	numout		stores node number at end of element
c			temporally for negative velocity check
c	o		output element number for a the four-way
c	out		number of output elements in a four-way
c			intersection
c			intersection under consideration
c	partime	--	the time of transport allowed to elapse before a
c			printout of [c] is wanted
c	psize		the number of nodes of the partitioned matrix
c	I*4 ARRAYS		
c	elmta	(599)	one of the elements flowing into a four-way

```

c      intersection
c      elmtc      (599)  the other element flowing into a four-way
c                      intersection
c      elmtck      (599,2) used to indicate if an the end nodes of an
c                      element has been considered in BREAKUP '
c                      (0=no 1=yes)
c      elmtx      (599,4) the inflow elements found in each
c                      four-way intersection
c      ignore      (599)  {ignore}=the constrained nodes left out
c                      by partitioning
c      input      (599,3) the elements flowing into an intersection
c      keep      (599)  {keep}=the free nodes kept by partitioning
c      nodc      (599,3) the renumbered nodes at each four-way
c                      intersection
c      node      (599,2) [node]=the node number at the end of each element
c
c      nodt      (599,2) the node numbers of each element end are stored
c                      here if BREAKUP is used
c      output      (599,3) the elements flowing out of an intersection

```

#### character VARIABLES

```

c      brk      indicates if BREAKUP is to be used or not
c      choice1      -- indicates continuous (c) or discontinuous (d)
c                      solute sources
c      choice2      -- indicates node (n), boundary (b) or circular
c                      boundary (c) sources
c      dtadjst      indicates if the initial value of dt is to
c                      be adjusted or not
c      pr3_d      indicates if output for 3_d plot is needed
c      prn1      directs output of general element data for
c                      verification
c      prn2      directs output of matrix values
c      prn3      directs output of concentration values
c                      at each partime

```

\*\*\*\*\*

```

^ .....
c ^ DOCUMENTATION: Variables and arrays are declared ^
c ^ ..... ^
c ^ .....

```

#### REAL VARIABLES

-----

```

real m(4),angle(2),tmin
real*8 elmt(599,5),a(599,599),s(599,599)
real*8 b(599),c(599),l(599),v(599),d(599)

```





```

c      ^ ..... nodes from element.dat and the control parame- ^
c      ^ ..... ters from choice.dat ..... ^
c
c      read (1,10) numelmt
c      read (1,10) numnode
c      read (3,11) choicel
c      read (3,11) choice2
c      read (3,10) cnode
c      read (3,10) alltime
c      read (3,10) partime
c      read (3,12) dt
c      read (3,12) alpha
c      read (3,12) coef
c      read (3,12) leaktime
c      read (3,13) brk,bkth,pr3_d,prn1,prn2,prn3,dtadjst
10 format (11x,i10)
11 format (19x,a)
12 format (11x,d12.6)
13 format (11x,7(a,4x))
      write (6,13) brk,bkth,pr3_d,prn1,prn2,prn3,dtadjst
c
c
c      .....
c      ^ DOCUMENTATION: Write input to nodconc.dat for verification ^
c      ^ ..... ^
c
c
c      if (prn1.eq.'Y'.or.prn1.eq.'y') then
c      write (2,*) 'CONTROL PARAMETERS'
c      write (2,*) '
c      write (2,*) 'numelmt = ',numelmt
c      write (2,*) 'numnode = ',numnode
c      write (2,*) 'choicel = ',choicel
c      write (2,*) 'choice2 = ',choice2
c      write (2,*) 'cnode = ',cnode
c      write (2,*) 'alltime = ',alltime
c      write (2,*) 'partime = ',partime
c      write (2,*) 'dt = ',dt
c      write (2,*) 'alpha = ',alpha
c      write (2,*) 'coef = ',coef
c      write (2,*) 'leaktime= ',leaktime
c      write (2,*) 'options = ',brk,bkth,pr3_d,prn1,prn2,prn3,dtadjst
c      write (2,*) '-----'
c      write (2,*) '
c      write (2,*) 'CO-ORDINATES AND VELOCITY DATA'
c      write (2,*) '
c      endif
c
c
c      .....

```

```

c   ^ DOCUMENTATION: Read element data from element.dat and assign
c   ^ the velocity to v.
c   ^
c   ^
c
do i=1,numelmt
  read (1,20) (elmt(i,j),j=1,5)
20 format (lx,5(d14.6))
  if (prnl.eq.'Y'.or.prnl.eq.'y') then
    write(2,20) (elmt(i,j),j=1,5)
  endif
  v(i)=elmt(i,5)
enddo
tmin=1000

c
c
c   ^ DOCUMENTATION: Read the values for element length, node number
c   ^ and aperture and determine the minimum length
c   ^
c   ^
c
do i=1,numelmt
  read (1,31) l(i),node(i,1),node(i,2),bb(i)
31 format(lx,d15.7,2i10,d15.7)
  if (abs(v(i)).gt.0.0d+00) then
    if (abs(l(i)/v(i)).lt.tmin) then
      tmin=abs(l(i)/v(i))
    endif
  endif
enddo

c
c
c   ^ DOCUMENTATION: The working value of dt is assigned so that only
c   ^ half the length of the shortest element is trav-
c   ^ ersed in one time step.
c   ^
c   ^
c
if (dtadjst.eq.'Y'.or.dtadjst.eq.'y')then
32 if (tmin.lt.dt*2.0) then
  dt=dt*0.9
endif
if (tmin.lt.dt*2.0) goto 32

c
c
c   ^ DOCUMENTATION: If the initial value of dt is such that less than
c   ^ half of the shortest element is traversed in one
c   ^ time step the value of dt is increased.
c   ^
c   ^
c

```

33

endif

endif

cc  
cc  
cc  
cc  
cc  
cc

```

..... the element data for the end nodes end of end
.....

```

endif

cccccccc

[illegible]

```

c
c      if (v(i).eq.0.0) then
c          pe(i)=0.1d+00
c          v(i)=0.1d-29
c          d(i)=v(i)*alpha
c      else
c          d(i)=v(i)*alpha
c          pe(i)=v(i)*l(i)/d(i)
c      endif
c
c
c      .....
c      ^ DOCUMENTATION: Determine if the value for the upstream weight-
c      ^ ..... function coefficient (alfa) is to be specified
c      ^ or the optimum value calculated.
c      ^ .....
c
c      if (coef.eq.0.0.or.coef.eq.1.0) then
c          alfa(i)=(1/dtanh(pe(i)/0.2d+01)-(0.2d+01/pe(i)))*coef
c      else
c          alfa(i)=coef
c      endif
c
c      30 format (f7.4,2(i4,2f7.4),d15.7)
c      if (prnl.eq.'Y'.or.prnl.eq.'y') then
c          write (2,30) l(i),node(i,1),(elmt(i,j),j=1,2),node(i,2),
c          &(elmt(i,j),j=3,4),bb(i)
c      endif
c      enddo
c
c
c      .....
c      ^ DOCUMENTATION: Write values of Peclet number, alfa and dispersion
c      ^ ..... coefficient to nodconc.dat for verification
c      ^ .....
c
c      if (prnl.eq.'Y'.or.prnl.eq.'y') then
c          write (2,*) '-----'
c          write (2,*) '
c          write (2,*) 'ELEMENT PECLT NUMBERS ALFA AND DISPERSION COEFF.'
c          write (2,*) '
c          do i=1,numelmt
c              write (2,3984) pe(i),alfa(i),d(i)
c      3984 format (3d14.6)
c          enddo
c          write (2,*) '-----'
c          write (2,*) '
c          endif
c          close (unit=1,status='keep')

```

```

^ DOCUMENTATION: Assign value to variable num and cross for use ^
^ .....in subroutine BREAKUP .....
^ .....
^
num=numnode
cross=0

*****
subroutine call ----- BREAKUP
*****

.....
^ DOCUMENTATION: This subroutine decouples all four way intersec- ^
^ .....tions and sets up all the arrays that co-ordinate ^
^ .....and direct the flow of solute into the appropri- ^
^ .....ate elements that drain the intersection. The ^
^ .....direction of such flow is governed by the angle ^
^ .....of intersection and the velocity. ^
^ .....
^
call breakup (elmt,c,node,numelmt,num,elmtx,output,input,
&cross,v,bb,nodc,elmta,elmtc,nodt,brk)

*****
subroutine call ----- CONCENTRATION *
*****

.....
^ DOCUMENTATION: This subroutine assigns a value of 1.0 to the ^
^ .....nodes where injection of a solute takes place and ^
^ .....a value of 0.0 to all other nodes. ^
^ .....The selection of the injection node/s is made ^
^ .....according to the value of CHOICE2 as follows: ^
^ .....if CHOICE2 = n the middle node on the left ^
^ .....boundary is chosen by the program ^
^ .....it CHOICE2 = b all nodes on the left boundary ^
^ .....are chosen by the program ^
^ .....if CHOICE2 = c the model has circular bound- ^
^ .....aries and the node where solute ^
^ .....is introduced must be specified ^
^ .....as CNODE in CHOICE.DAT ^
^ .....
^
call concentration (nodt,elmt,c,choice2,num,numelmt,l,cnode)

```

```

c   ^ DOCUMENTATION: The concentration assigned to each node is output
c   ^ ***** to NODCONC.DAT for verification
c   ^ *****
c
c   if (prn1.eq.'Y'.or.prn1.eq.'y') then
c       write (2,*) 'CONCENTRATION DATA'
c       write (2,*) '_____ '
c       do i=1,numnode
c           write (2,40)i,c(i)
40 format ('concentration at node',i4,' is',f22.15)
c       enddo
c       write (2,*) '-----'
c       write (2,*) ' '
c   endif
c
c   *****
c   subroutine call ----- MATRICIES *
c   *****
c
c   ^ DOCUMENTATION: This subroutine calculates the coefficient matrix
c   ^ ***** of the left hand side of the matrix equation
c   ^ ***** defined above. The elemental matrices are out
c   ^ ***** to NODCOND.DAT for verification.
c   ^ *****
c
c   call matricies (podt,v,d,l,a,dt,num,numelmt,s,alfa)
c
c   ^ *****
c   ^ DOCUMENTATION: The coefficients of [a] and [s] are output by
c   ^ ***** column to NODCOND.DAT for verification
c   ^ *****
c
c   if (prn2.eq.'Y'.or.prn2.eq.'y') then
c       write (2,*) 'DISPERSION ADVECTION MATRIX' AND 'SMATRIX'
c       write (2,*) '_____ '
c       do j=1,numnode
c           write (2,*) 'COLUME ',j
c           write (2,*) '_____ '
c           do i=1,numnode
c               write (2,8008) i,a(i,j),s(i,j)
8008 format ('ROW = ',i3,2f22.15)
c           enddo
c           write (2,*) ' '
c       enddo
c       write (2,*) '-----'
c       write (2,*) ' '
c   endif
c

```

```

C *****
C subroutine call ----- PARTITION *
C *****
C
C
C
C
C ^ DOCUMENTATION: This subroutine partitions the matrices ^
C ^ ^ determined above to leave out the constrained ^
C ^ nodes. ^
C ^
C
C call partition (c,s,a,num,ignore,keep,afc,psize,sfc,choice2,
&numelmt,nodt,nodc,cross)
C
C
C
C ^ DOCUMENTATION: The coefficients of the partitioned [a], [s], ^
C ^ ^ [afc] and {c} are output by column to NODCONC.DAT ^
C ^ for verification ^
C ^
C
C if (prn2.eq.'Y'.or.prn2.eq.'y') then
C   write (2,*) 'PARTITIONED MATRICES'
C   write (2,*) '*****'
C   write (2,*) '
C   write (2,*) 'ADVECTION DISPERSION MATRIX AND SMATRIX'
C   write (2,*) '
C   do i=1,psize
C     write (2,*) ' COLUMN',i
C     write (2,*) '
C     do j=1,psize
C       write (2,8024) j,a(j,i),s(j,i)
8024 format (' row = ',i3,2f22.15)
C     enddo
C     write (2,*) '
C   enddo
C   write (2,*) '-----'
C   write (2,*) '
C   write (2,*) 'CONCENTRATION AND AFC'
C   write (2,*) '
C   do i=1,psize
C     write (2,8034) c(i),afc(i)
8034 format (f6.5,f22.15)
C   enddo
C   write (2,*) '-----'
C   write (2,*) '
C endif
C
C *****
C subroutine call ----- LINV2F *
C *****

```



```

c
c
c
c  ^ DOCUMENTATION: This subroutine is an ISML routine available on ^
c  ^ the VAX computer for the inversion of a matrix. ^
c  ^ The definition of the variables follows: ^
c  ^
c  ^      a      = The input matrix ^
c  ^      psize  = The actual dimension of a ^
c  ^      ia     = The row size of a and ainv as ^
c  ^              specified in the dimension ^
c  ^              statement. ^
c  ^      ainv   = The output matrix containing the ^
c  ^              inverse of a. ^
c  ^      idgt   = The error option: ^
c  ^              If idgt>0 the elements are assumed ^
c  ^              to be correct and an accuracy test ^
c  ^              is done. ^
c  ^              If idgt=0 no test. ^
c  ^      wkarea = The work area = to or > than ^
c  ^              psize**2+3*psize. ^
c  ^      ier    = Error Parameter put out by routine ^
c  ^              if it fails. ^
c  ^
c  ^
c
c  call linv2f (a,psize,ia,ainv,idgt,wkarea,ier)
c
c
c
c  ^ DOCUMENTATION: The number of iterations is calculated. This ^
c  ^ variable is used to provide concentration output ^
c  ^ at regular time intervals which are less than the ^
c  ^ total simulation time (ie. every partime). It ^
c  ^ not be mistaken for the number of iterative steps ^
c  ^ that are controlled by the time step dt. This ^
c  ^ variable is calculated and used in the subroutine ^
c  ^ SOLVEC. ^
c  ^
c  ^
c
c  iterations=alltime/partime
c
c
c
c  ^ DOCUMENTATION: Check the value of the control character CHOICE1 ^
c  ^ If CHOICE1 = c then the sources are continuous ^
c  ^ the subroutine SOLVEC is used. ^
c  ^ If CHOICE1 = d then the sources are discontinuous ^
c  ^ and the subroutine SOLVED is used. ^
c  ^
c  ^
c
c  do i=1,iterations
c      time = i*partime

```

```

C
C *****
C subroutine call ----- SOLVEC *
C *****
C
C
C
C
C ^ DOCUMENTATION: This subroutine calculates the new value of c at ^
C ^ time = t+dt for continuous solute sources. It ^
C ^ uses another subroutine called MULTIPLY to do ^
C ^ this. The value of the nodal concentration is ^
C ^ outputed to NODCONC.DAT every partime ^
C ^
C
C call solvec (ainv,c,s,afc,sfc,b,partime,psize,dt,cc,keep,
&num,i,v,cross,choicel,choice2,bb,elmtx,nodt,time,leaktime)
C
C
C ^ DOCUMENTATION: The number of four way intersections is checked ^
C ^ (cross) to see if the subroutine RECONSTITUTE ^
C ^ needs to be called. ^
C ^
C
C if (cross.gt.0) then
C
C *****
C subroutine call ----- RECONSTITUTE *
C *****
C
C
C
C ^ DOCUMENTATION: This subroutine reverses the effects of the sub- ^
C ^ routine BREAKUP with respect to the nodal concern- ^
C ^ tration values. After BREAKUP there is four ^
C ^ values for each intersection. RECONSTITUTE cal- ^
C ^ culates the one representative value for that ^
C ^ node for output purposes only. The four internal ^
C ^ values are not changed. ^
C ^
C
C call reconstitute (cross,nodc,cc,elmta,elmtc,bb,v)
C endif
C
C
C
C ^ DOCUMENTATION: The nodal concentrations are output to NODCONC. ^
C ^ DAT for verification ^
C ^
C
C
C if (prn3.eq.'Y'.or.prn3.eq.'y') then

```

```

        write(2,110)
110 format (' _____')
        write (2,120) i*partime
120 format (' RELATIVE NODAL CONCENTRATION AT TIME = ',i4)
        write (2,130) dt
130 format (' Timestep = ',f8.6)
    endif

```

C  
C  
C  
C  
C  
C  
C  
C  
C

```
^ DOCUMENTATION: The absolute values of concentration are substituted ^
^   ^^^^^^^^^ substituted. This is necessary because the finite ele- ^
^ ,      ^ ment solution can give negative values when the ^
^          ^ concentration is very low near the front. ^
```

```

do j=1,numnode
  cc(j)=abs(cc(j))
  if (prn3.eq.'Y'.or.prn3.eq.'y') then
    write (2,140) j,cc(j)
140 format (' AT NODE # ',i4,' CONCENTRATION = ',f22.15)
  endif
enddo

```

C  
C  
C  
C  
C  
C  
C  
C  
C  
C  
C

```

DOCUMENTATION: The concentration values for the first 27 nodes
^
^ are output to BRKTHR.DAT for plotting the break-
^
^ curves for these nodes with-time. The reason why
^
^ only the first 27 nodes are specified is that
^
^ the LOTUS spread sheet program was used to do the
^
^ plotting and it only accepts this length of line.

```

```

        if (bkth.eq.'Y'.or.bkth.eq.'y') then
            write (4,150) i*partime,(cc(j),j=1,27)
150 format (1x,i3,9(1x,f4.2))
        endif
    enddo

```

C  
C  
C  
C  
C  
C  
C  
C

```

^ DOCUMENTATION: The number of elements and nodes is written to
^ ~~~~~ THRED.DAT for the 3-D plot of the concentration
^ at each fracture intersection

```

```

      if (pr3_d.eq.'Y'.or.pr3_d.eq.'y') then
        write (5,160) numelmt
        write (5,160) numnode
160  format(i4)

```

[illegible]

```

c      ^ ~~~~~ ia assigned the values of NODE. ~~~~~ ^
c      ^ ~~~~~
c
c
c      do i=1,numelmt
c        do j=1,2
c          elmtck(i,j)=0
c          nodd(i,j)=node(i,j)
c        enddo
c      enddo

c
c      ^ ~~~~~
c      ^ DOCUMENTATION: All elements are checked to see if they begin or ^
c      ^ ~~~~~ end at a four way intersection. Each end is ^
c      ^ ~~~~~ checked to see if it has been so identified ^
c      ^ ~~~~~ already. ^
c      ^ ~~~~~
c
c
c      if (brk.eq.'N'.or.brk.eq.'n') goto 600
c      do i=1,numelmt
c        if (elmtck(i,1).eq.1.and.elmtck(i,2).eq.1) goto 450
c        out=0
c        in=1
c        input(i,in)=i
c        elmtck(i,2)=1
c        do j=i+1,numelmt
c          if (node(i,2).eq.node(j,1).and.elmtck(j,1).eq.0) then
c            out=out+1
c            output(i,out)=j
c            elmtck(j,1)=1
c          endif
c          if (node(i,2).eq.node(j,2).and.elmtck(j,2).eq.0) then
c            in=in+1
c            input(i,in)=j
c            elmtck(j,2)=1
c          endif
c        enddo

c
c      ^ ~~~~~
c      ^ DOCUMENTATION: If the intersection is anything but a four-way ^
c      ^ ~~~~~ intersection the next element is considered. If ^
c      ^ ~~~~~ a five way or greater intersection is found the ^
c      ^ ~~~~~ program issues an ERROR message and stops. If a ^
c      ^ ~~~~~ four way intersection is found the routine cont- ^
c      ^ ~~~~~ inues. ^
c      ^ ~~~~~
c
c
c

```

```

if (out+in.gt.4) goto 500
if (out.eq.3.or.in.eq.3) goto 450
if (out.le.1.or.in.le.1) goto 450

```

c  
c  
c  
c  
c  
c  
c  
c  
c  
c

```

^ ~~~~~
^ DOCUMENTATION: The number of four way intersections is increment
^ ~~~~~ ed and an the intersection is cataloged by the ^
^ ~~~~~ first input element of same. ^
^ ~~~~~

```

```

cross=cross+1
elmtx(cross,1)=i
do j=1,2
  n=input(i,j)
  o=output(i,j)

```

c  
c  
c  
c  
c  
c  
c  
c  
c  
c  
c  
c

```

^ ~~~~~
^ DOCUMENTATION: The elements are examined to see if they are ^
^ ~~~~~ perpendicular and if so they are assigned a fin- ^
^ ~~~~~ ite but very large slope. If they are not perpen- ^
^ ~~~~~ dicular the slope is calculated and the angle of ^
^ ~~~~~ of intersection between the input element and ^
^ ~~~~~ both output elements is calculated. ^
^ ~~~~~

```

```

if (elmt(n,3).eq.elmt(n,1)) then
  m(j)=1.0D+30
else
  m(j)=(elmt(n,4)-elmt(n,2))/(elmt(n,3)-elmt(n,1))
endif
if (elmt(o,3).eq.elmt(o,1)) then
  m(j+2)=1.0D+30
else
  m(j+2)=(elmt(o,4)-elmt(o,2))/(elmt(o,3)-elmt(o,1))
endif

```

c  
c  
c  
c  
c  
c  
c  
c  
c  
c

```

^ ~~~~~
^ DOCUMENTATION: The slope of the input element and the first out- ^
^ ~~~~~ put element are compared. If they are equal then ^
^ ~~~~~ angle # 1 is assigned a value of 3.14 radians. ^
^ ~~~~~

```

```

if (abs(m(1)-m(j+2)).le.0.0001) then
  angle(j)=3.141592
else

```

-

```

        angle(j)=atan((m(j+2)-m(1))/(1+m(j+2)*m(1)))
    endif
enddo

c
c
c ~~~~~
c ^ DOCUMENTATION: The direction of solute flow is determined from ^
c ^ the two angles. ^
c ~~~~~

    if (angle(1).lt.angle(2)) then
        n1=1
        n2=2
    else
        n1=2
        n2=1
    endif

c
c
c ~~~~~
c ^ DOCUMENTATION: The temporary node numbers are assigned, the arr-^
c ^ ay used to catalog the flow configuration at the ^
c ^ intersection is assigned values according to the ^
c ^ input and output elements that create it, and the ^
c ^ total number of nodes is increased by 3. ^
c ~~~~~

    nodt(input(i,1),2)=node(i,2)
    nodt(output(i,n1),1)=num+1
    nodt(input(i,2),2)=num+2
    nodt(output(i,n2),1)=num+3
    elmtx(cross,2)=output(i,n1)
    elmtx(cross,3)=input(i,2)
    elmtx(cross,4)=output(i,n2)
    nodec(cross,1)=node(i,2)
    nodec(cross,2)=num+2
    nodec(cross,3)=node(i,2)
    num=num+3
    write (6,*) num

c
c
c ~~~~~
c ^ DOCUMENTATION: The input flow configuration is assigned and cat-^
c ^ alogged according to the intersection number. ^
c ^ The program skips the next section which deals ^
c ^ with the situation when the last element is chosen ^
c ~~~~~

```

```

      elmta(cross)=input(i,1)
      elmtc(cross)=input(i,2)
450  continue
      enddo
      goto 600
C
C
C
C  ^ DOCUMENTATION: If there are more than four elements intersecting
C  ^ at the one point then an error message is output
C  ^ and the program stops.
C  ^
C  ^
C
C
500  write (6,*) '** ERROR **'
      write (6,*) 'TO MANY FRACTURES INTERSECTING AT THE SAME POINT'
      write (6,*) 'LOOK AT ELEMENT NUMBER',i
      call exit
600  continue
      end
C
C  ***** subroutine CONCENTRATION *****
C
C  subroutine concentration (nodd,elmt,c,choice2,num,
&ncl,l,cnode)
      real*8 c(599),elmt(599,5),l(599),ymin,yoff
      integer nodd(599,2),cnode
      character*1 choice2
C
C
C  ^ DOCUMENTATION: All nodes are assigned a value of 0.0
C  ^
C  ^
C
C
C  do i=1,num
      c(i)=0.0d+00
    enddo
      if (choice2.eq.'C'.or.choice2.eq.'c') then
        c(cnode)=0.1d+01
      endif
C
C
C  ^ DOCUMENTATION: If CHOICE2 = b then all nodes on the left boundary
C  ^ are assigned a concentration value of 1.0 and all
C  ^ interior nodes are left at 0.0
C  ^
C  ^
C
C
C
```



```

if ((choice2 .eq. 'b').or.(choice2 .eq. 'B')) then
  do i=1,nel
    if (elmt(i,1).eq.0.0d+00) then
      c(nodt(i,1))=0.1d+01
    endif
  enddo

```

c  
c  
c  
c  
c  
c  
c  
c

```

^ DOCUMENTATION: If CHOICE2 = N then the middle node is assigned ^
^ a value of 1.0 ^

```

```

elseif (choice2.eq.'n'.or.choice2.eq.'N') then
  ymin=1000.0
  yoff=0.0
  do i=1,nel
    if (elmt(i,1).eq.0.0d+00) then
      if (elmt(i,2).lt.ymin) then
        ymin=elmt(i,2)
      elseif (elmt(i,2).gt.yoff)then
        yoff=elmt(i,2)
      endif
    endif
  enddo
  yoff=(yoff-ymin)/2.0
  ymin=1000.0
  do i=1,nel
    if (elmt(i,1).eq.0.0d+00) then
      if(abs(yoff-elmt(i,2)).lt.ymin) then
        ymin=abs(yoff-elmt(i,2))
      endif
    endif
  enddo
  do i=1,nel
    if (elmt(i,1).eq.0.0d+00) then
      if (abs(yoff-elmt(i,2)).eq.ymin) then
        c(nodt(i,1))=0.1d+01
      endif
    endif
  enddo
endif
end

```

c  
c  
c

```

***** subroutine MATRICIES *****

```

```

subroutine matricies (nodt,v,d,l,a,dt,num,nel,s,alfa)
real*8 v(599),d(599),l(599),a(599,599)
real*8 dt,s(599,599),alfa(599)

```

```
real*8 r11,r12,r21,r22,s11,s22,s12,s21
real*8 a11,a12,a21,a22
integer nodd(599,2)
```

```
~~~~~
^ DOCUMENTATION: [a] and [s] are initialized to 0.0
^ ~~~~~
```

```
do i=1,num
  do j=1,num
    a(i,j)=0.0d+00
    s(i,j)=0.0d+00
  enddo
enddo
```

```
~~~~~
^ DOCUMENTATION: The coefficients of [r] and [s] are calculated
^ and the coefficients of [a] are obtained from
^ [r]+[s].
^ ~~~~~
```

```
do i=1,nel
  ii=nodd(i,1)
  jj=nodd(i,2)
  write (2,*) 'VALUES OF D,L,V,&DT FOR ELEMENT # ',i
  write (2,*) ':::::::::::::::::::::::::::::::::::::'
  write (2,*) '(d,l)',d(i),l(i)
  write (2,*) '(v,dt)',v(i),dt
  r11=(d(i)/l(i))-(v(i)/0.2D+01)+alfa(i)*v(i)/0.2D+01
  r12=(-d(i)/l(i))+(v(i)/0.2D+01)-alfa(i)*v(i)/0.2D+01
  r21=(-d(i)/l(i))-(v(i)/0.2D+01)-alfa(i)*v(i)/0.2D+01
  r22=(d(i)/l(i))+(v(i)/0.2D+01)+alfa(i)*v(i)/0.2D+01
  s11=(l(i)/0.3D+01-l(i)*alfa(i)/2.4D+01)*0.2D+01/dt
  s12=(l(i)/0.6D+01-l(i)*alfa(i)/2.4D+01)*0.2D+01/dt
  s21=(l(i)/0.6D+01+l(i)*alfa(i)/2.4D+01)*0.2D+01/dt
  s22=(l(i)/0.3D+01+l(i)*alfa(i)/2.4D+01)*0.2D+01/dt
  write (2,*) 'ELEMENTAL [R] MATRIX FOR ELEMENT # ',i
  write (2,*) ':::::::::::::::::::::::::::::::::::::'
  write (2,*) '(r11,r12)',r11,r12
  write (2,*) '(r21,r22)',r21,r22
  write (2,*) 'ELEMENTAL [S] MATRIX FOR ELEMENT # ',i
  write (2,*) ':::::::::::::::::::::::::::::::::::::'
  write (2,*) '(s11,s22)',s11,s22
  a11 = r11+s11
  a12 = r12+s12
  a21 = r21+s21
```

```

a22 = r22+s22
c   write (2,*) 'ELEMENTAL [A] MATRIX FOR ELEMENT # ',i
c   write (2,*) ':::::::::::::::::::::::::::::::::::::'
c   write (2,*) '(A11,A12)',a11,a12
c   write (2,*) '(A21,A22)',a21,a22
a(ii,ii)=a(ii,ii)+a11
a(ii,jj)=a(ii,jj)+a12
a(jj,ii)=a(jj,ii)+a21
a(jj,jj)=a(jj,jj)+a22
s(ii,ii)=s(ii,ii)+s11
s(ii,jj)=s(ii,jj)+s12
s(jj,ii)=s(jj,ii)+s21
s(jj,jj)=s(jj,jj)+s22
enddo
end

c
c ***** subroutine PARTITION *****
c
c   subroutine partition (c,s,a,num,ignore,keep,afc,psize,sfc
&,choice2,numelmt,nodt,nodc,cross)
c   real*8 c(599),s(599,599),a(599,599),afc(599),sfc(599)
c   integer psize,ignore(599),keep(599)
c   integer numelmt,nodt(599,2),nodc(599,3),cross
c   character*1 choice2
c
c   ~~~~~
c   ^ DOCUMENTATION: The counters n and m are initialized to 0.
c   ^ ~~~~~
c   ^
c   ^
c   n=0
c   m=0
c
c   ~~~~~
c   ^ DOCUMENTATION: The constrained nodes are determined by the value^
c   ^ of c at that node. If c=1.0 then the node is
c   ^ constrained and it is cataloged as such in the
c   ^ array IGNORE. If c=0.0 then the node is not con-
c   ^ strained and it is cataloged in the array KEEP.
c   ^ ~~~~~
c
c
c   do i=1,num
c     if (c(i).eq.0.1D+01) then
c       n=n+1
c       ignore(n)=i
c       do k=1,numelmt
c         do l=1,2

```

```

        if (nodd(k,1).ge.i) then
            nodd(k,1)=nodd(k,1)-1
        endif
    enddo
enddo
else
    m=m+1
    keep(m)=i
endif
enddo

```

```

^ DOCUMENTATION: The partitioned size of the matrices "m" is ass-^
^ igned to the variable psize.

```

```
psize=m
```

```

^ DOCUMENTATION: {afc} and {sfc} are initialized to 0.0 and {c} is^
^ reassigned according to the array KEEP.

```

```

do i=1,psize
    ii=keep(i)
    afc(i)=0.0d+00
    sfc(i)=0.0d+00
    c(i)=c(ii)

```

```

^ DOCUMENTATION: {afc} and {sfc} are assembled from the parts of ^
^ [a] and [s] that are not used according to the ^
^ array IGNORE.

```

```

do j=1,n
    jj=ignore(j)
    afc(i)=afc(i)+a(ii,jj)
    sfc(i)=sfc(i)+s(ii,jj)
enddo

```

```

^ DOCUMENTATION: [a] and [s] are partitioned
^ according to the array KEEP.

```

```

C
C
C
      do j=1,psize
        jj=keep(j)
        a(i,j)=a(ii,jj)
        s(i,j)=s(ii,jj)
      enddo
    enddo
  end

C
C
C
  *****  subroutine SOLVEC  *****

  subroutine solvec(ainv,c,s,afc,sfc,b,part,p,dt,cc,keep,
&num,ii,v,cross,choicel,choice2,bb,elmtx,nodt,time,
&leaktime)
    real*8 ainv(599,599),c(599),s(599,599)
    real*8 afc(599),b(599),cc(599),time
    real*8 sfc(599),v(599),bb(599),leaktime
    integer p,part,steps,keep(599),cross
    integer elmtx(599,4),nodt(599,2),num
    character*1 choicel,choice2

C
C
C
    ~~~~~
    ^ DOCUMENTATION: The number of time steps that are to be performed
    ^ ~~~~~ before output of concentration values is required
    ^ ~~~~~ is calculated from the control parameters.
    ^ ~~~~~
    ~~~~~

    steps=int(part/dt)

C
C
C
    ~~~~~
    ^ DOCUMENTATION: For each time step the subroutine BRIDGIT is cal-
    ^ ~~~~~ led if the number of four way intersections is
    ^ ~~~~~ more than zero.
    ^ ~~~~~
    ~~~~~

    do j=1,steps
      if (cross.gt.0) then
        *****
        * SUBROUTINE CALL BRIDGIT*
        *****
        call bridgit(c,cross,v,bb,elmtx,nodt)
      endif
    enddo
  end

```

```

C      ^ DOCUMENTATION: {b} is assembled from {s}, {c}, {afc}, and {sfc}.^
C      ^ ~~~~~^
C      ^ ~~~~~^
C      ^ ~~~~~^
C
C      do i=1,p
C          b(i)=0.0D+00
C          do k=1,p
C              b(i)=b(i)+s(i,k)*c(k)
C          enddo
C
C
C      ^ DOCUMENTATION: The value of CHOICE1 is checked to see if the ^
C      ^ ~~~~~ [B] is assembled with {Cc} = 0.0 or 1.0. ^
C      ^ ~~~~~^
C      ^ ~~~~~^
C
C      if (choice1.eq.'d'.or.choice1.eq.'D'.and.time+j*dt.ge.
C      &leaktime) goto 700
C          b(i)=b(i)-afc(i)+sfc(i)
C      700 continue
C      enddo
C
C
C      ^ DOCUMENTATION: To calculate the concentration values the subrou-^
C      ^ ~~~~~ tine MULTIPLY is called which multiplies {b} by ^
C      ^ ~~~~~ the inverse of {a}. ^
C      ^ ~~~~~^
C      ^ ~~~~~^
C
C      *****
C      subroutine call ----- MULTIPLY *
C      *****
C
C      call multiply (b,ainv,c,p)
C      enddo
C
C
C      ^ DOCUMENTATION: The values for nodal concentration are assigned ^
C      ^ ~~~~~ to {cc} according to the original numbering of ^
C      ^ ~~~~~ nodes. ^
C      ^ ~~~~~^
C      ^ ~~~~~^
C
C      j=1
C      do i=1,num
C          jj=keep(j)

```

```

        if (jj.eq.i) then
            cc(i)=c(j)
            j=j+1
        elseif (choice2.eq.'n'.or.choice2.eq.'N'.and.c(i).eq.
&0.0d+00) then
            cc(i)=0.0d+00
        elseif (choicel.eq.'d'.or.choicel.eq.'D'.and.time+j*dt
&.ge.leaktime) then
            cc(i)=0.0d+00
        else
            cc(i)=0.1d+01
        endif
    enddo
end

***** subroutine BRIDGIT *****

subroutine bridgit(c,cross,v,bb,elmtx,nodt)
real*8 c(599),bb(599),v(599)
integer cross,elmtx(599,4),nodt(599,2)
integer el,e2,e3,e4,n1,n2,n3,n4

~~~~~
^ DOCUMENTATION: For each four way intersection the variables el, ^
^ e2, e3, e4, n1, n2, n3, and n4 are assigned the ^
^ element numbers and node numbers respectively of ^
^ those elements and nodes that make up the inter- ^
^ section. The order of these assignments are det- ^
^ ermined in the subroutine breakup according to ^
^ the angle of intersection. ^
~~~~~

do i=1,cross
    el=elmtx(i,1)
    e2=elmtx(i,2)
    e3=elmtx(i,3)
    e4=elmtx(i,4)
    n1=nodt(el,2)
    n2=nodt(e2,1)
    n3=nodt(e3,2)
    n4=nodt(e4,1)

~~~~~
^ DOCUMENTATION: The appropriate concentration from the end of the ^
^ input elements is transferred to the beginning of ^
^ output elements according to the differences in ^
^ flow in the elements. ^
~~~~~

```

c  
c  
c

1

c  
c  
c  
c  
c  
c  
c  
c

c  
c  
c  
c  
c  
c  
c  
c

```
do i=1,p
  do j=1,p
    c(i)=c(i)+ainv(i,j)*b(j)
  enddo
enddo
do i=1,p
  c(i)=0.2d+01*c(i)-cold(i)
enddo
end
```



```

C
C ***** SUBROUTINE RECONSTITUTE *****
C
C      subroutine reconstitute(cross,nodc,cc,elmta,elmtc,
C      &bb,v)
C      real*8 cc(599),bb(599),v(599)
C      integer cross,nodc(599,3)
C      integer elmta(599),elmtc(599)
C
C      ^^^^^^^^^^^^^^^^^^^^^^^^^^^^^^^^^^^^^^^^^^^^^^^^^^^^^^^^^^^^^
C      ^ DOCUMENTATION: For each four-way intersection the representative ^
C      ^ concentration is calculated from the components ^
C      ^ in each of the input fractures. This value is ^
C      ^ a representative value only for output a specifi- ^
C      ^ ed times. The value does enter into the calcula- ^
C      ^ tions at any point. ^
C      ^^^^^^^^^^^^^^^^^^^^^^^^^^^^^^^^^^^^^^^^^^^^^^^^^^^^^^^^^^^^^
C
C      do i=1,cross
C         cc(nodc(i,3))=(cc(nodc(i,1))*bb(elmta(i))*v(elmta(i))+cc(
C      &nodc(i,2))*bb(elmtc(i))*v(elmtc(i)))/(bb(elmta(i))*v(elmta(i)
C      &)+bb(elmtc(i))*v(elmtc(i)))
C      enddo
C      end

```

APPENDIX D

DATA FILE USED TO GENERATE FIGURE 4.3  
AND THRED.DAT FOR FIGURE 4.4

2	0	4.0	0.5	8.	1	1	1	2
-1.0	7.0	7.0	-1.0	0.0	6.0	6.0	0.0	
1		0.0	0.0	1	12.0			
0								
1		0.0	6.0	0				
0								
1		6.0	6.0	1	0.0			
0								
1		6.0	0.0	0				
0								
	1.0	1	1	1				
	1.0	1	1	1				
	8.0				0.			15.
.0001								
	8.0				0.			75.
.0001								

COORDINATE AND CONCENTRATION DATA  
AS RECORDED IN THRED.DAT FOR  
FIGURE 4.4

67  
48  
0.5000 0.2720 0.5539 0.3080  
0.5539 0.3080 0.6078 0.3440  
0.6078 0.3440 0.6616 0.3800  
0.6616 0.3800 0.7155 0.4160  
0.7155 0.4160 1.0000 0.6061  
0.0000 0.0099 0.4461 0.3080  
0.4461 0.3080 0.5000 0.3440  
0.5000 0.3440 0.5539 0.3800  
0.5539 0.3800 0.6078 0.4160  
0.6078 0.4160 0.6616 0.4520  
0.6616 0.4520 1.0000 0.6781  
0.0000 0.0819 0.3922 0.3440  
0.3922 0.3440 0.4461 0.3800  
0.4461 0.3800 0.5000 0.4160  
0.5000 0.4160 0.5539 0.4520  
0.5539 0.4520 0.6078 0.4880  
0.6078 0.4880 1.0000 0.7501  
0.0000 0.1539 0.3384 0.3800  
0.3384 0.3800 0.3922 0.4160  
0.3922 0.4160 0.4461 0.4520  
0.4461 0.4520 0.5000 0.4880  
0.5000 0.4880 0.5539 0.5240  
0.5539 0.5240 1.0000 0.8221  
0.0000 0.2259 0.2845 0.4160  
0.2845 0.4160 0.3384 0.4520  
0.3384 0.4520 0.3922 0.4880  
0.3922 0.4880 0.4461 0.5240  
0.4461 0.5240 0.5000 0.5600  
0.5000 0.5600 1.0000 0.8941  
0.0000 0.2979 0.2306 0.4520  
0.2306 0.4520 0.2845 0.4880  
0.2845 0.4880 0.3384 0.5240  
0.3384 0.5240 0.3922 0.5600  
0.3922 0.5600 0.4461 0.5960  
0.4461 0.3080 0.5000 0.2720  
0.3922 0.3440 0.4461 0.3080  
0.3384 0.3800 0.3922 0.3440  
0.2845 0.4160 0.3384 0.3800  
0.2306 0.4520 0.2845 0.4160  
0.0000 0.6061 0.2306 0.4520  
0.5539 0.3080 1.0000 0.0099  
0.5000 0.3440 0.5539 0.3080  
0.4461 0.3800 0.5000 0.3440  
0.3922 0.4160 0.4461 0.3800  
0.3384 0.4520 0.3922 0.4160

0.2845	0.4880	0.3384	0.4520
0.0000	0.6781	0.2845	0.4880
0.6078	0.3440	1.0000	0.0819
0.5539	0.3800	0.6078	0.3440
0.5000	0.4160	0.5539	0.3800
0.4461	0.4520	0.5000	0.4160
0.3922	0.4880	0.4461	0.4520
0.3384	0.5240	0.3922	0.4880
0.0000	0.7501	0.3384	0.5240
0.6616	0.3800	1.0000	0.1539
0.6078	0.4160	0.6616	0.3800
0.5539	0.4520	0.6078	0.4160
0.5000	0.4880	0.5539	0.4520
0.4461	0.5240	0.5000	0.4880
0.3922	0.5600	0.4461	0.5240
0.0000	0.8221	0.3922	0.5600
0.7155	0.4160	1.0000	0.2259
0.6616	0.4520	0.7155	0.4160
0.6078	0.4880	0.6616	0.4520
0.5539	0.5240	0.6078	0.4880
0.5000	0.5600	0.5539	0.5240
0.4461	0.5960	0.5000	0.5600
1.0000	0.6061	0.0002	
1.0000	0.6781	0.0000	
0.0000	0.0099	0.0000	
1.0000	0.7501	0.0000	
0.0000	0.0819	0.0000	
1.0000	0.8221	0.0000	
0.0000	0.1539	0.0000	
1.0000	0.8941	0.0000	
0.0000	0.2259	0.0000	
0.0000	0.2979	1.0000	
0.0000	0.6061	0.0000	
0.0000	0.6781	0.0000	
1.0000	0.0099	0.0586	
0.0000	0.7501	0.0000	
1.0000	0.0819	0.0304	
0.0000	0.8221	0.0000	
1.0000	0.1539	0.0072	
1.0000	0.2259	0.0009	
0.5000	0.2720	0.0548	
0.5539	0.3080	0.0600	
0.6078	0.3440	0.0297	
0.6616	0.3800	0.0069	
0.7155	0.4160	0.0008	
0.4461	0.3080	0.0647	
0.5000	0.3440	0.0611	
0.5539	0.3800	0.0214	
0.6078	0.4160	0.0033	
0.6616	0.4520	0.0002	
0.3922	0.3440	0.0822	
0.4461	0.3800	0.0545	

0.5000	0.4160	0.0122
0.5539	0.4520	0.0010
0.6078	0.4880	0.0000
0.3384	0.3800	0.0993
0.3922	0.4160	0.0410
0.4461	0.4520	0.0044
0.5000	0.4880	0.0000
0.5539	0.5240	0.0000
0.2845	0.4160	0.1171
0.3384	0.4520	0.0211
0.3922	0.4880	0.0000
0.4461	0.5240	0.0000
0.5000	0.5600	0.0000
0.2306	0.4520	0.1107
0.2845	0.4880	0.0000
0.3384	0.5240	0.0000
0.3922	0.5600	0.0000
0.4461	0.5960	0.0000

00479





